(2)

CONTRACT REPORT SL-89-3

SIMPLIFIED ANALYSIS OF CONCRETE GRAVITY DAMS INCLUDING FOUNDATION FLEXIBILITY

by

James M. Nau

Department of Civil Engineering
North Carolina State University
Raleigh, North Carolina 27695

US Army Corps of Engineers

September 1989
Final Report

Approved For Public Release, Distribution Unlimited

Prepared for DEPARTMENT OF THE ARMY
US Army Corps of Engineers
Washington, DC 20314-1000

Under Contract No. DACW39-88-K-0033
Work Unit 31588

Monitored by Structures Laboratory
US Army Engineer Waterways Experiment Station
3909 Halls Ferry Road, Vicksburg, Mississippi 39180-6199

STRUCTURES LABORATORY

Unclassified
SECURITY CLASSIFICATION OF THIS PAGE

REPORT DOCUMENTATION PAGE

Form Approved
OMB No 0704-0188

1a REPORT SECURITY CLASSIFICATION Unclassified	1b RESTRICTIVE MARKINGS
2a SECURITY CLASSIFICATION AUTHORITY	3 DISTRIBUTION/AVAILABILITY OF REPORT Approved for public release; distribution unlimited.
2b DECLASSIFICATION/DOWNGRADING SCHEDULE	
4 PERFORMING ORGANIZATION REPORT NUMBER(S)	5 MONITORING ORGANIZATION REPORT NUMBER(S) Contract Report SL-89-3
6a NAME OF PERFORMING ORGANIZATION Department of Civil Engineering North Carolina State University 6b OFFICE SYMBOL (If applicable)	7a NAME OF MONITORING ORGANIZATION USAEWES Structures Laboratory
6c ADDRESS (City, State, and ZIP Code) Raleigh, NC 27695	7b ADDRESS (City, State, and ZIP Code) 3909 Halls Ferry Road Vicksburg, MS 39180-6199
8a NAME OF FUNDING/SPONSORING ORGANIZATION US Army Corps of Engineers 8b OFFICE SYMBOL (If applicable)	9 PROCUREMENT INSTRUMENT IDENTIFICATION NUMBER Contract No. DACW39-88-K-0033
8c ADDRESS (City, State, and ZIP Code) Washington, DC 20314-1000	10 SOURCE OF FUNDING NUMBERS PROGRAM ELEMENT NO / PROJECT NO / TASK NO / WORK UNIT ACCESSION NO 31588
11 TITLE (Include Security Classification) Simplified Analysis of Concrete Gravity Dams Including Foundation Flexibility	
12 PERSONAL AUTHOR(S) Nau, James M.	
13a TYPE OF REPORT Final report 13b TIME COVERED FROM _____ TO _____	14 DATE OF REPORT (Year, Month, Day) September 1989 15 PAGE COUNT 83
16 SUPPLEMENTARY NOTATION Available from National Technical Information Service, 5285 Port Royal Road, Springfield, VA 22161.	
17 COSATI CODES FIELD / GROUP / SUB-GROUP	18 SUBJECT TERMS (Continue on reverse if necessary and identify by block number) Concrete gravity dams Foundation flexibility Seismic Analysis Simplified procedure

19 ABSTRACT (Continue on reverse if necessary and identify by block number)

The objective of this study was to develop a model for the flexible foundation rock beneath a dam and to incorporate this model into the finite element procedure and a two-dimensional model of the monolith, SDFDAM. To account for foundation flexibility, the theory of Flamant, assuming the foundation to be an isotropic, elastic half-plane, was used. The findings of this study indicate that it is important to include the effects of foundation flexibility in the seismic analysis of concrete gravity dams on the supposition that reliable foundation properties can be obtained from field or laboratory measurements.

20 DISTRIBUTION/AVAILABILITY OF ABSTRACT ☐ UNCLASSIFIED/UNLIMITED ☒ SAME AS RPT ☐ DTIC USERS	21 ABSTRACT SECURITY CLASSIFICATION Unclassified
22a NAME OF RESPONSIBLE INDIVIDUAL	22b TELEPHONE (Include Area Code) / 22c OFFICE SYMBOL

DD Form 1473, JUN 86 Previous editions are obsolete

Preface

This report describes a simplified analysis procedure for seismic analysis of concrete gravity dams that includes flexible foundations. The research was accomplished with funds provided to the Structures Laboratory (SL), US Army Engineer Waterways Experiment Station (WES), by the Engineering and Construction Directorate, Headquarters, US Army Corps of Engineers (HQUSACE), under Structural Engineering Work Unit 31588. The Technical Monitor was Mr. Lucian G. Guthrie, HQUSACE.

The research was accomplished for the Structural Mechanics Division (SMD), SL, WES. Dr. J. M. Nau, North Carolina State University, conducted this research under Contract No. DACW39-88-K-0033 and is the author of this report. Dr. R. L. Hall, SMD, managed and coordinated the study under the general supervision of Messrs. Bryant Mather, Chief, SL, James T. Ballard, Assistant Chief, SL, and under the direct supervision of Dr. Jimmy P. Balsara, Chief, SMD.

Commander and Director of WES during preparation of this report was COL Larry B. Fulton, EN. Technical Director was Dr. Robert W. Whalin.

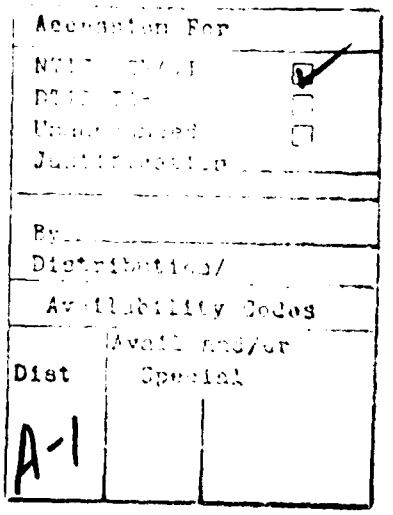

Contents

List of Tables

List of Figures

Conversion Factors, Non-SI to SI (metric) Units of Measurement

Non-SI units of measurement used in this report can be converted to SI (metric) units as follows:

Multiply	By	To Obtain
feet	0.3048	metres
inches	25.4	millimetres
pounds (mass) per cubic foot	16.01846	kilograms per cubic metre
pounds (force) per square inch	0.006894757	megapascals

1. INTRODUCTION

In the simplified method for seismic analysis of concrete gravity dams, the hydrodynamic forces arising from the fundamental mode of vibration are calculated and applied to the upstream face of the dam as an equivalent static load (Chopra, 1978). The stresses throughout the dam are computed using the finite element procedure and a two dimensional model of the monolith (Cole and Cheek, 1986). In this analysis, the effects of foundation flexibility are ignored. The objective of this study is to develop a model for the flexible foundation rock beneath a dam and to incorporate this model into the Cole and Cheek procedure, hereinafter referred to as SDFDAM. To assess the influence of the added foundation flexibility, a parametric study is conducted. Solutions obtained from SDFDAM are compared with those from the well-established computer program EAGD-84 (Fenves and Chopra, 1984). The program EAGD-84 provides a time history solution of the dam and includes all the significant modes of vibration. Four dams are used in this study which range in height from 130 feet to 638 feet.* The maximum principal tensile stresses on the upstream and downstream faces are compared to judge the suitability of the simplified equivalent lateral force method, including dam-foundation rock interaction.

---

* A table of factors for converting non-SI units of measurement to SI (metric) units is presented on page vi.

SIMPLIFIED ANALYSIS OF FUNDAMENTAL MODE RESPONSE

2.1 Equivalent Single Degree-of-Freedom System

The fundamental mode of vibration has the greatest effect on the response of short-period structures subjected to earthquake excitation. Since concrete gravity dams fall into this category, using only the fundamental mode should provide a good approximation in the calculation of the forces produced by an earthquake. To simplify the approach further, only the response to horizontal ground motion is considered. This response has been shown to be more significant than the response from vertical ground motion. Figure 1 shows the dam-reservoir-foundation system. The dam is supported on flexible foundation rock and impounds a reservoir with a horizontal bottom. The reservoir is assumed to be of infinite extent in the upstream direction, and the absorptive effects of accumulated reservoir-bottom sediments are ignored.

In the simplified analysis procedure, an equivalent single degree-of-freedom system is defined. This system has the same properties as the dam with an empty reservoir, but is modified by an added mass for the hydrodynamic effects. The mass per unit height of the equivalent system can be expressed as,

$$\tilde{m}_s(y) = m_s(y) + m_a(y) \tag{1}$$

where

y = height above the base,

$m_s(y)$ = mass of the dam without water,

$m_a(y) = \dfrac{p_1(y,\tilde{\omega}_s)}{\psi(Y)}$ = added mass of the water,

$p_1(y,\tilde{\omega}_s)$ = impulsive water pressure,

$\psi(y)$ = shape of the fundamental mode of vibration of the dam on a rigid foundation with empty reservoir,

$\tilde{\omega}_s$ = fundamental resonant frequency of the dam on a rigid foundation, including hydrodynamic effects.

The analysis is simplified further by introducing a standard mode shape and fundamental period. This approximation is possible since the cross-sectional properties of concrete gravity dams do not vary significantly. The standard mode shape is shown in Figure 2. As shown in this figure, the equation for the fundamental period of the dam on a rigid foundation with an empty reservoir is

$$T_s = 1.4 \frac{H_s}{\sqrt{E_s}} \tag{2}$$

where

H_s = the height of the dam, in ft, and

E_s = modulus of elasticity of the dam concrete, in psi.

The fundamental natural vibration period of the dam is lengthened by the presence of water in the reservoir and by the flexible foundation rock. The period of the fundamental mode is thus given by

$$\tilde{T}_s = R_1 R_f T_s, \tag{3}$$

where R_1 = period lengthening ratio due to dam-water interaction (Fig. 3), and

R_f = period lengthening ratio due to dam-foundation rock interaction (Fig. 4).

The damping for the equivalent SDOF system is given by

$$\tilde{\xi}_s = \frac{1}{R_1}\frac{1}{(R_f)^3}\,\xi_s + \xi_f\,, \tag{4}$$

where ξ_s = damping ratio of the dam on a rigid foundation with empty reservoir, and

ξ_f = damping ratio due to dam-foundation rock interaction (Fig. 5).

Typically, ξ_s is taken as 0.05. Values for ξ_f are given in Fig. 5. In this figure, η_f is the hysteretic damping factor for the foundation rock, taken as 0.1 in this study.

2.2 Earthquake Induced Loads and Stress Calculations

The loads resulting from the horizontal ground motion can be approximated by a set of equivalent horizontal static forces applied to the dam. These earthquake induced loads consist of two parts: the hydrodynamic forces and the inertial mass of the dam. The hydrodynamic effects are represented by an added mass of water moving with the dam. This added mass depends on several factors including compressibility of the water and the fundamental mode shape and frequency of the dam. The impulsive pressure resulting from the stored water during an earthquake can be computed in dimensionless form from,

$$\frac{gp_1}{wH}\left(\hat{y},\ \frac{\omega_s}{\omega_s}\right) =$$

$$\frac{4}{\pi}\sum_{n=1}^{\infty}\frac{1}{(2n-1)}\frac{\hat{I}_{1n}}{\sqrt{1-\frac{1}{(2n-1)^2}\left(\frac{\tilde{\omega}_s}{\omega_s}\right)^2}}\cos[(2n-1)\pi\hat{y}/2] \tag{5}$$

where

$\hat{y} = y/H$,

$\omega_r = C/2H$ = the fundamental resonant frequency for impulsive pressure in water,

$\tilde{\omega}_s = 2\pi/R_1 T_s$ = the fundamental resonant frequency of the dam and reservoir,

$$I_{1n} = \int_0^1 \psi(y)\cos[(2n - 1)\pi y/2]dy,$$

y = height above base,

H = height of the water,

C = the velocity of sound in water = 4720 fps,

w = unit weight of water = 62.4 pcf, and

g = acceleration of gravity.

From equation (5), normalized values of p_1 are computed as a function of $\hat{y}$ for various values of the ratio $\tilde{\omega}_s/\omega_r = R_2$, and the results are shown in Figure 6. These plots were made for a full reservoir, i.e., $H = H_s$. To obtain the impulsive pressure, p_1, when the reservoir is not full, the value from Figure 6 is multiplied by the ratio of the height of the water to the height of the dam squared $(H/H_s)^2$. Thus, the impulsive pressure is

$$p_1(y) = (\text{value from Figure 6})wH(H/H_s)^2. \tag{6}$$

The lateral earthquake forces over the height of the dam, including the hydrodynamic effects are computed from

$$f_s(y) = \frac{\tilde{\Gamma}}{\tilde{m}^*} \frac{S_a(\tilde{T}_s)}{g} [w_s(y)\psi(y) + gp_1(y,\tilde{\omega}_s)], \tag{7}$$

where

$\tilde{\Gamma}$ = modal earthquake-excitation factor

$\tilde{m}^*$ = generalized mass

$S_a(\tilde{T}_s, \tilde{\xi}_s)$ = ordinate of the earthquake spectrum in g,

$w_s(y)$ = weight per unit height of the dam, lb/ft, and

$\psi(y)$ = the fundamental mode shape of the dam.

Calculations for several cross sections and water levels show the value of $\tilde{\Gamma}/\tilde{m}^*$ is about 4.0. This value is used throughout the study.

Because the cross-section of the dam is not symmetric, the earthquake forces must be applied separately in both the upstream and downstream directions. The principal tensile stresses are of most concern, since concrete is much weaker in tension. To calculate the principal tensile stresses on the upstream face, the earthquake-induced forces are applied to the dam in the downstream direction. Likewise, to calculate the principal tensile stresses on the downstream face, the earthquake-induced forces are applied to the dam in the upstream direction. For each loading case, the earthquake-induced forces are combined with the hydrostatic and gravity loads.

The computer program SDFDAM (Cole and Cheek, 1986) incorporates Chopra's original simplified procedure for the analysis a concrete gravity dams. SDFDAM uses a two-dimensional finite element method for the stress analysis of the dam monolith. For this analysis, subroutines from the standard finite-element package SAP (Wilson, 1970) are used. An automatic mesh generating package is incorporated into SDFDAM. The only input parameters required for generating the mesh are the dimensions that describe the cross section. An example of the mesh generated by SDFDAM is shown in Figure 7.

3. DEVELOPMENT OF THE FOUNDATION FLEXIBILITY MATRIX

3.1 Theory of Flamant

To more accurately predict the behavior of a concrete gravity dam during an earthquake, the flexibility of the foundation rock should be taken into consideration. The classic theory of Flamant (Christian and Desai, 1977) is used. This theory assumes an isotropic, elastic half-plane.

For a state of plane stress, the equation for the relative vertical displacements, w_{mn}, of points m and n, shown in Figure 8(a), resulting from a vertically loaded strip is

$$w_{mn} = 2V_n/(\pi E_f a) \int_{(m-n-0.5)a}^{(m-n+0.5)a} \ln(d/x)\,dx \,, \tag{8}$$

where

a = width of loaded strip,

V_n = magnitude of the vertical load,

E_f = modulus of elasticity of foundation,

v_f = Poisson's ratio of foundation,

m = distance from point n to point of desired displacement, and

n = point beneath the center of loading.

To determine the constant d, a reference point is chosen for the deformed surface. If the deflection w_{nn} is assumed to be zero,

$$d = a/(2e) \tag{9}$$

where e is the base for the natural logarithm. Now, the equation for w_{mn} can be rewritten as

$$w_{mn} = 2V_n/(\pi E_f a) \int_{(m-n-0.5)a}^{(m-n+0.5)a} \ln[a/(2ex)]dx \qquad (10)$$

which, after integrating, becomes

$$w_{mn} = \frac{2V_n}{\pi E_f} F_{mn} , \qquad (11)$$

where

$$F_{mn} = A \ln(A) - B \ln(B),$$

$$A = 2(m - n) - 1, \text{ and}$$

$$B = 2(m - n) + 1.$$

The coefficient F_{mn} depends upon m and n. This dependence may be expressed in terms of x/a, the dimensionless distance from the loaded area. Table 1 shows the variation of F_{mn} with x/a.

The horizontal displacement, u_{mn}, resulting from the vertical load is constant and is given by

$$u_{mn} = \pm \frac{1 - \nu_f}{2E_f} V_n , \qquad (12)$$

except in the case of a point at the center of the loaded area (x = 0), where the horizontal displacement is zero.

Similar considerations can be used to determine equations which will give the vertical and horizontal displacements resulting from a horizontal (shear) load over a length a, (H_n/a). For horizontal displacements,

$$u_{MN} = \frac{H_n}{\pi E_f} F_{MN}, \tag{13}$$

where

H_n = magnitude of the horizontal load, and

$F_{MN} = F_{mn}$.

For vertical displacements,

$$w_{MN} = \pm \frac{1 - \nu_f}{2E_f} H_n \tag{14}$$

except where $x = 0$, $w_{MN} = 0$.

For plane strain E_f and ν_f are replaced by $E_f/(1-\nu_f^2)$ and $\nu_f/(1-\nu_f)$.

3.2 Procedure

The foundation flexibility must be formulated in matrix form for implementation into the computer program SDFDAM. SDFDAM automatically generates a finite element mesh that has 11 equally spaced nodes at the base of the dam. Because planar quadrilateral elements with two degrees of freedom per node are used to model the dam, a total of 22 degrees of freedom result at the dam-foundation interface. To create the flexibility matrix for the foundation, a unit load is applied at each DOF at a time. As the unit load is applied to a DOF, the displacements are calculated for every DOF. These displacements are the flexibility coefficients and form a column in the flexibility matrix. This procedure is repeated until the unit load has been applied to each DOF and all the corresponding flexibility coefficients are calculated. Since the nodes at the foundation are equally spaced, the distance between each node can be set equal to the constant a. The load width

also is set equal to this distance a. Therefore, when either the vertical load (V_n) or the horizontal load (H_n) is applied at a node, it will be equally spaced a distance a/2 from each adjacent node, as shown in Figure 8(b). With this arrangement, the ratio x/a used in the determination of F_{mn} in the Flamant equation will increase in increments of 1 from node to node away from the load. From Table 1, it is observed that the F_{mn} coefficient increases at a decreasing rate as the distance x/a increases. Directly beneath the center of the load, F_{mn} is equal to 0, since all other displacements are relative to it. To approximate the displacement at the load, a coefficient (F_{mn}) must be computed at a ratio of x/a that is "far" from the load. In this study, an x/a ratio equal to 40 was chosen to determine the displacement directly beneath the load. Since the width of the dam at its base is equal to 10a, the foundation at four dam widths away from the applied unit load is assumed not to be influenced by the dam. To calculate the surface displacements for the other nodes, the F_{mn} coefficients at these nodes are subtracted from the F_{mn} coefficient for x/a equal to 40.

The only other variables required in the Flamant equations are the horizontal (H_n) or vertical (V_n) load, the modulus of elasticity of the foundation (E_f), and Poisson's ratio of the foundation (ν_f). For purposes of creating the flexibility matrix, V_n and H_n are always equal to unity. Obviously, symmetry can be used in calculating the flexibility coefficients.

To illustrate how the flexibility matrix is developed, column 12 will be derived. Figure 9 shows the locations and positive directions of the 22 degrees-of-freedom. In addition, Figure 9 shows the location and direction of the unit load and flexibility coefficients, and the deformed shape after the unit load is applied. Flexibility coefficients $f_{1,12}$, $f_{2,12}$, and $f_{12,12}$ are selected to be calculated here. Plane strain is assumed.

$$f_{12,12} = \frac{(1 - \nu_f^2)}{\pi E_f} F_{mn} .$$

At $x/a = 40$,

$$A = 2(m - n) - 1 = 2(40 - 0) - 1 = 79,$$

$$B = 2(m - n) + 1 = 2(40 - 0) + 1 = 81, \text{ and}$$

$$F_{mn} = A \ln(A) - B \ln(B) = -10.764 .$$

For $\nu_f = 0.25$ and $E_f = 7.9 \times 10^6$ psi, the flexibility coefficients become

$$f_{12,12} = \frac{[1 - (0.25)^2]}{\pi(7.9 \times 10^6)} (10.764) = 4.066 \times 10^{-7} \text{ in., and}$$

$$f_{2,12} = \frac{(1 - \nu_f^2)}{\pi E_F} [F_{mn}(x/a = 40) - F_{mn}(x/a = 5)].$$

From Table 1, for $x/a = 5$, $F_{mn} = -6.602$ and

$$f_{2,12} = \frac{(1 - 0.25^2)}{\pi(7.9 \times 10^6)} (10.764 - 6.602) = 1.572 \times 10^{-7} \text{ in.},$$

$$f_{1,12} = \frac{1 - \nu_f - 2\nu_f^2}{2E_f} = \frac{1 - .25 - 2(.25)^2}{(2)(7.9 \times 10)^6}$$

$$f_{1,12} = 3.956 \times 10^{-8} \text{ in} .$$

The results for the remaining coefficients for column 12 of the flexibility matrix are shown in Table 2. Once all the flexibility coefficients are calculated, the matrix is inverted and appropriately combined with the stiffness matrix of the dam.

4. PARAMETRIC STUDY

4.1 Objective

The objective of the parametric study is to verify that the modified version of SDFDAM produces acceptable results for the preliminary analysis of concrete gravity dams. The principal stresses computed from the simplified analysis of SDFDAM (Cole and Cheek, 1986) are compared with the time history results of EAGD-84 (Fenves and Chopra, 1984). In addition, the stresses computed from the block or layered model and elementary beam theory (Fenves and Chopra, 1986) are evaluated and compared.

4.2 Selection of Dams and Response Parameters

Four dams are used in this study. These dams were previously used in a study by the Corps of Engineers for verifying their program SDFDAM (Cole and Cheek, 1986). Table 3 lists the dimensions and properties of each dam. The "standard" dams designated as S130, S200, and S300 are dimensioned to be typical of dams between 130 and 300 feet in height. These standard cross sections represent over 90 percent of the dams built by the Corps in the United States. The dam designated as D638 is the existing Dworshak dam located in Clearwater, Idaho. This dam was chosen since its great height presents an extreme case for checking the validity of the approximate procedure used by SDFDAM. Since the major modification to SDFDAM was the addition of foundation rock flexibility, the one parameter which will be varied is the ratio E_f/E_s. Four E_f/E_s ratios are used for this study: 1/2, 1, 2, and ∞ (rigid). The dam modulus, E_s, remains constant for all dams, so only the foundation modulus, E_f, is varied to obtain the desired ratio.

Two earthquakes, one of moderate and one of high intensity, were selected for the study. The San Fernando earthquake recorded at the Pacoima Dam on

February 9, 1971 is selected as the high intensity earthquake and will be referred to as EQ 1. This earthquake has a maximum acceleration of 1.17 g. The Imperial Valley earthquake recorded at El Centro, California on May 18, 1940 represents the moderately intense earthquake, and will be referred to as EQ 2. It has a maximum acceleration of 0.348 g. The horizontal accelerogram for each earthquake is shown in Figure 10, and the response spectra for 5 percent viscous damping are shown in Figure 11. Results from SDFDAM (Cole and Cheek, 1986), BLOCK (Fenves and Chopra, 1986), and EAGD-84 (Fenves and Chopra, 1984) are generated for all four dams, for both earthquakes, and for the four E_f/E_s ratios. Thus a total of 32 cases arise. Table 4 identifies each of these cases. The period and damping for each case, calculated using Eqs. 3 and 4, are shown in Table 5. The spectral acceleration values are also shown in Table 5.

Before EAGD-84 is run for each of the 32 cases, the parameters which control the response computations must be carefully selected to ensure that the computed dynamic response is accurate. Dam S130 was of particular concern because of its low fundamental period, as shown in Table 5. To insure that the proper time step is selected for this dam, time intervals (DT) of .005, .01, and .02 seconds are used in EAGD-84 for the rigid foundation ($E_f/E_s = \infty$), case 4. For these calculations, ten modes are combined. The maximum principal stresses for the upstream and downstream faces of the dam are plotted in Figure 12. The stresses for DT of .02 seconds are only slightly greater than those for .005 and .01 seconds. The same investigation was conducted for dam S200 with a rigid foundation (case 12) and a DT of .01 and .02 seconds. Again there is good agreement in the results for these time steps, which are shown in Figure 13. On the basis of these findings, a time step equal to .02 seconds is used for all 32 cases.

Another response parameter of concern is the selection of the number of modes. General guidelines are to use five modes if the foundation rock is rigid, and ten modes if the foundation rock is flexible. To insure that the correct selection is made for this parameter, the number of modes should be increased until there is little change in the stresses on the upstream and downstream faces of the dam. Again, the rigid foundation case for dam S130 (case 4) is used to investigate the effects of the number of modes. For these analyses, 1, 2, 5, and 10 modes are included. For these calculations a time step of .02 seconds is used. The results are shown in Figure 14. As shown in this figure, the case with 1 mode generally overestimates the dynamic response; the inclusion of higher modes reduces the response. Although the recommendation to include five modes is appropriate for the rigid foundation, ten modes are considered, for convenience, for all foundation conditions in the parametric study.

4.3 Results of Parametric Study

The maximum principal stresses from EAGD-84, SDFDAM, and BLOCK for the upstream and downstream faces are plotted and compared for all 32 cases. Plots for the rigid base cases (4, 8, 12, 16, 20, and 24) for the three standard dams, and all cases (25 through 32) for dam D638 are presented in this section. These plots are shown in Figures 15 through 28. The figures containing the plots of the other cases are shown in the Appendix. These selections were made because all of the results for the three standard dams show the same general trend. However, the results for dam D638 show a departure from this pattern. For the three standard dams, the tensile stresses from SDFDAM are greater than those from EAGD-84 for all ratios of E_f/E_s. The closest agreement in stresses from the two procedures is observed for the cases in which $E_f/E_s = \infty$. The stresses of perhaps greatest concern

are located near the top one-fourth of the dam, where the slope of the downstream face changes abruptly. Tables 6 and 7 list the stresses at this location on the upstream and downstream faces. For comparison, these tables also give the ratios of stresses from SDFDAM and BLOCK to those of EAGD-84. For the three standard dams, the ratio of the SDFDAM stress to the EAGD-84 stress, (1)/(3), ranges from a high of 2.11 in case 2 to a low of 0.88 in case 8. In other words, the approximate fundamental mode analysis may provide an overestimate of the maximum principal stress by as much as 111 percent. Only in case 8 is the stress from SDFDAM on the unconservative side; however, this underestimate is insignificant. On the other hand, for the 638 ft Dworshak Dam, D638, there are several cases that show SDFDAM to produce unconservative results. These cases (cases 25, 26, 27, and 28) are for the higher intensity earthquake, EQ1. The maximum underestimate is about 30 percent on the upstream face. Similar conclusions may be reached when the stresses computed from the oversimplified block model are compared with those from EAGD-84. The maximum overestimate is about 150 percent; in no case does the underestimate exceed 10 percent. It is worthy to note that the stresses from BLOCK compare favorably with those of SDFDAM on the upstream face, but exceed the SDFDAM results on the downstream face. This result may be due to the limitation of the elementary beam theory in predicting principal stresses near inclined surfaces.

Because of the apparent conservative of SDFDAM for the majority of dams considered in this study, one final investigation was conducted for dam S130 on a rigid foundation. Referring to Figure 14, which contains EAGD-84 solutions for various numbers of modes, the results show larger stresses over about the top half of the dam when only 1 mode is considered. This observation explains at least part of the overestimate in the equivalent

lateral force method, since all SDFDAM results in Figures 15-28 include one mode only. To see how the results compare for one mode, Figure 29 is presented. In this figure, the results from EAGD-84 (from Figure 14 for one mode) are compared with the stresses from SDFDAM from Figure 15. These results compare favorably, again indicating the general conservatism introduced into the simplified method when only one mode is considered.

5. SUMMARY AND CONCLUSIONS

The US Army Corps of Engineers developed the computer code SDFDAM (Cole and Cheek, 1986) for the analysis of concrete gravity dams subjected to earthquakes. The approximate procedure reported by Chopra for the determination of the earthquake-induced loads is incorporated into SDFDAM. This procedure considers the response in the fundamental mode of vibration. In the current version of SDFDAM, the stresses in the dam are computed under the assumption that the foundation is rigid. Subsequent studies have shown that the effects of dam-foundation rock interaction may be significant and should be included in the analysis. The purpose of this study was to develop and implement a procedure into SDFDAM to account for foundation flexibility. The theory of Flamant, in which the foundation is assumed to be an isotropic elastic half-plane, was used.

A parametric study was conducted to assess the validity of the modified version of SDFDAM. The computer program EAGD-84 (Fenves and Chopra, 1984) was used as the standard for this investigation. Four dam cross sections, ranging in height from 130 to 638 ft, four foundation moduli, and two earthquake ground motions were used. The maximum principal stresses on the upstream and downstream faces of each dam were plotted and compared. In general, the stresses for the 130 ft, 200 ft, and 300 ft dams obtained from SDFDAM are greater than those from EAGD-84. Thus, for these dams, the simplified procedure including foundation interaction effects provides conservative estimates of the earthquake-induced stresses, regardless of the foundation modulus and the intensity of the earthquake motion. It should be noted, however, that the approximate stresses obtained from SDFDAM may exceed the exact values of EAGD-84 by as much as 100 percent. This overestimate may be

attributed in part to the inclusion of only one mode in the simplified procedure.

For the 638 ft dam subjected to the high intensity earthquake, the results of SDFDAM are not on the conservative side for all foundation conditions. The stresses obtained from the approximate procedure of SDFDAM are as much as 30 percent lower than those of EAGD-84. When subjected to the earthquake motion of lesser intensity, however, the simplified procedure is conservative for all foundation moduli. While it is difficult to draw general conclusions from these limited results, it is evident that for the extreme case of a high dam subjected to an intense earthquake, the simplified analysis procedure may be inadequate.

Finally, the results of this study reveal, as expected, that the stresses in a dam subjected to earthquake loading are a function of the foundation modulus. Because foundation compliance alters the fundamental natural period of the dam, the response is increased or decreased, depending upon the frequency content of the ground motion. These findings indicate that it is important to include the effects of foundation flexibility in the seismic analysis of concrete gravity dams. Of course, this conclusion assumes that reliable foundation properties can be obtained from field or laboratory measurements.

6. REFERENCES

1. Chopra, A. K., "Earthquake Resistant Design of Concrete Gravity Dams," Journal of the Structural Division, ASCE, Vol. 104, No. ST6, June, 1978, pp. 953-971.

2. Christian, J. T., and Desai, C. S. Numerical Methods In Geotechnical Engineering, McGraw-Hill, Inc., New York, 1977.

3. Cole, R. A., and Cheek, J. B., "Seismic Analysis of Gravity Dams," Technical Report SL-86-44, U.S. Army Engineer Waterways Experiment Station, Vicksburg, Mississippi, Dec., 1986.

4. Fenves, G., and Chopra, A. K., "EAGD-84, A Computer Program for Earthquake Analysis of Concrete Gravity Dams," Report No. UCB/EERC-84/11, Earthquake Engineering Research Center, University of California, Berkeley, California, Aug., 1984.

5. Fenves, G., and Chopra, A. K., "Simplified Analysis for Earthquake Resistant Design of Concrete Gravity Dams," Report No. UCB/EERC-85/10, Earthquake Engineering Research Center, University of California, Berkeley, California, June, 1986.

6. Wilson, E. L., "SAP - A General Structural Analysis Program," SESM Report 70-20, Department of Civil Engineering, University of California, Berkeley, 1970.

x/a	F_{mn}
0	0
1	-3.296
2	-4.751
3	-5.574
4	-6.154
5	-6.602
6	-6.967
7	-7.276
8	-7.544
9	-7.780
10	-7.991
11	-8.181
12	-8.356
13	-8.516
14	-8.664
15	-8.802
16	-8.931
17	-9.052
18	-9.167
19	-9.275
20	-9.378

Table 1. The Coefficient F_{mn} for the Half-Plane Problem

Flexibility Coefficient Location (f_{RxC})	Coefficient (in.)
1 , 12	3.956×10^{-8}
2 , 12	1.572×10^{-7}
3 , 12	3.956×10^{-8}
4 , 12	1.741×10^{-7}
5 , 12	3.956×10^{-7}
6 , 12	1.960×10^{-7}
7 , 12	3.956×10^{-8}
8 , 12	2.271×10^{-7}
9 , 12	3.956×10^{-8}
10 , 12	2.821×10^{-7}
11 , 12	0
12 , 12	4.066×10^{-7}
13 , 12	-3.956×10^{-8}
14 , 12	2.821×10^{-7}
15 , 12	-3.956×10^{-8}
16 , 12	2.271×10^{-7}
17 , 12	-3.956×10^{-8}
18 , 12	1.960×10^{-7}
19 , 12	-3.956×10^{-7}
20 , 12	1.741×10^{-7}
21 , 12	-3.956×10^{-8}
22 , 12	1.572×10^{-7}

Table 2. Flexibility Coefficients for Column 12 of the Foundation Rock Flexibility Matrix

	Dams			
Dimensions, ft.	S130	S200	S300	D638
HEIGHT	130.	200.	300.	638.
W	14.	17.	21.	27.
BASE	130.5	146.83	230.83	495.
HWATER	115.	185.	285.	570.
BH_1	95.	158.	250.	---
BH_2	110.	175.	270.	585.
S_u	0.120	0.083	0.083	0.0
S_d	0.710	0.667	0.700	0.800
Material Properties				
Modulus of Elasticity (million psi)	3.0	3.0	3.0	5.0
Poisson's Ratio	0.2	0.2	0.2	0.2
Unit Weight (lb/ft^3)	144.0	144.0	144.0	144.0

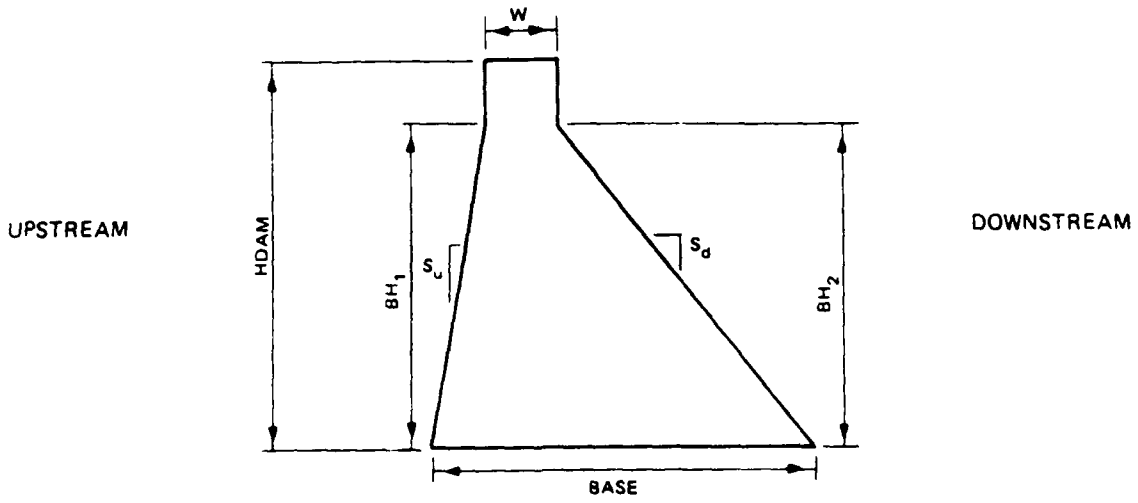

Table 3. Properties of Dams Used for the Parametric Study

Case	E_f/E_s	E_f	Earthquake	Dam
1	1/2	1.5	EQ1	S130
2	1	3.0	EQ1	S130
3	2	6.0	EQ1	S130
4	∞	∞	EQ1	S130
5	1/2	1.5	EQ2	S130
6	1	3.0	EQ2	S130
7	2	6.0	EQ2	S130
8	∞	∞	EQ2	S130
9	1/2	1.5	EQ1	S200
10	1	3.0	EQ1	S200
11	2	6.0	EQ1	S200
12	∞	∞	EQ1	S200
13	1/2	1.5	EQ2	S200
14	1	3.0	EQ2	S200
15	2	6.0	EQ2	S200
16	∞	∞	EQ2	S200
17	1/2	1.5	EQ1	S300
18	1	3.0	EQ1	S300
19	2	6.0	EQ1	S300
20	∞	∞	EQ1	S300
21	1/2	1.5	EQ2	S300
22	1	3.0	EQ2	S300
23	2	6.0	EQ2	S300
24	∞	∞	EQ2	S300
25	1/2	2.5	EQ1	D638
26	1	5.0	EQ1	D638
27	2	10.0	EQ1	D638
28	∞	∞	EQ1	D638
29	1/2	2.5	EQ2	D638
30	1	5.0	EQ2	D638
31	2	10.0	EQ2	D638
32	∞	∞	EQ2	D638

Note: E_f in million psi

Table 4. Cases Considered in this Study

Case	Natural Period of Vibration (sec)	Viscous Damping Factor	Spectral Acceleration Value (g)
1	0.163	0.139	1.360
2	0.145	0.094	1.810
3	0.134	0.067	2.030
4	0.122	0.043	1.720
5	0.163	0.139	0.500
6	0.145	0.094	0.517
7	0.134	0.067	0.670
8	0.122	0.043	0.684
9	0.261	0.138	1.360
10	0.232	0.093	1.740
11	0.215	0.066	2.230
12	0.195	0.041	2.090
13	0.261	0.138	0.525
14	0.232	0.093	0.637
15	0.215	0.066	0.639
16	0.195	0.041	0.703
17	0.402	0.138	1.520
18	0.357	0.092	1.890
19	0.331	0.065	1.710
20	0.301	0.040	2.150
21	0.402	0.138	0.438
22	0.357	0.092	0.515
23	0.331	0.065	0.609
24	0.301	0.040	0.753
25	0.682	0.137	0.687
26	0.607	0.091	0.696
27	0.562	0.064	0.898
28	0.511	0.039	1.710
29	0.682	0.137	0.507
30	0.607	0.091	0.717
31	0.562	0.064	0.853
32	0.511	0.039	0.904

Table 5. Natural Periods, Viscous Damping Factors, and Spectral Acceleration Values

Maximum Principal Stress on the Upstream Face (psi)

Case	SDFDAM (1)	BLOCK (2)	EAGD-84 (3)	Ratio (1)/(3)	Ratio (2)/(3)
1	376	401	251	1.50	1.60
2	514	519	266	1.93	1.95
3	581	578	352	1.65	1.64
4	486	495	478	1.02	1.04
5	114	131	65	1.75	2.02
6	119	135	111	1.07	1.22
7	166	176	135	1.23	1.30
8	170	180	193	0.88	0.93
9	541	567	443	1.22	1.28
10	704	706	487	1.45	1.45
11	915	917	671	1.36	1.37
12	855	860	657	1.30	1.31
13	182	190	120	1.52	1.58
14	231	233	141	1.64	1.65
15	231	234	147	1.57	1.59
16	259	259	211	1.23	1.23
17	772	772	444	1.74	1.74
18	972	932	674	1.44	1.38
19	875	889	760	1.15	1.17
20	1112	1118	742	1.50	1.51
21	187	203	165	1.13	1.23
22	229	237	178	1.29	1.33
23	280	280	215	1.30	1.30
24	358	347	214	1.67	1.62
25	584	838	638	0.92	1.31
26	592	845	872	0.68	0.97
27	782	992	1100	0.71	0.90
28	1548	1676	1866	0.83	0.91
29	414	441	431	0.96	1.02
30	612	632	573	1.07	1.10
31	740	758	776	0.95	0.98
32	788	805	795	0.99	1.01

Table 6. Maximum Principal Stresses on the Upstream Face

Maximum Principal Stress on the
Downstream Face (psi)

Case	SDFDAM (1)	BLOCK (2)	EAGD-84 (3)	RATIO (1)/(3)	RATIO (2)/(3)
1	520	622	309	1.68	2.01
2	697	809	330	2.11	2.45
3	784	901	443	1.77	2.03
4	662	771	626	1.06	1.23
5	180	217	103	1.75	2.11
6	186	224	137	1.36	1.64
7	247	289	168	1.47	1.72
8	252	295	270	0.93	1.09
9	700	860	383	1.83	2.25
10	903	1080	620	1.46	1.74
11	1164	1366	850	1.37	1.61
12	1098	1283	848	1.29	1.51
13	237	311	177	1.34	1.76
14	314	376	205	1.53	1.83
15	315	378	207	1.52	1.83
16	327	415	302	1.08	1.37
17	995	1192	592	1.68	2.01
18	1245	1460	746	1.67	1.96
19	1123	1329	888	1.26	1.50
20	1421	1650	906	1.57	1.82
21	263	325	239	1.10	1.36
22	315	385	263	1.20	1.46
23	378	450	288	1.31	1.56
24	476	556	289	1.65	1.92
25	892	1172	893	1.00	1.31
26	904	1180	1204	0.75	0.98
27	1177	1378	1521	0.77	0.91
28	2275	2286	2541	0.90	0.90
29	649	682	611	1.06	1.12
30	933	933	805	1.16	1.16
31	1116	1099	1012	1.10	1.09
32	1185	1161	1155	1.03	1.01

Table 7. Maximum Principal Stresses on the Downstream Face

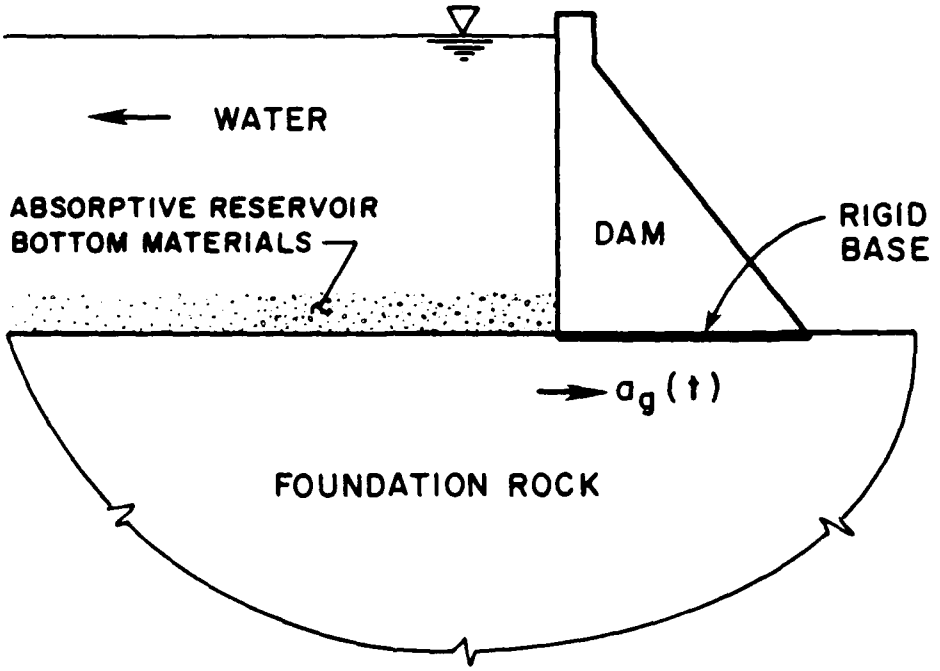

Figure 1. Dam-Water Foundation Rock System

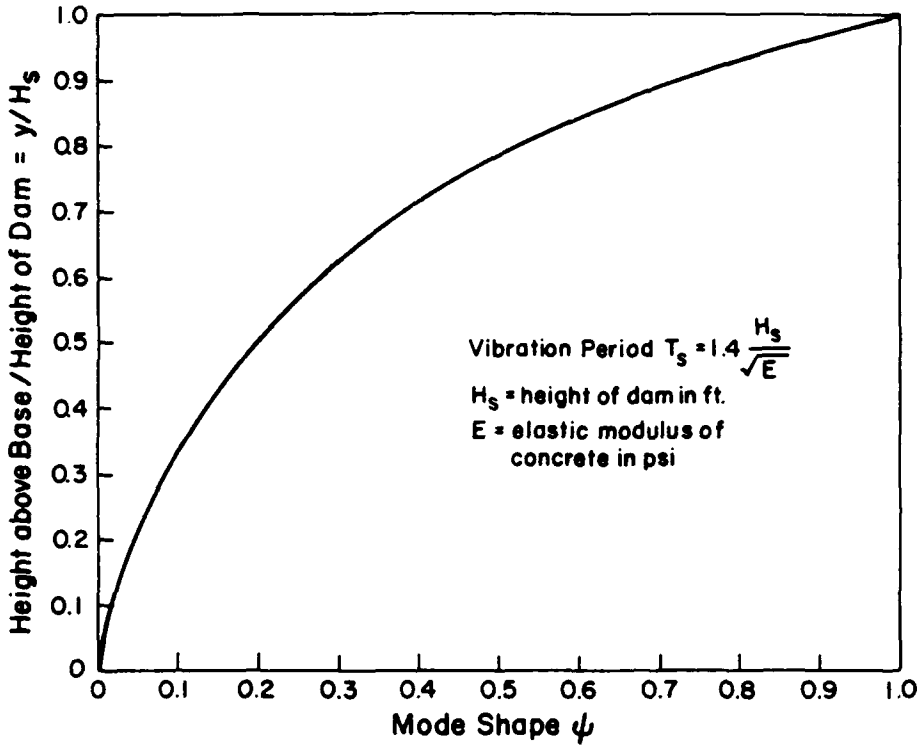

Figure 2. Standard Mode Shape and Fundamental Period for the Dam on a Rigid Foundation and Empty Reservoir. After Chopra (1978)

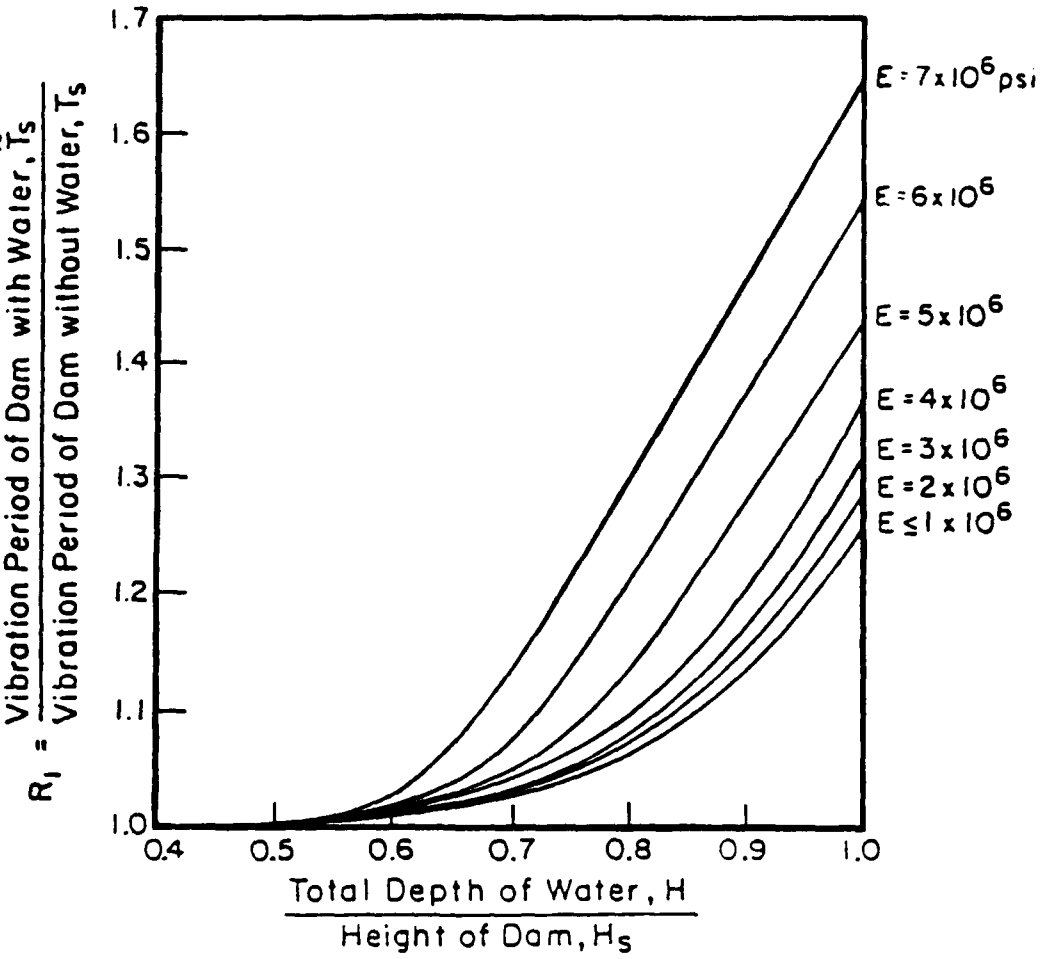

Figure 3. Standard Values for R_1, the Ratio of Fundamental Vibration Periods of the Dam with and without Water. After Chopra (1978).

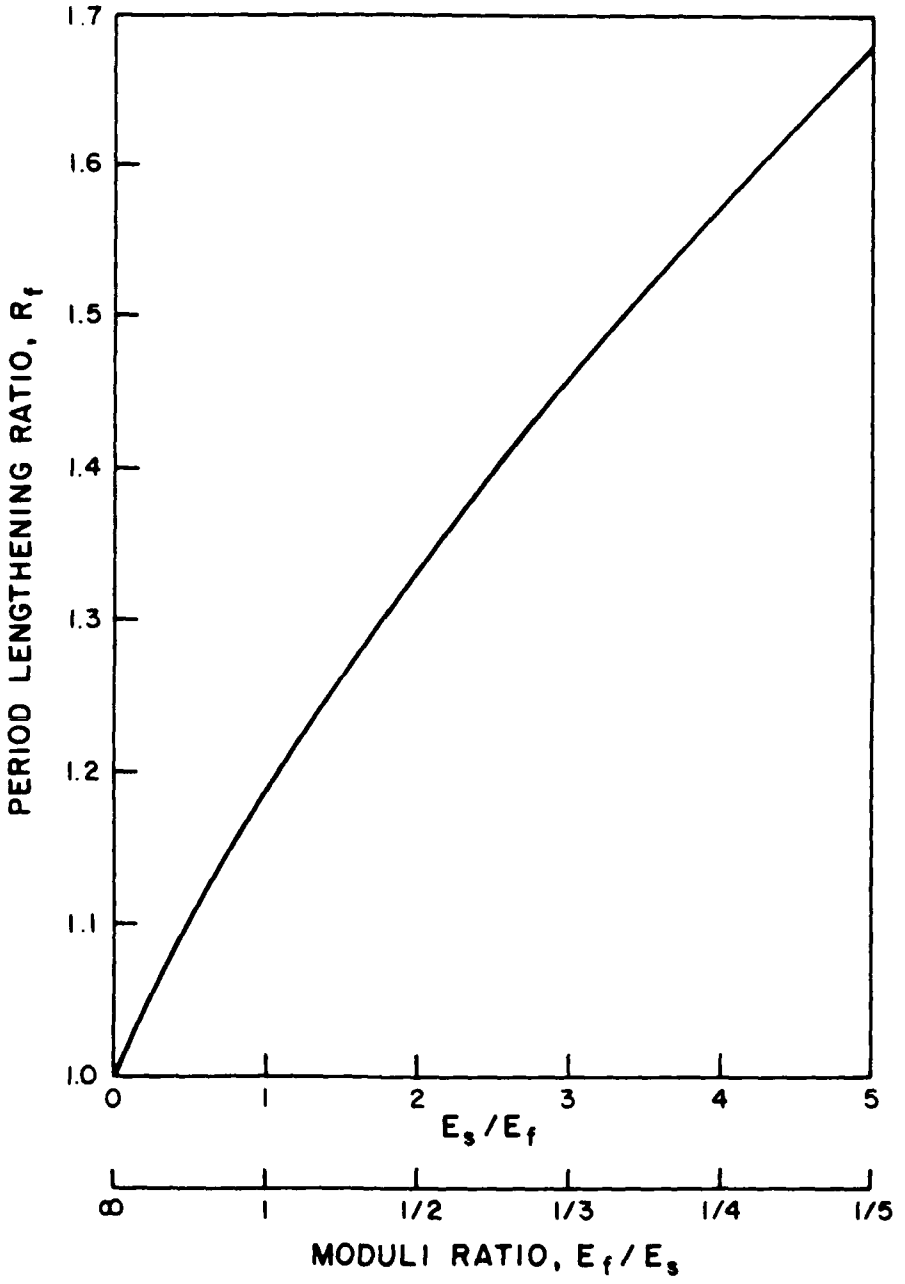

Figure 4. Standard Values for R_f, the Period Lengthening Ratio Due to Dam-Foundation Rock Interaction. After Fenves and Chopra (1986).

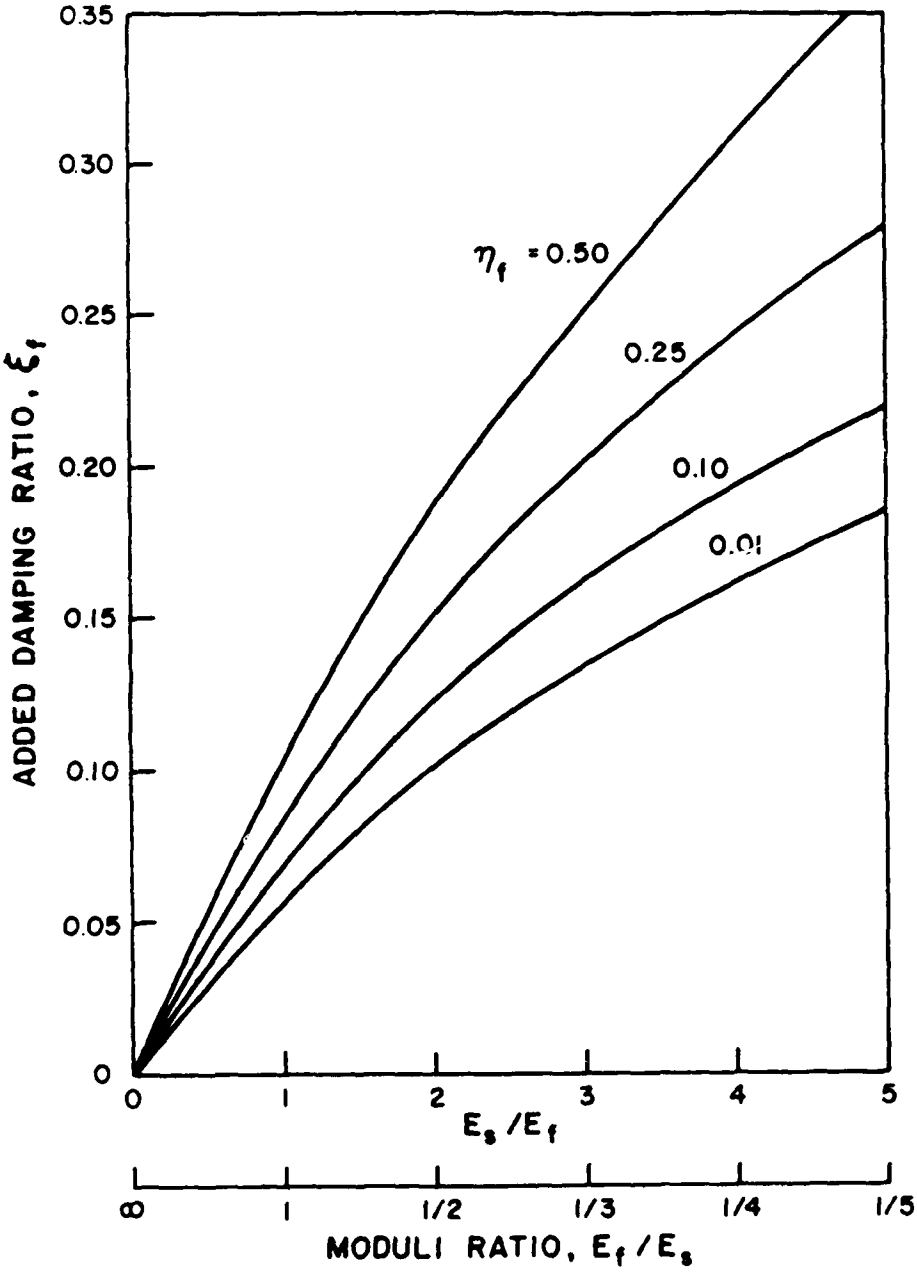

Figure 5. Standard Values for ξ_f, the Added Damping Due to Dam-Foundation Rock Interaction. After Fenves and Chopra (1986).

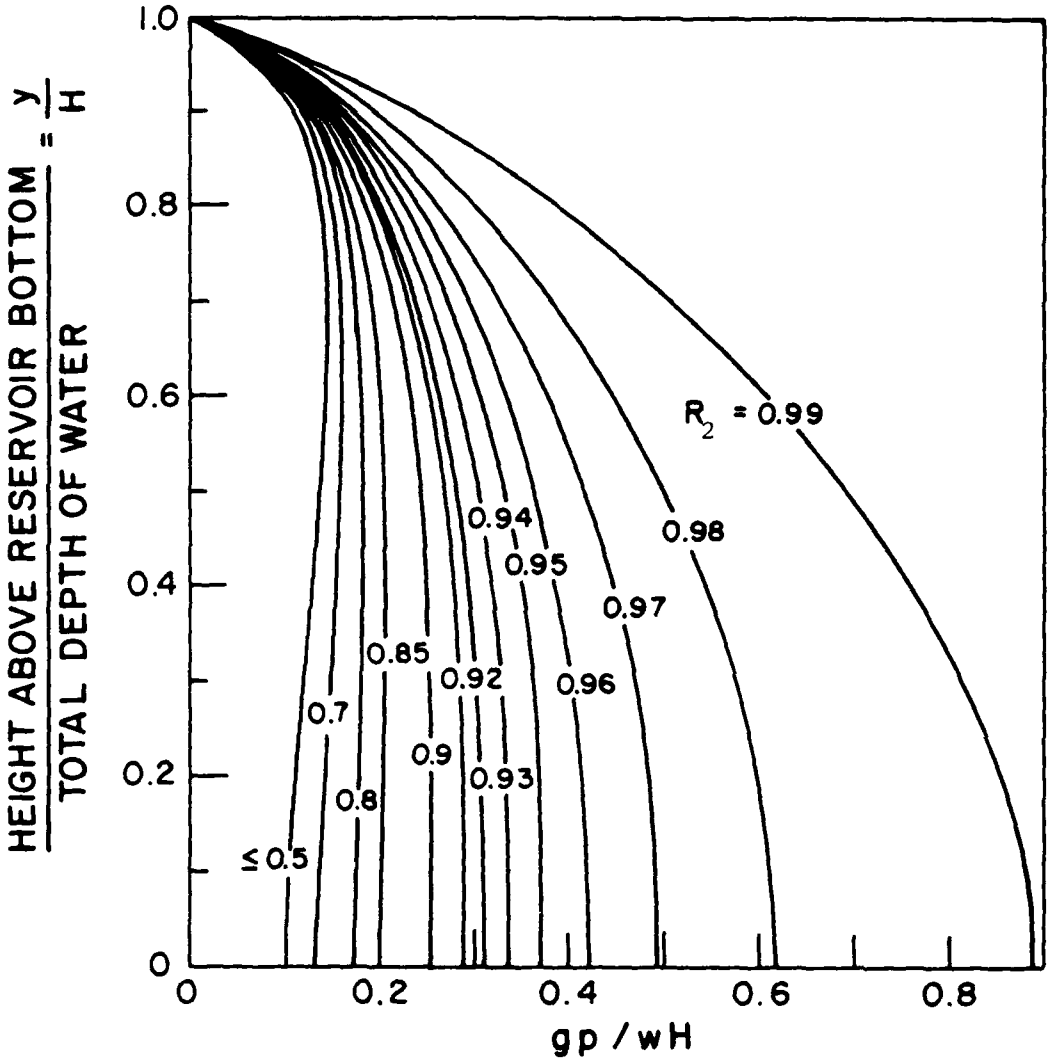

Figure 6. Standard Plots for Variation of p_1 over Depth of Water for $H/H_s = 1$ and Various Values of $R_2 = \hat{\omega}_s/\omega_r$. After Chopra (1978).

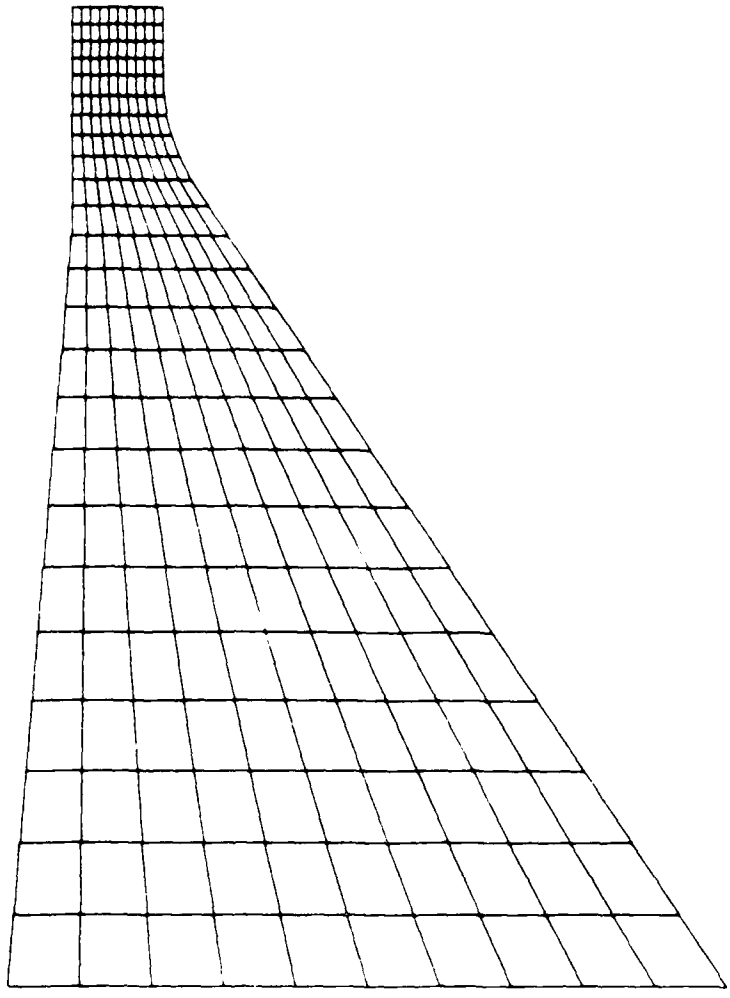

Figure 7. Finite Element Mesh Generated by SDFDAM for DAM S130

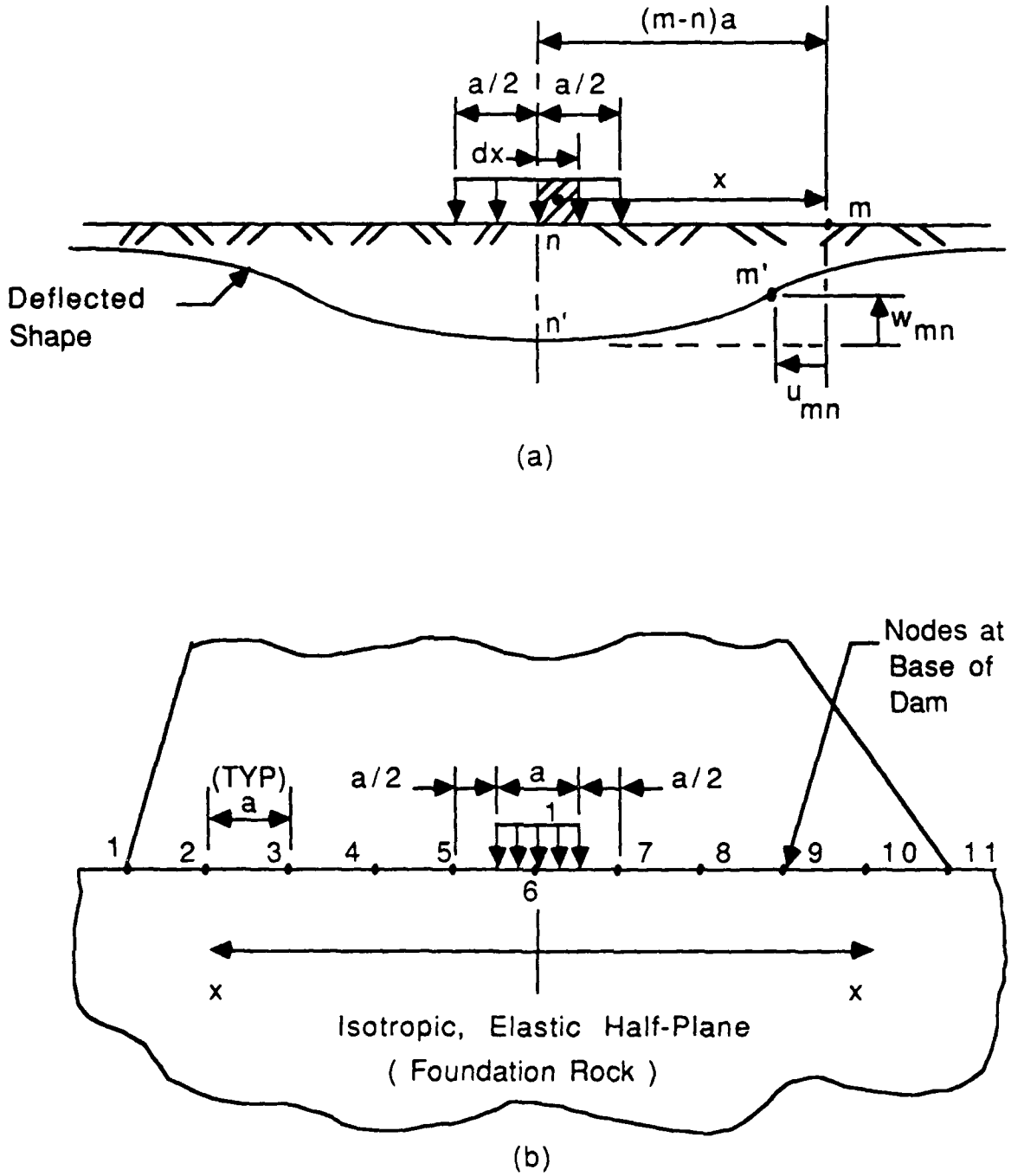

Figure 8. Flamant Isotropic, Elastic Half-Plane: (a) Vertical and Horizontal Displacements Due to a Uniformly Loaded Strip. (b) Location of Nodes and Load for Using the Flamant Equation

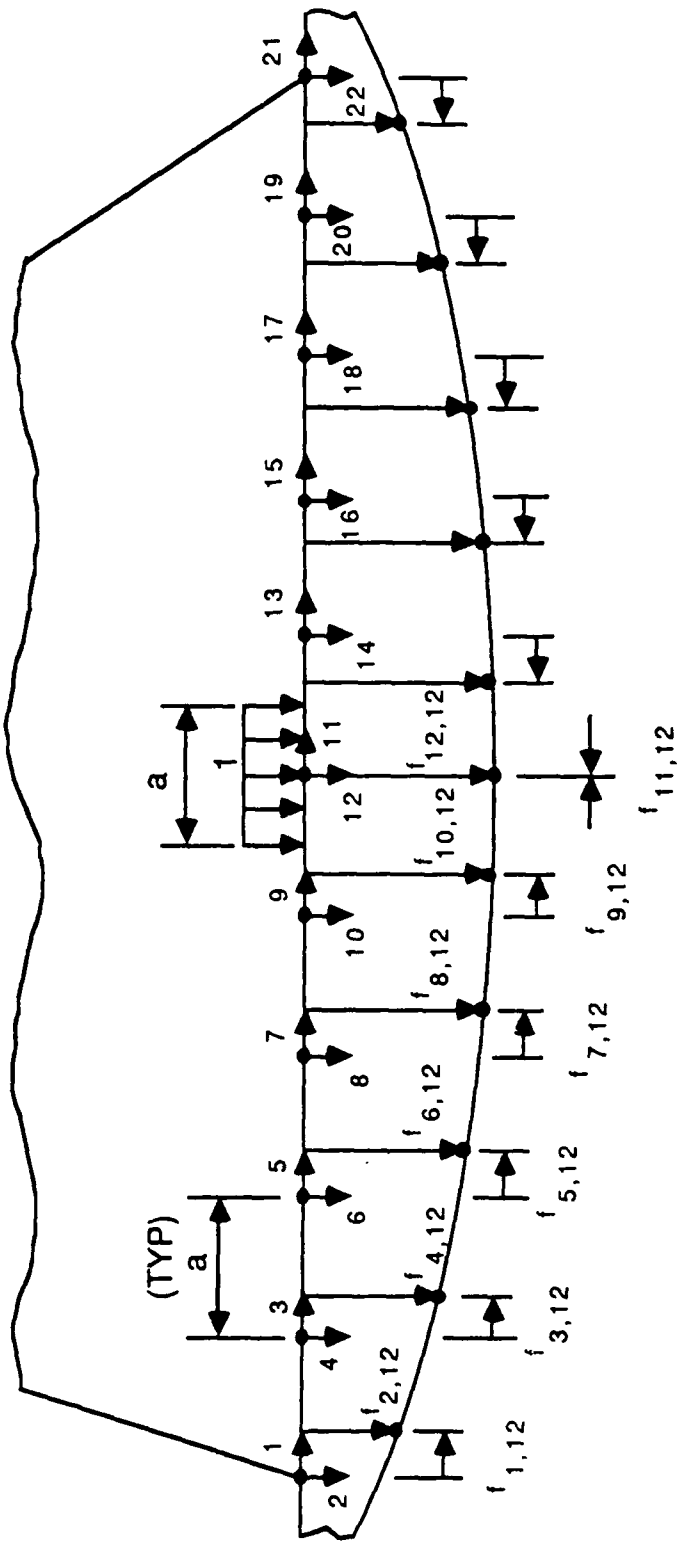

Figure 9. Location and Direction of Coefficients for Column 12 of Flexibility Matrix

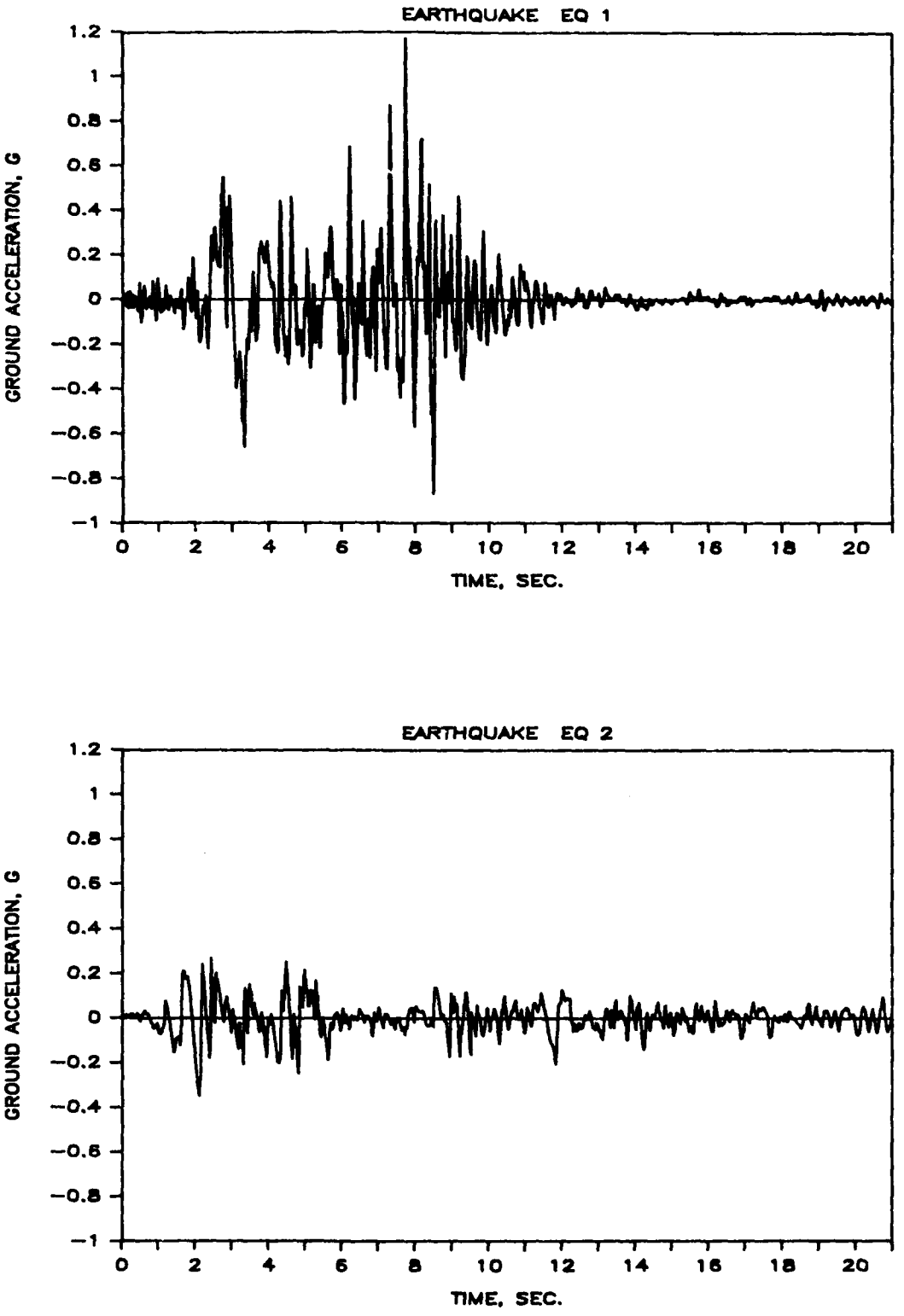

Figure 10. Horizontal Earthquake Time Histories

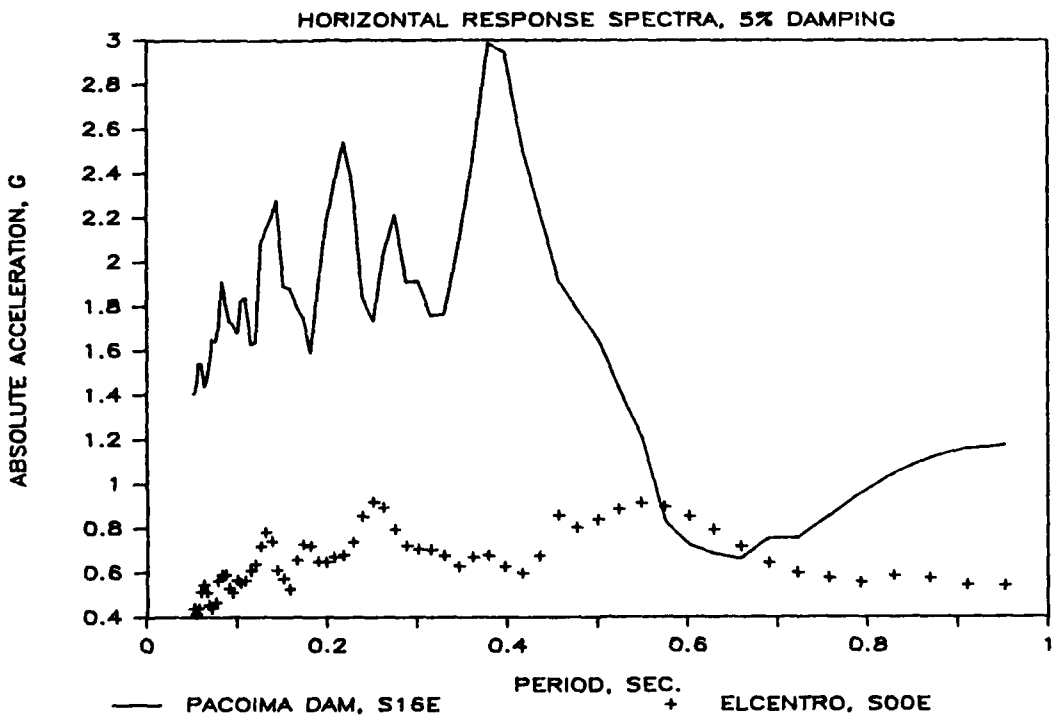

Figure 11. Response Spectra for 5-Percent Viscous Damping

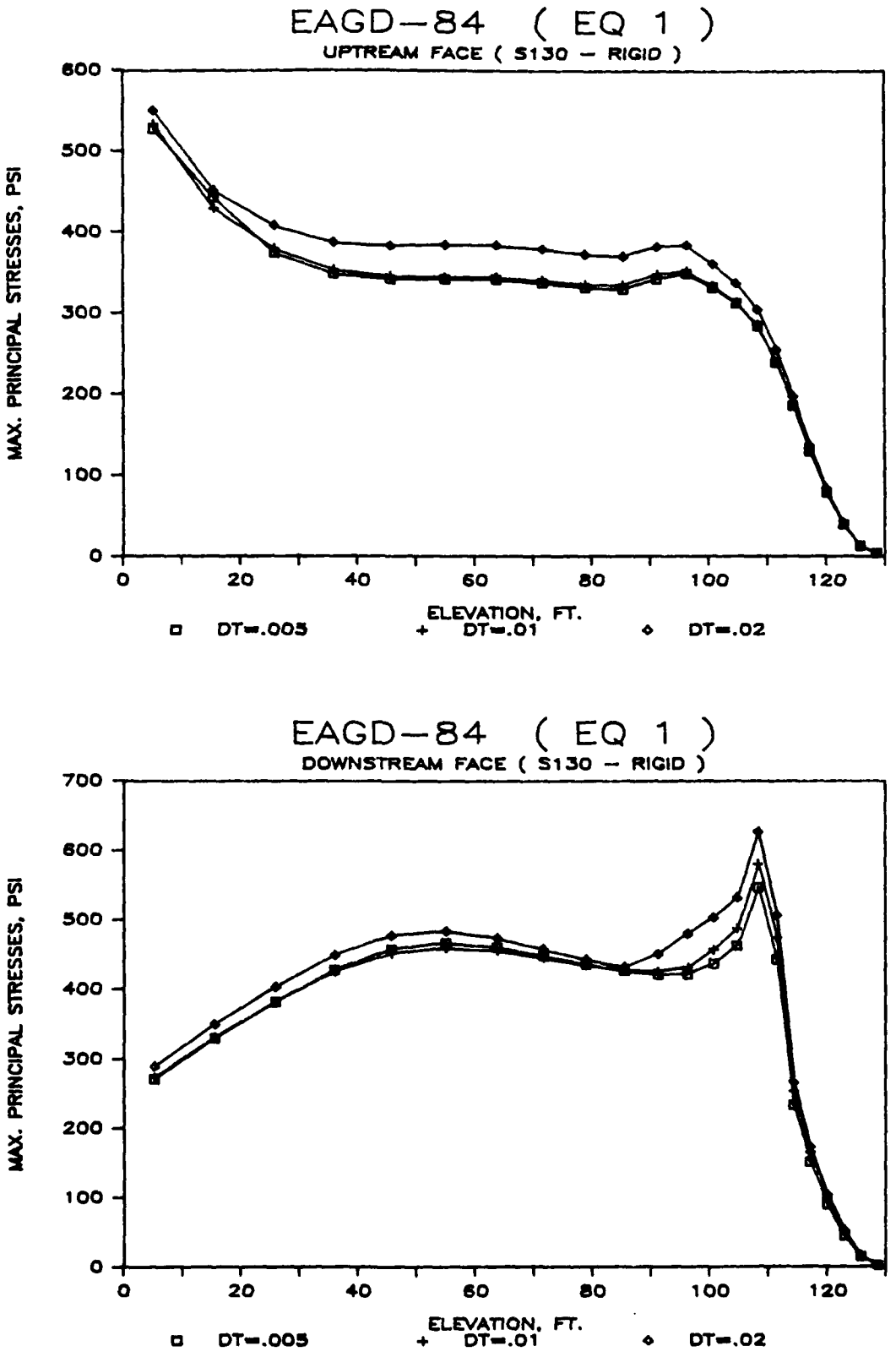

Figure 12. Effect of Time Increment on the Computation of the Response of Dam S130 (Case 4)

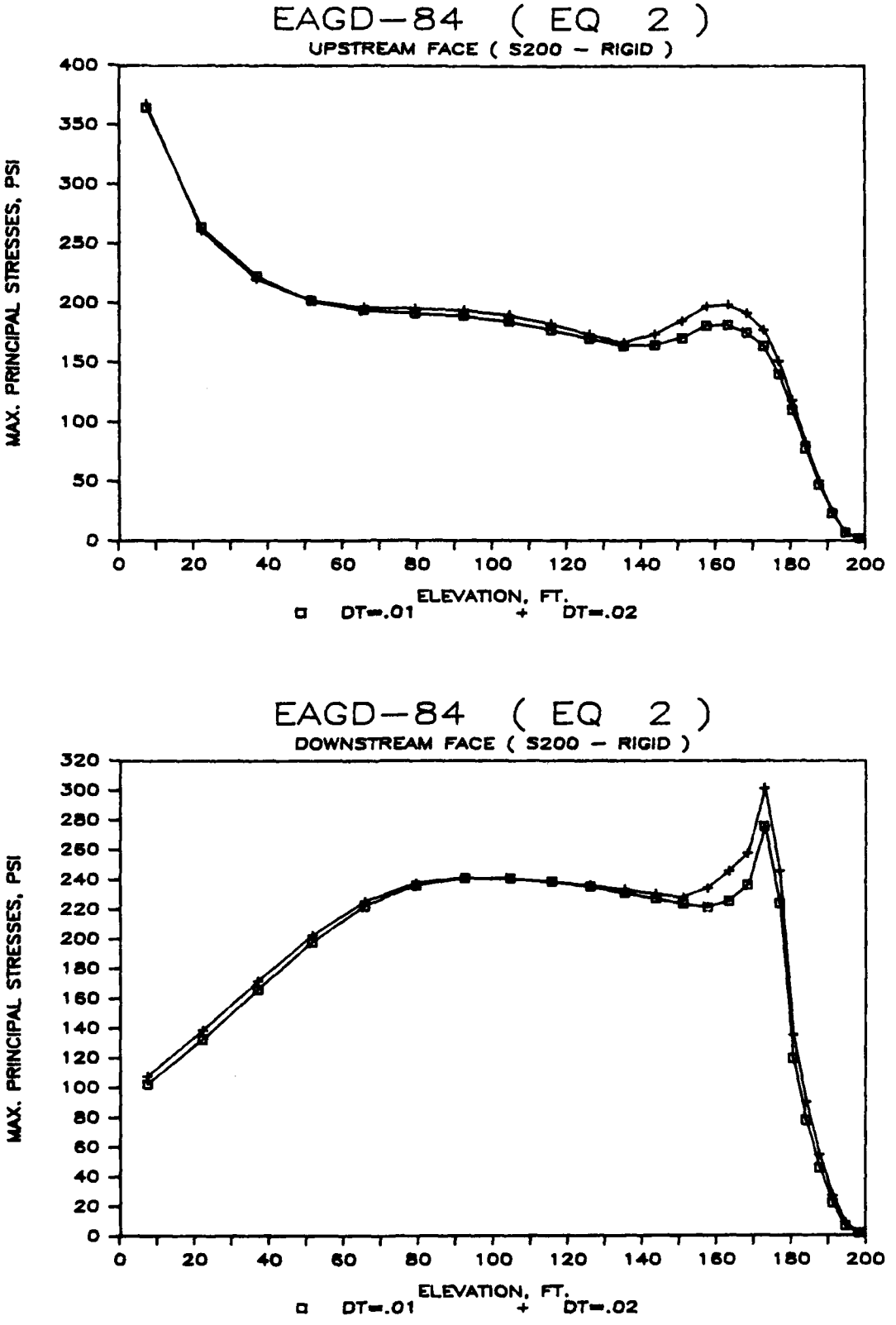

Figure 13. Effect of Time Increment on the Computation of the Response of Dam S200 (Case 12)

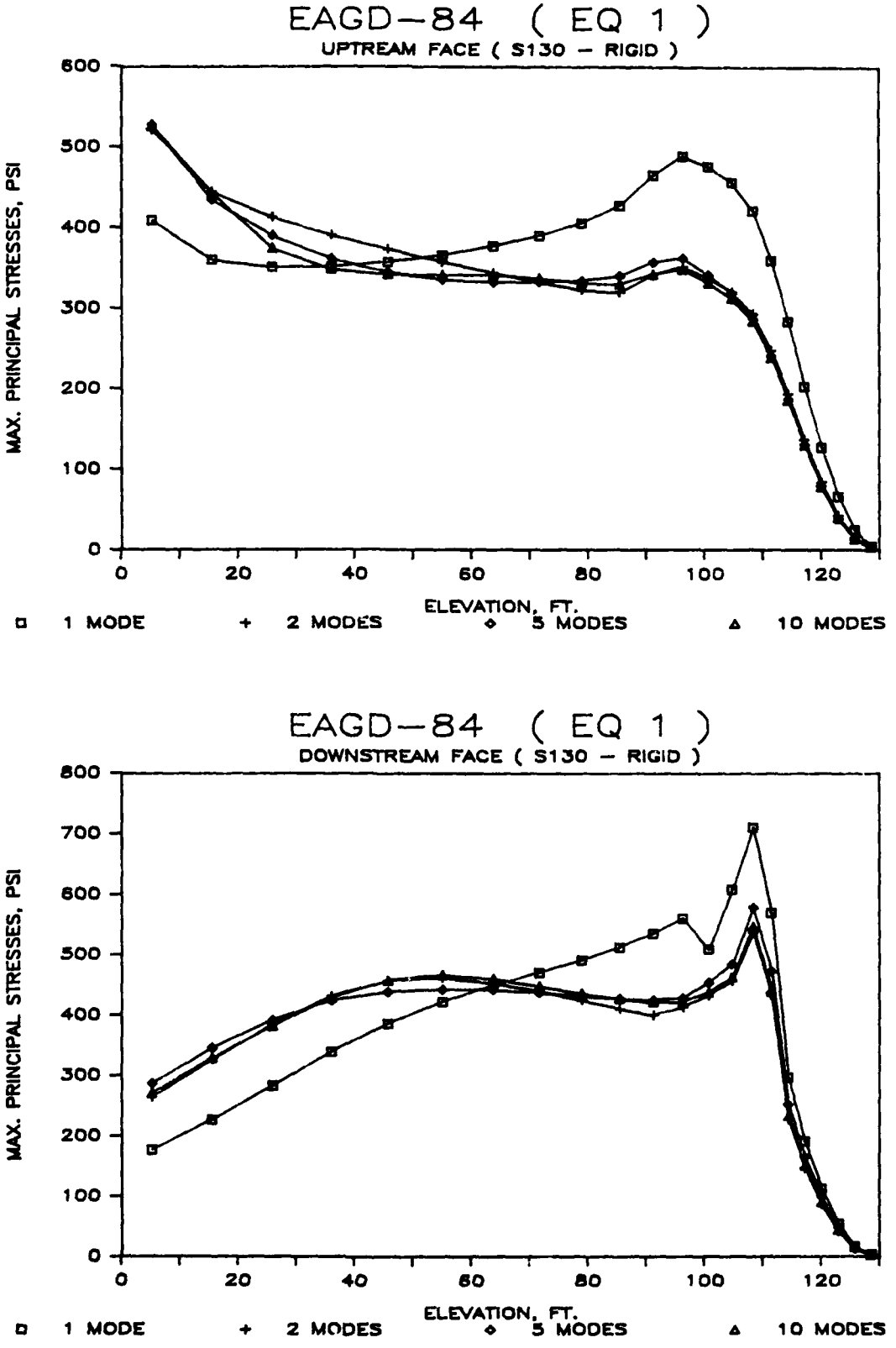

Figure 14. Effect of the Number of Modes Used in the Computation of Response of Dam S130 (Case 4)

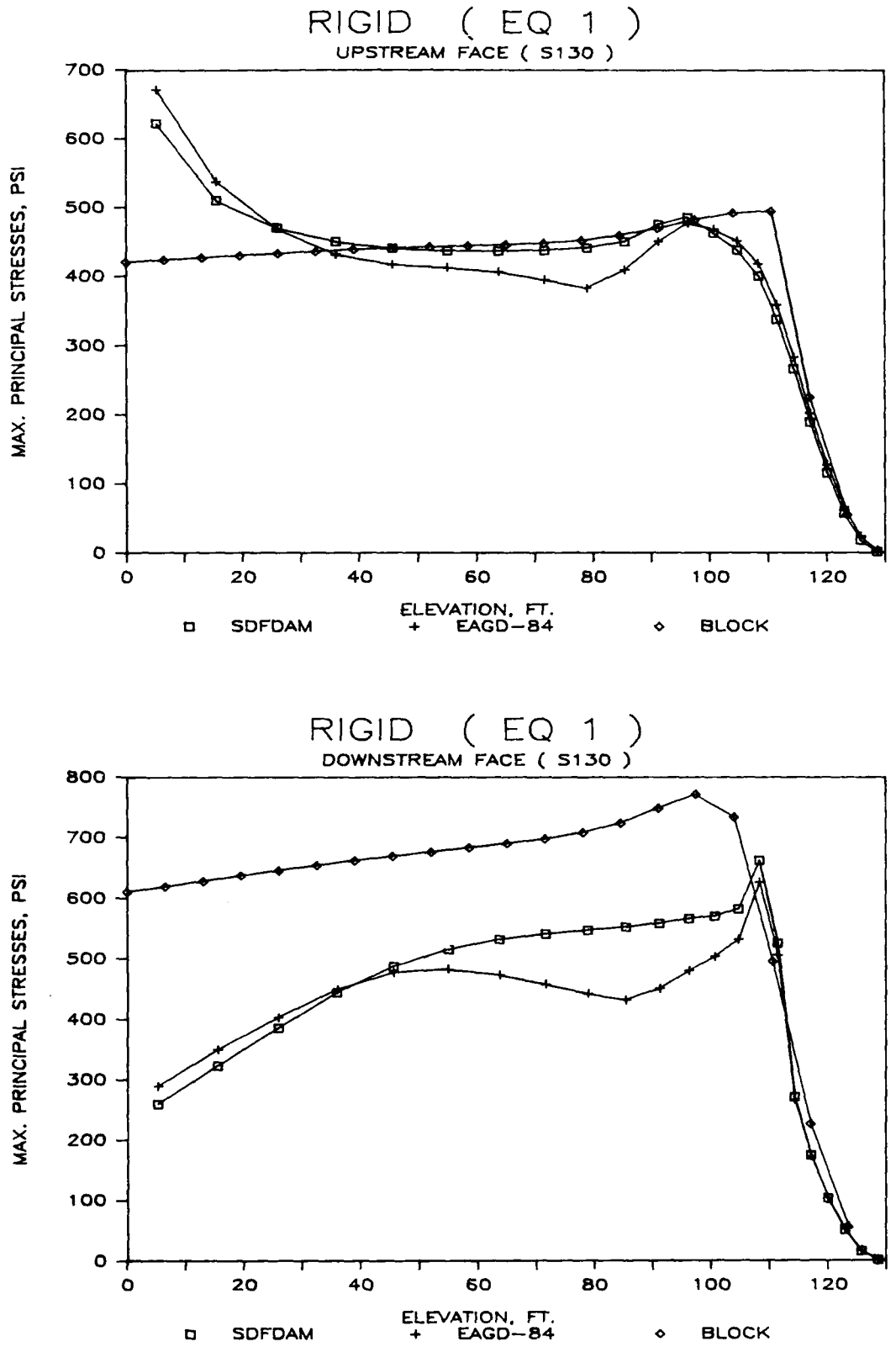

Figure 15. Effect of Foundation Modulus, F_f (Case 4)

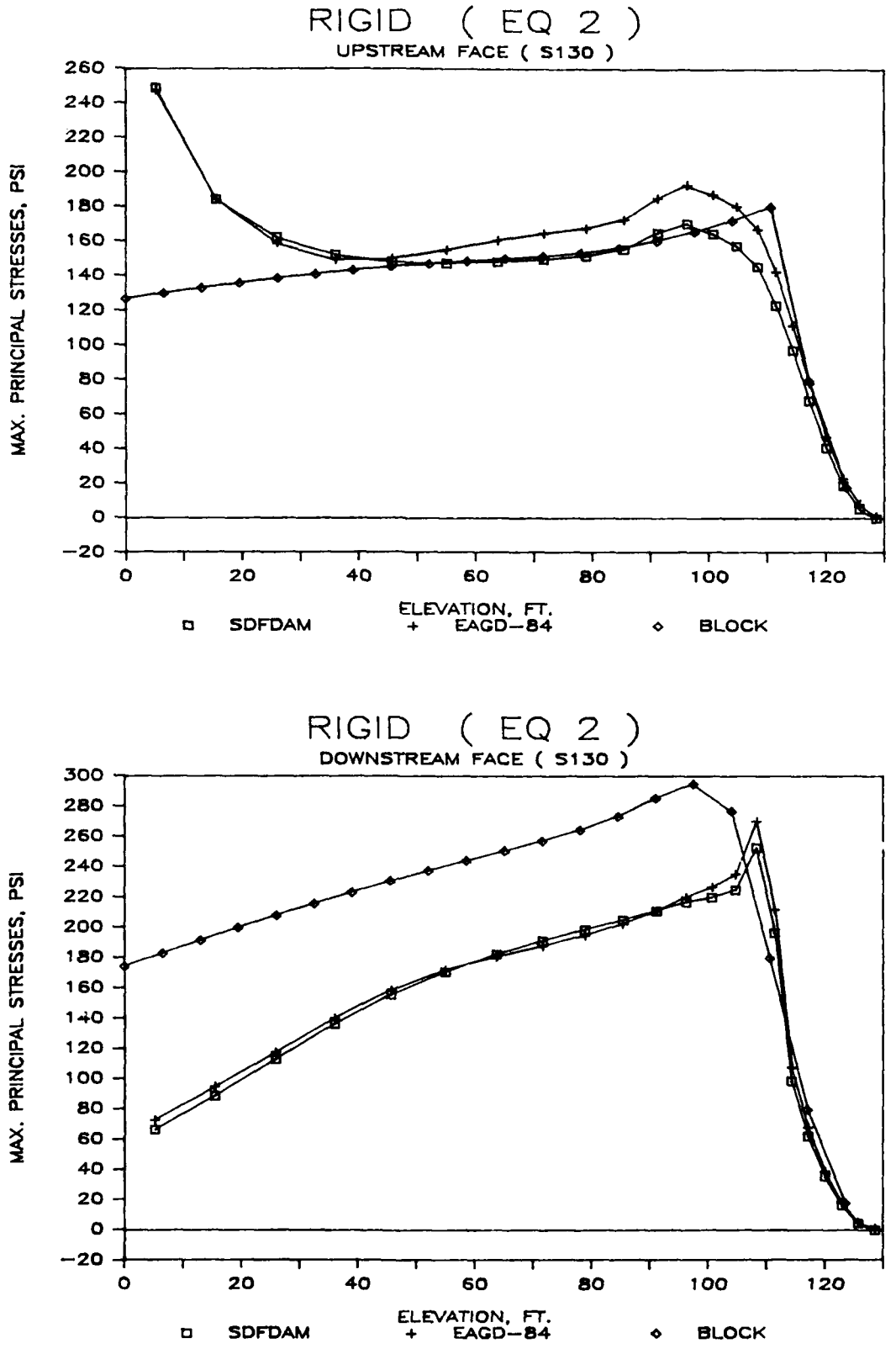

Figure 16. Effect of Foundation Modulus, E_f (Case 8)

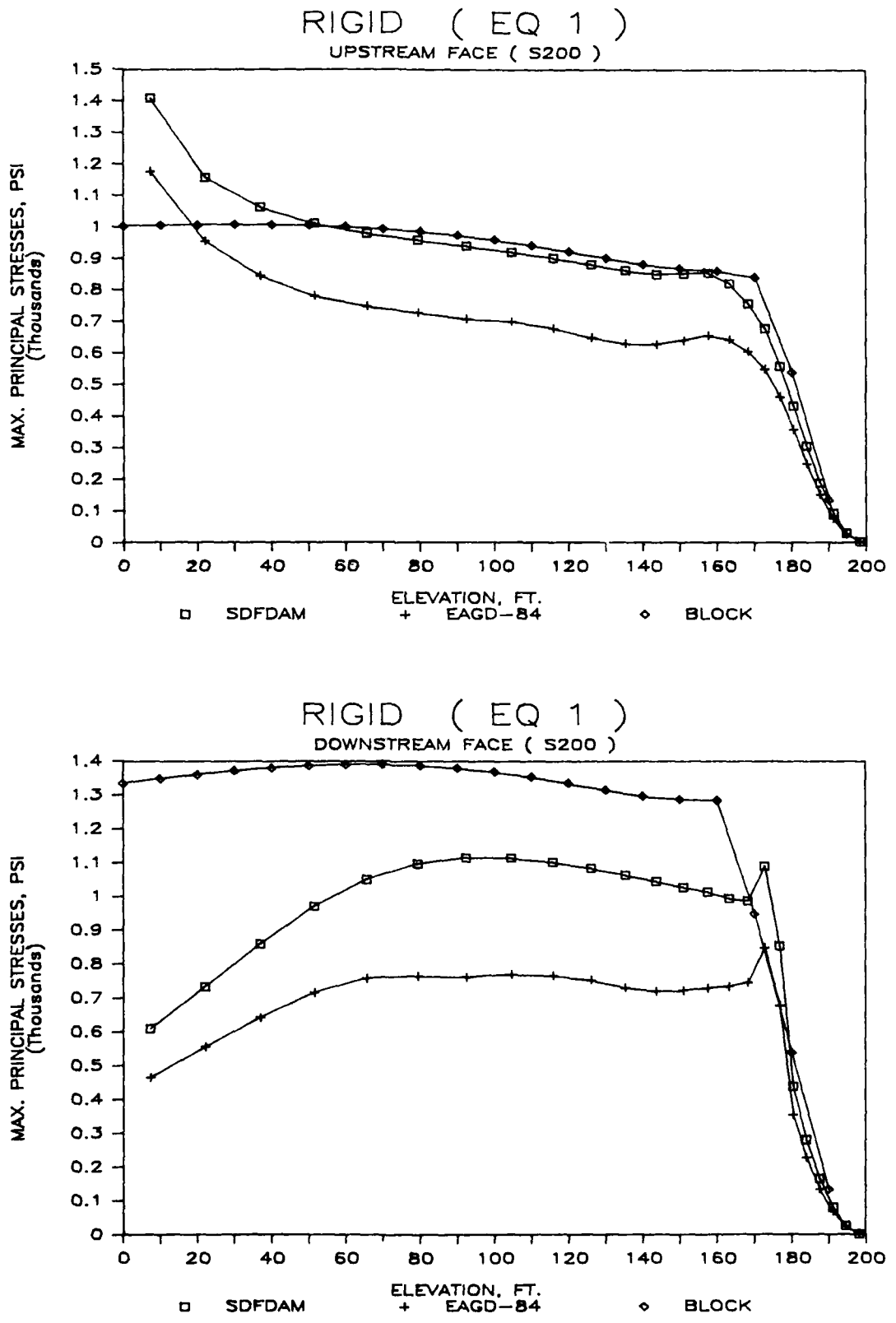

Figure 17. Effect of Foundation Modulus, E_f (Case 12)

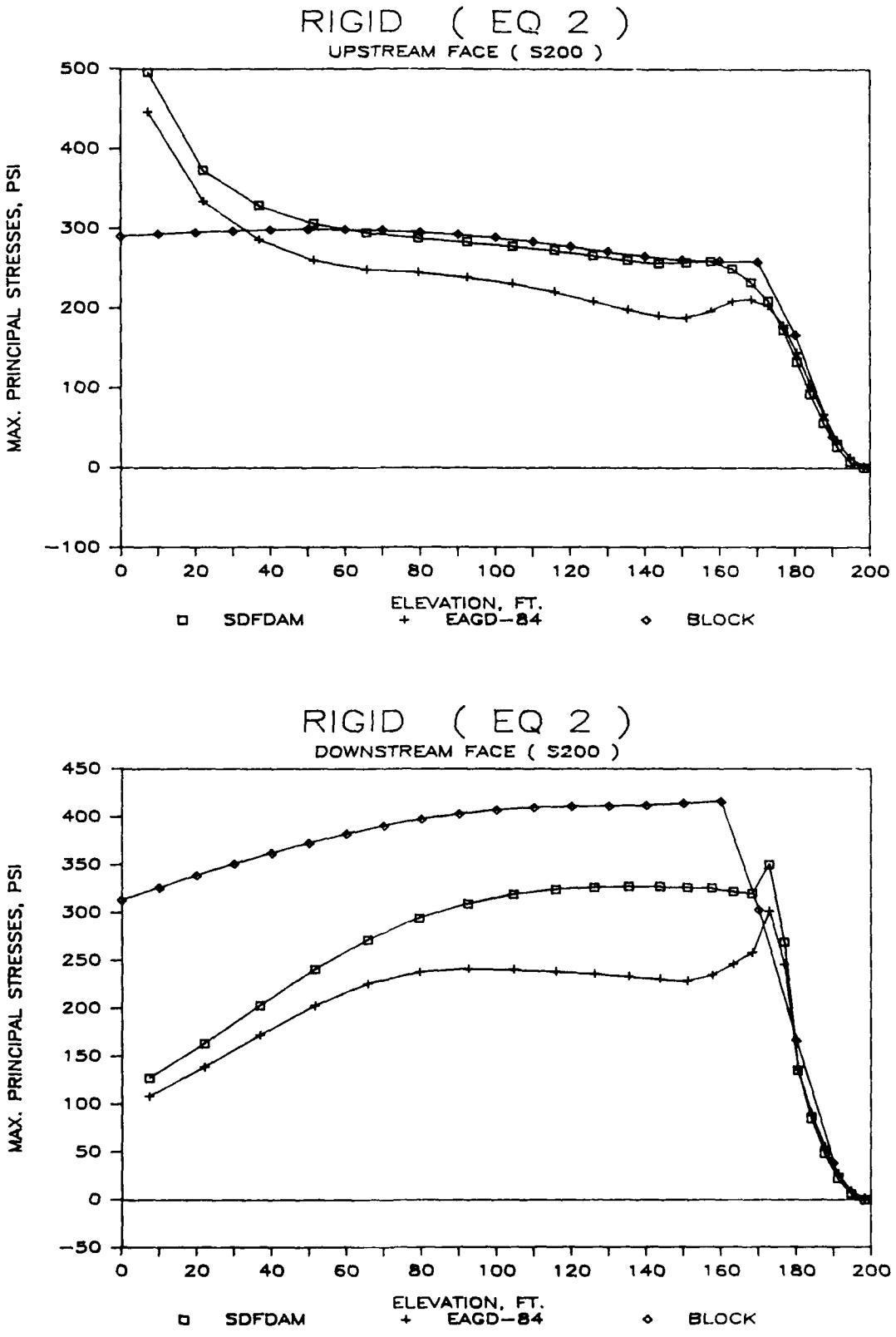

Figure 18. Effect of Foundation Modulus, E_f (Case 16)

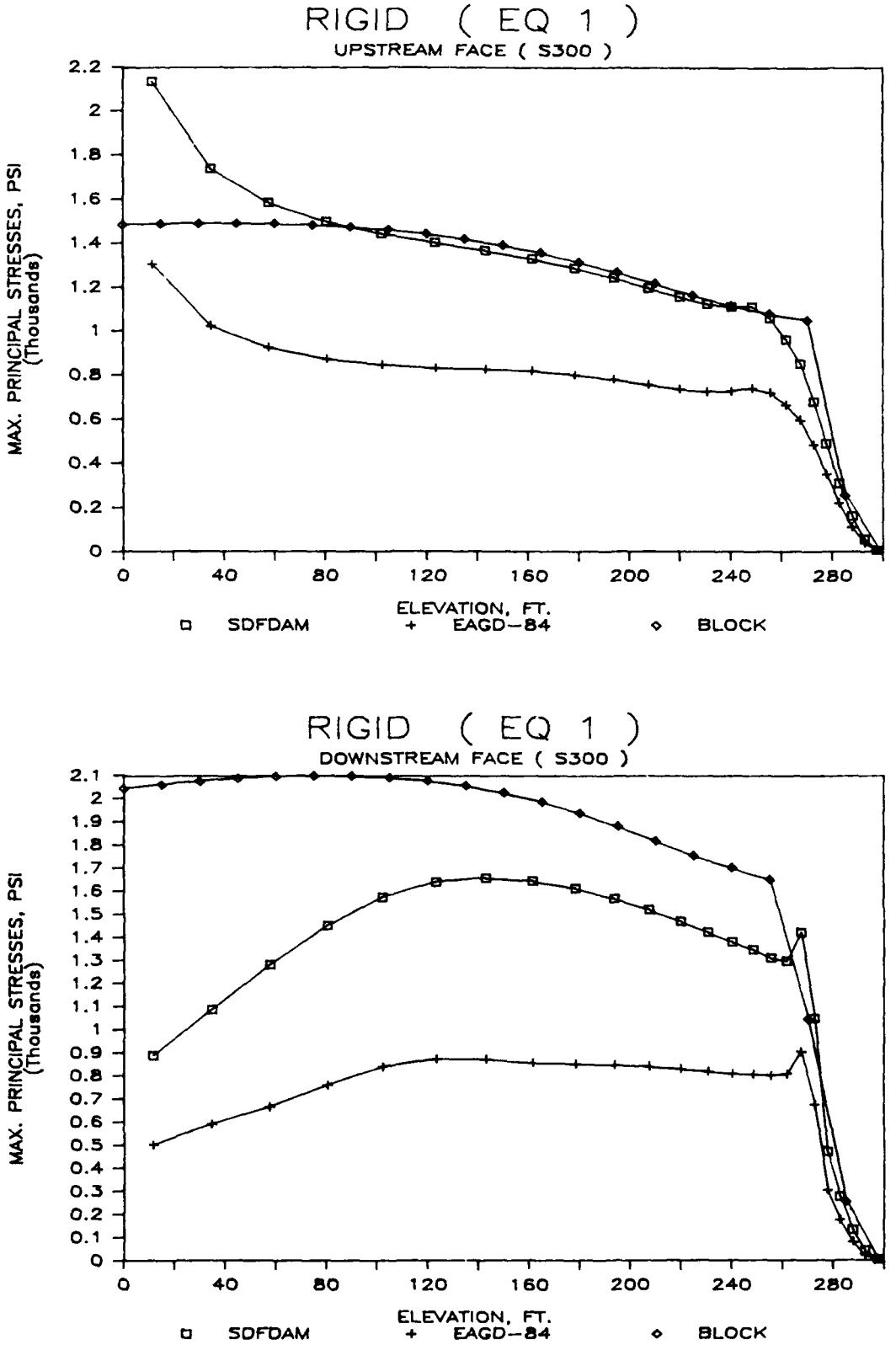

Figure 19. Effect of Foundation Modulus, E_f (Case 20)

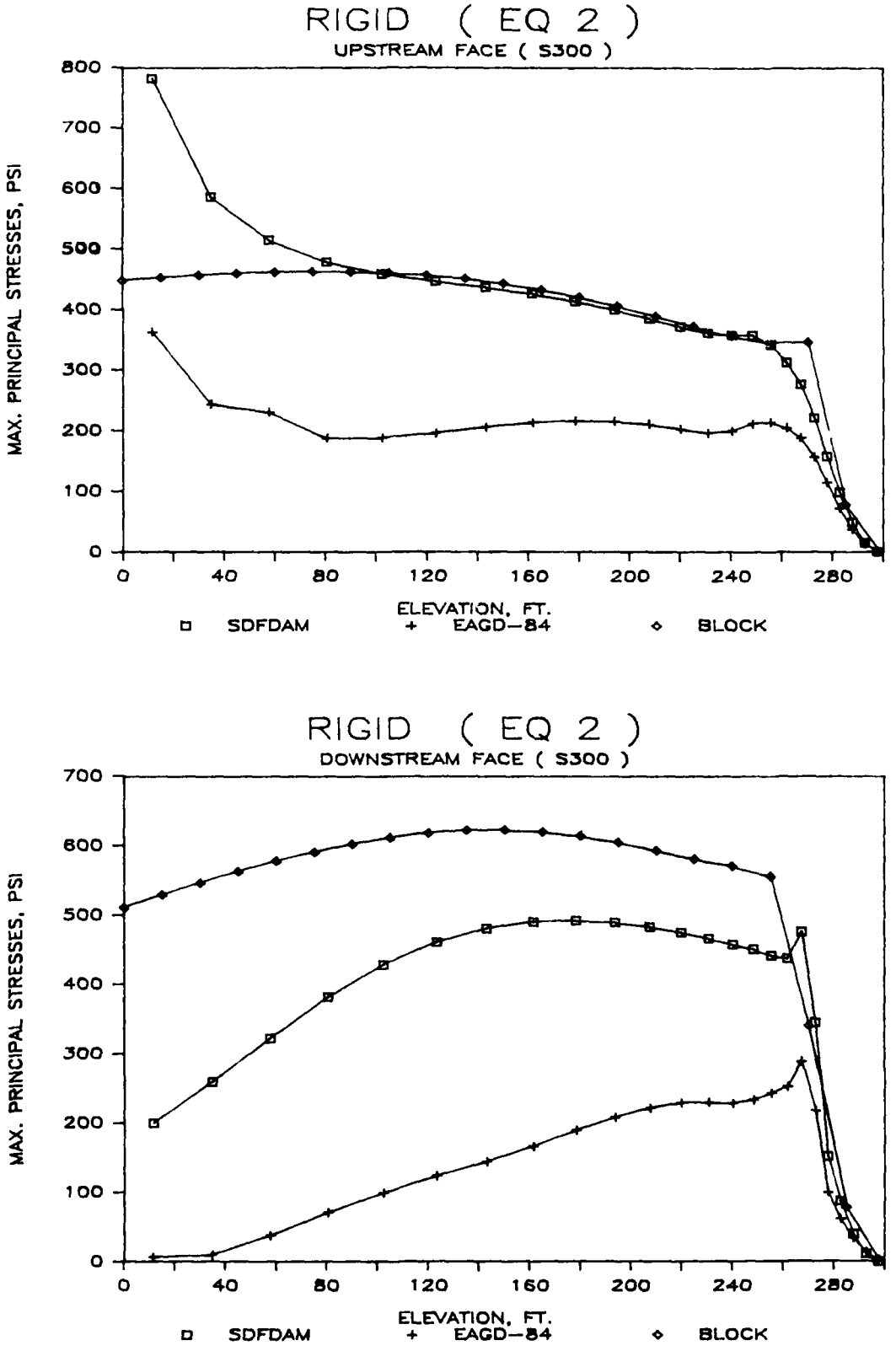

Figure 20. Effect of Foundation Modulus, E_f (Case 24)

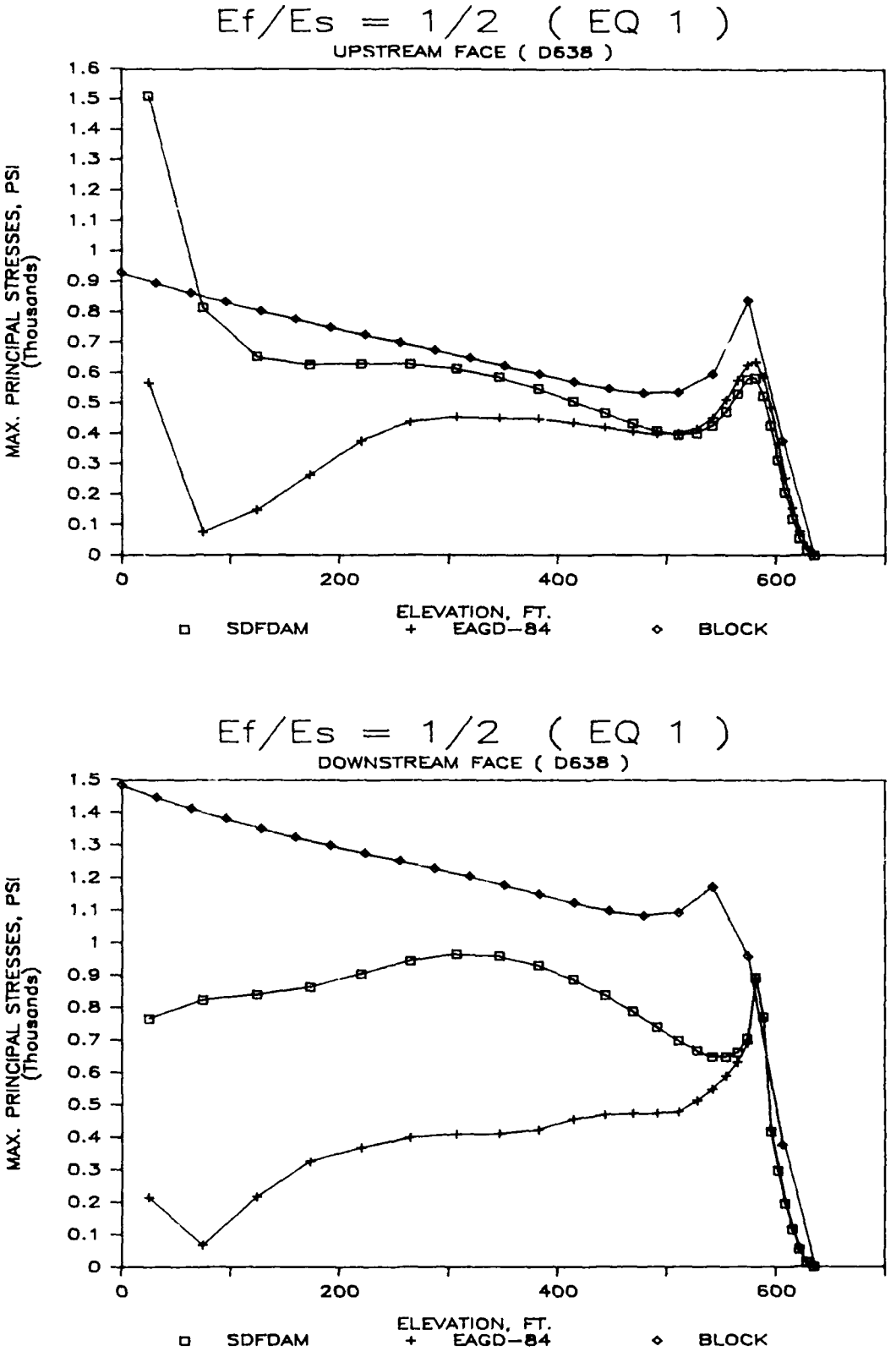

Figure 21. Effect of Foundation Modulus, E_f (Case 25)

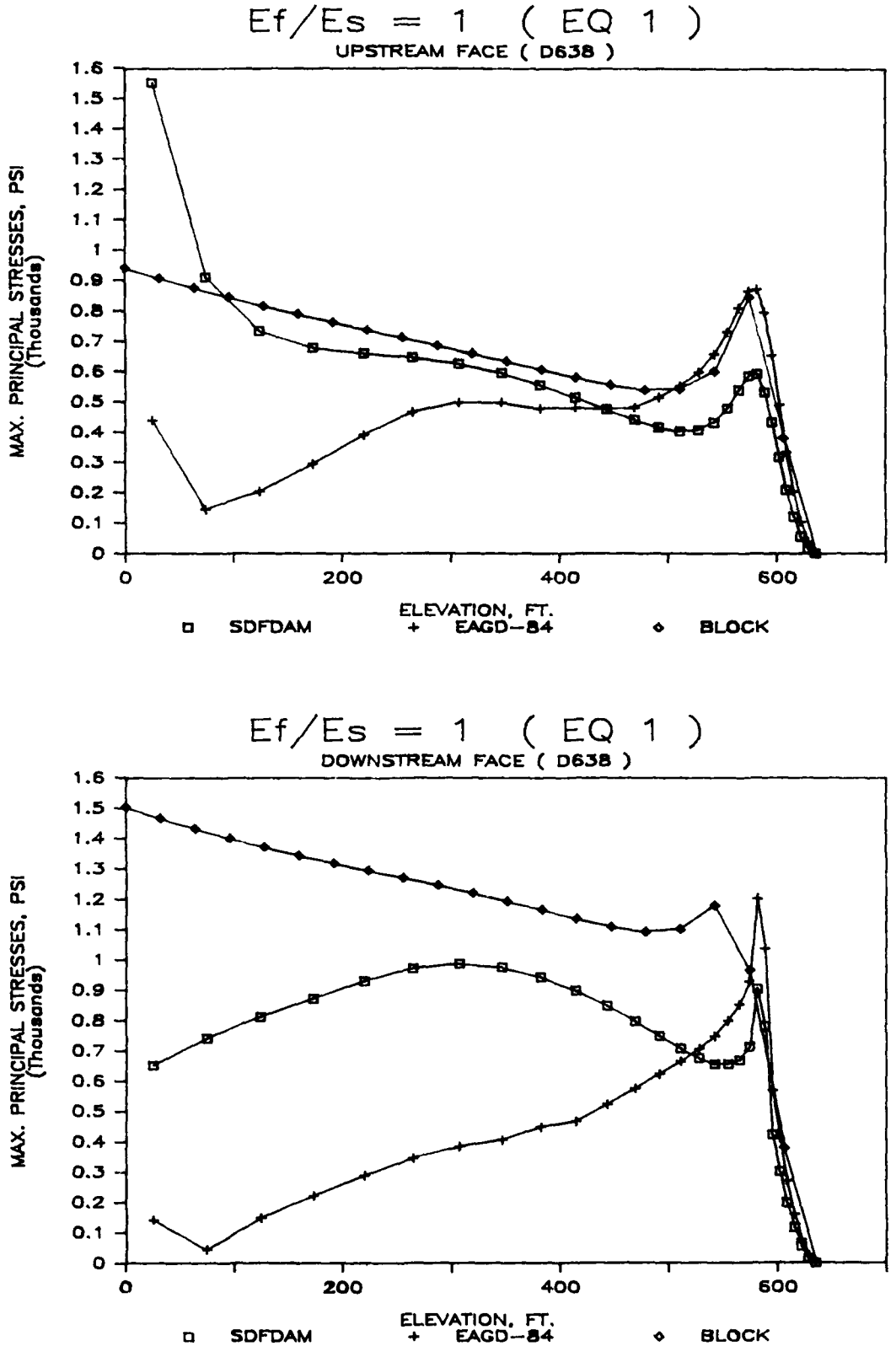

Figure 22. Effect of Foundation Modulus, E_f (Case 26)

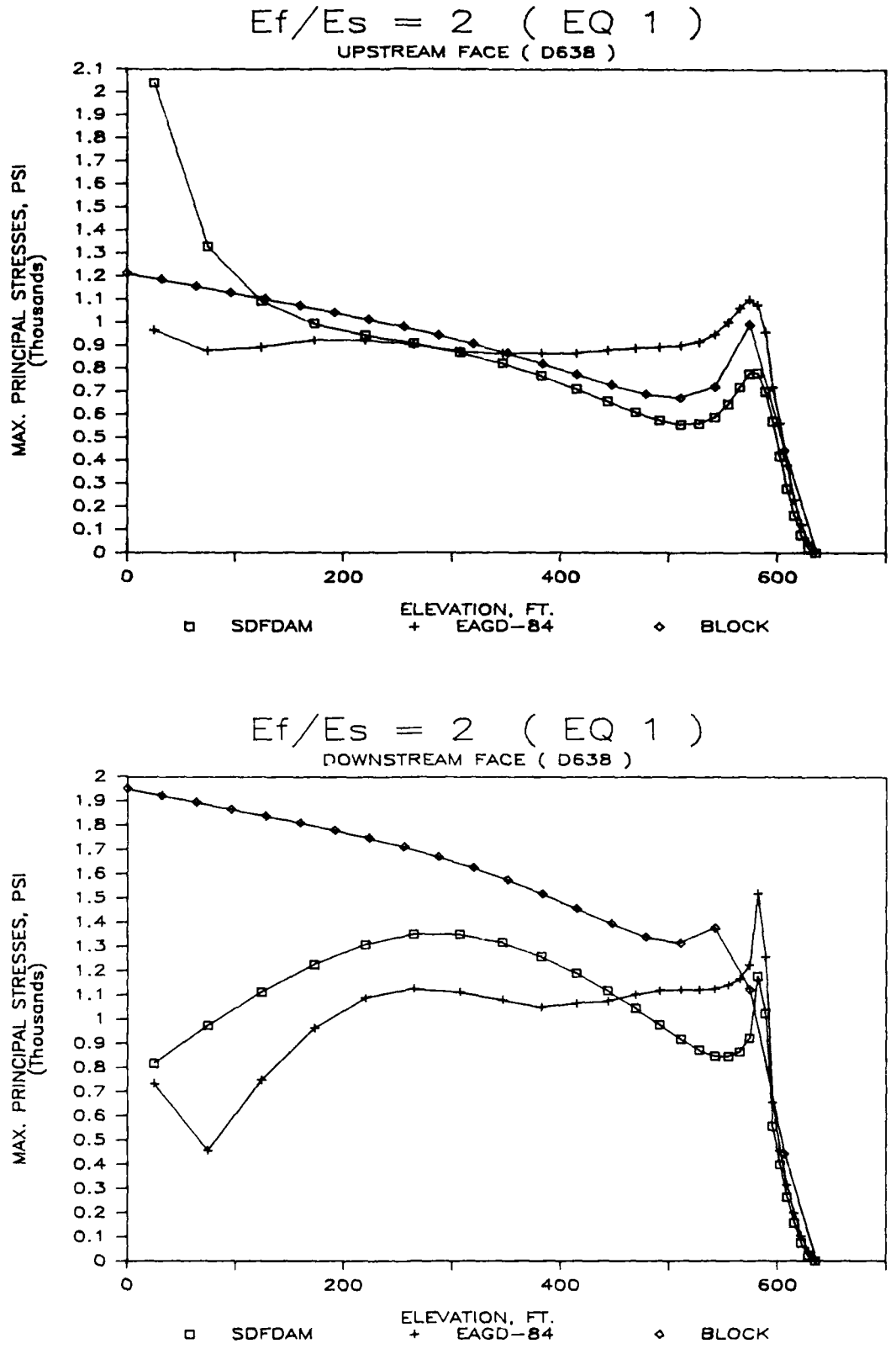

Figure 23. Effect of Foundation Modulus, E_f (Case 27)

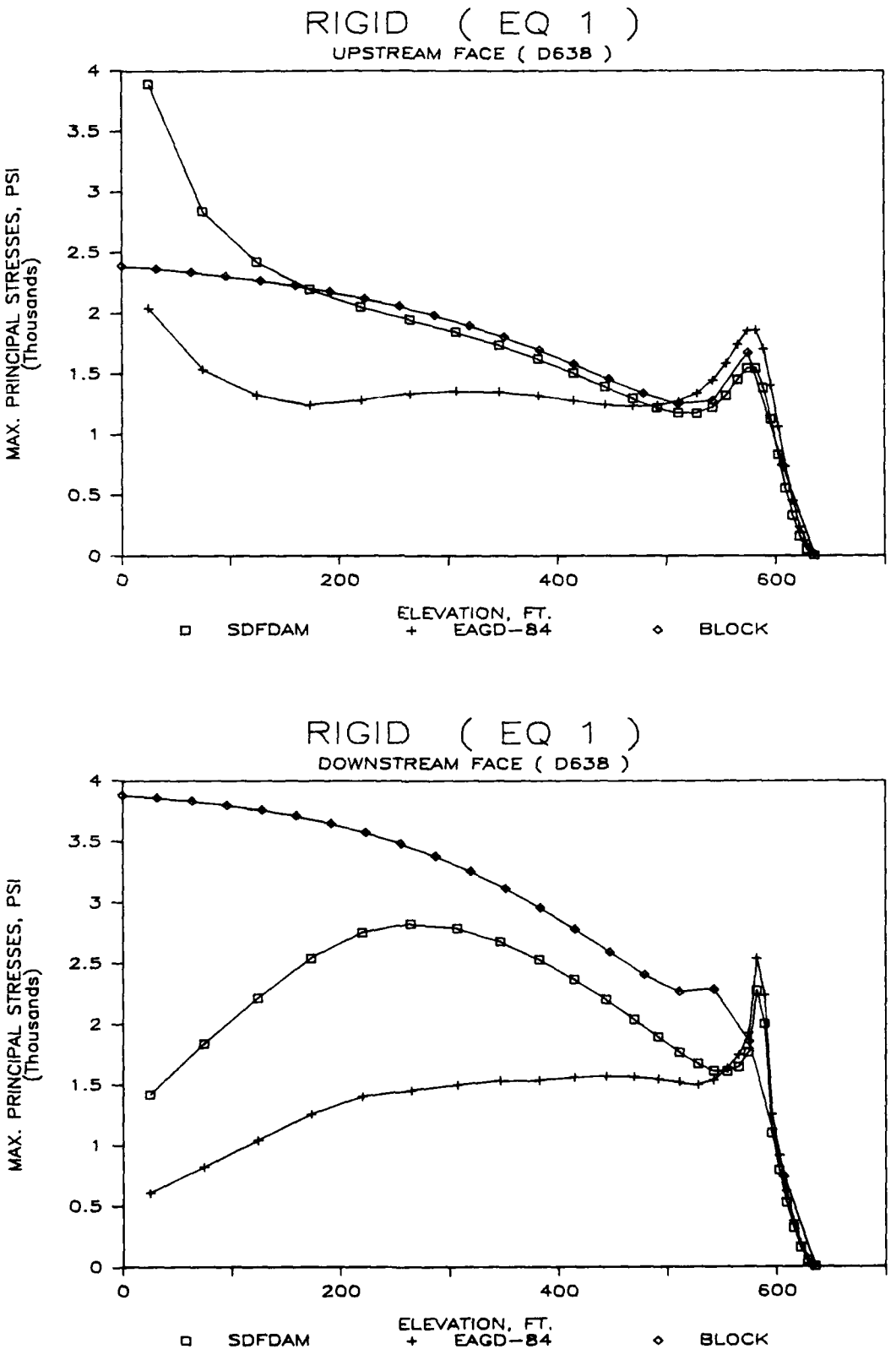

Figure 24. Effect of Foundation Modulus, E_f (Case 28)

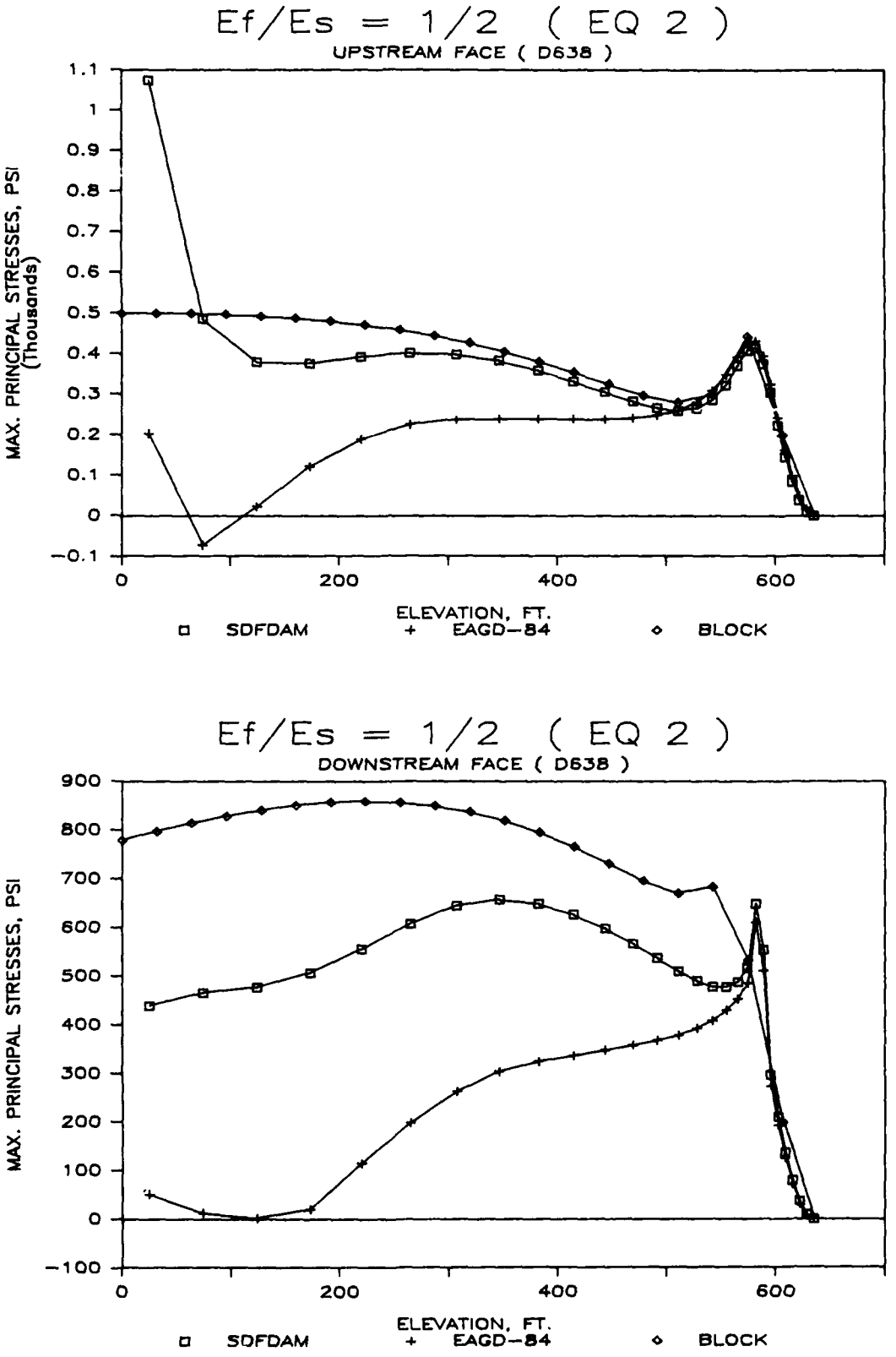

Figure 25. Effect of Foundation Modulus, E_f (Case 29)

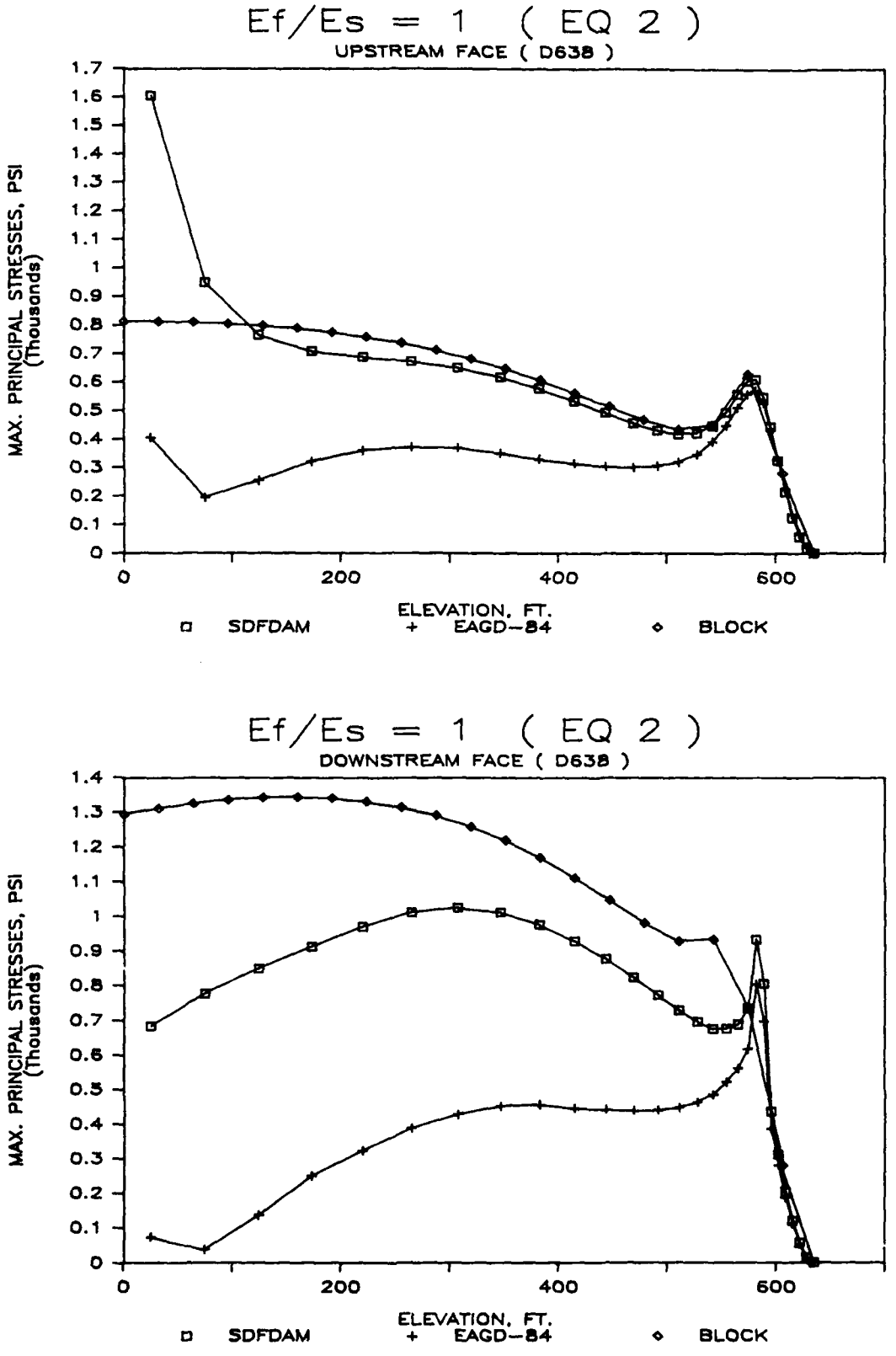

Figure 26. Effect of Foundation Modulus, E_f (Case 30)

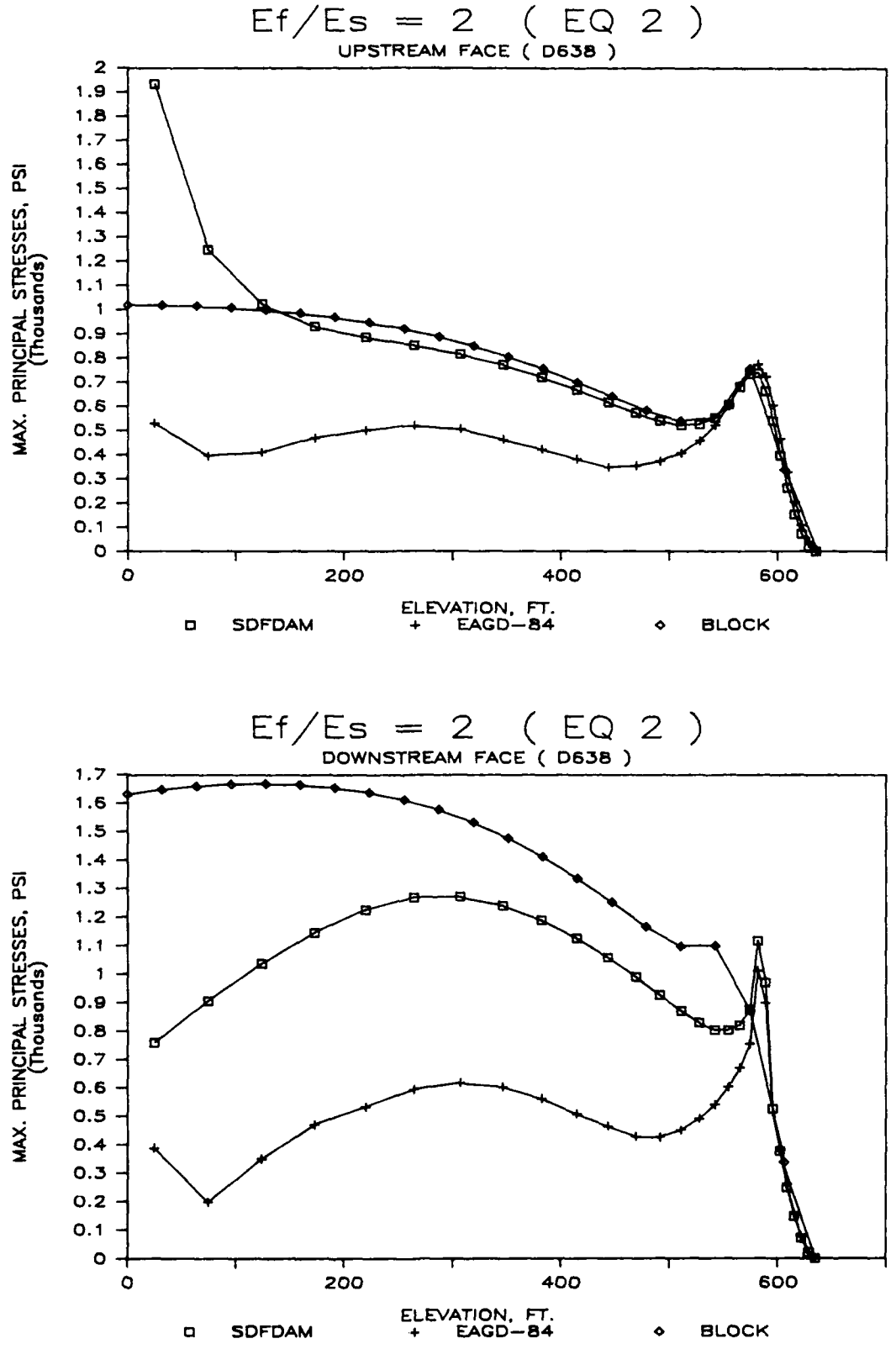

Figure 27. Effect of Foundation Modulus, E_f (Case 31)

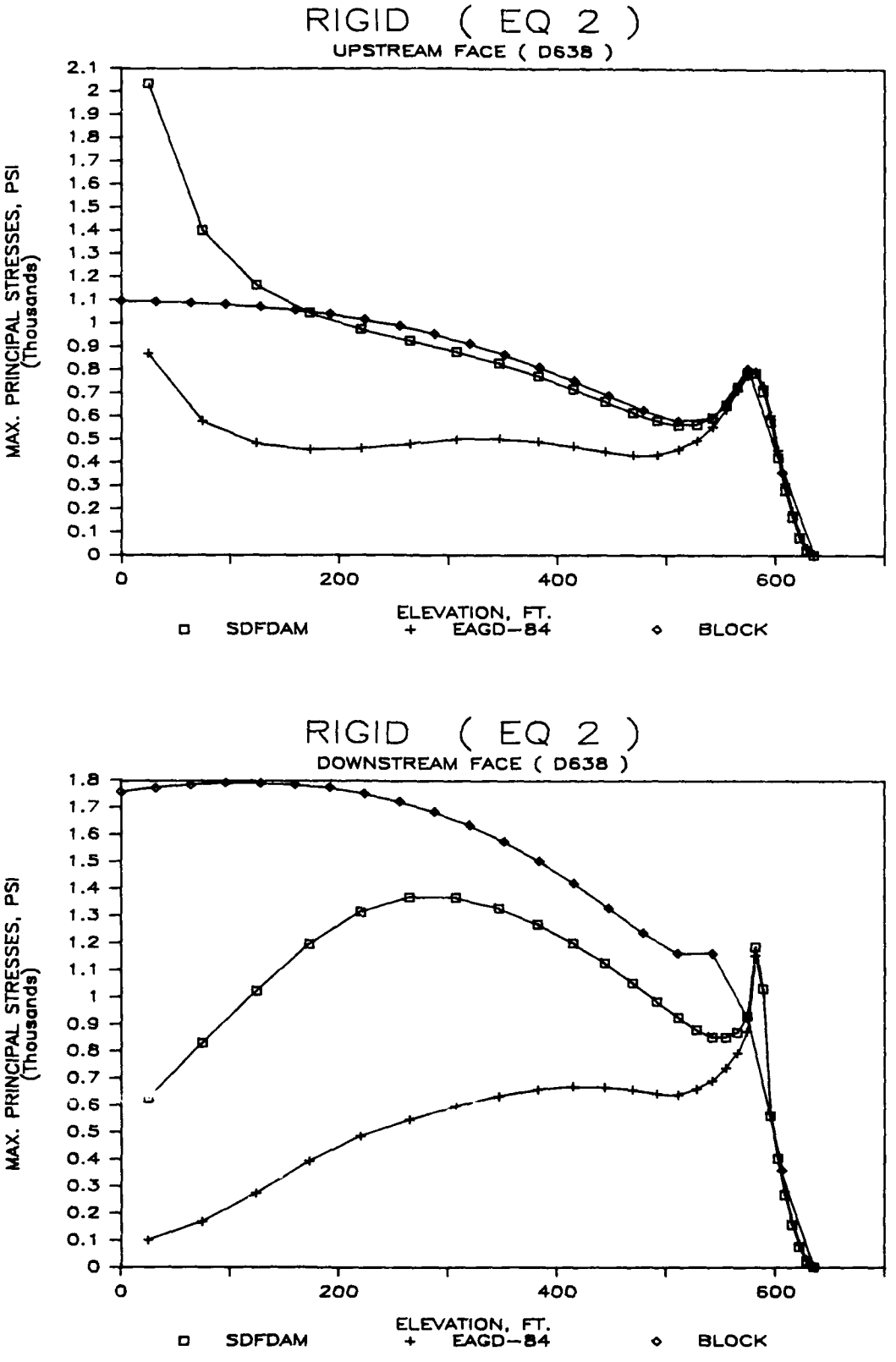

Figure 28. Effect of Foundation Modulus, E_f (Case 32)

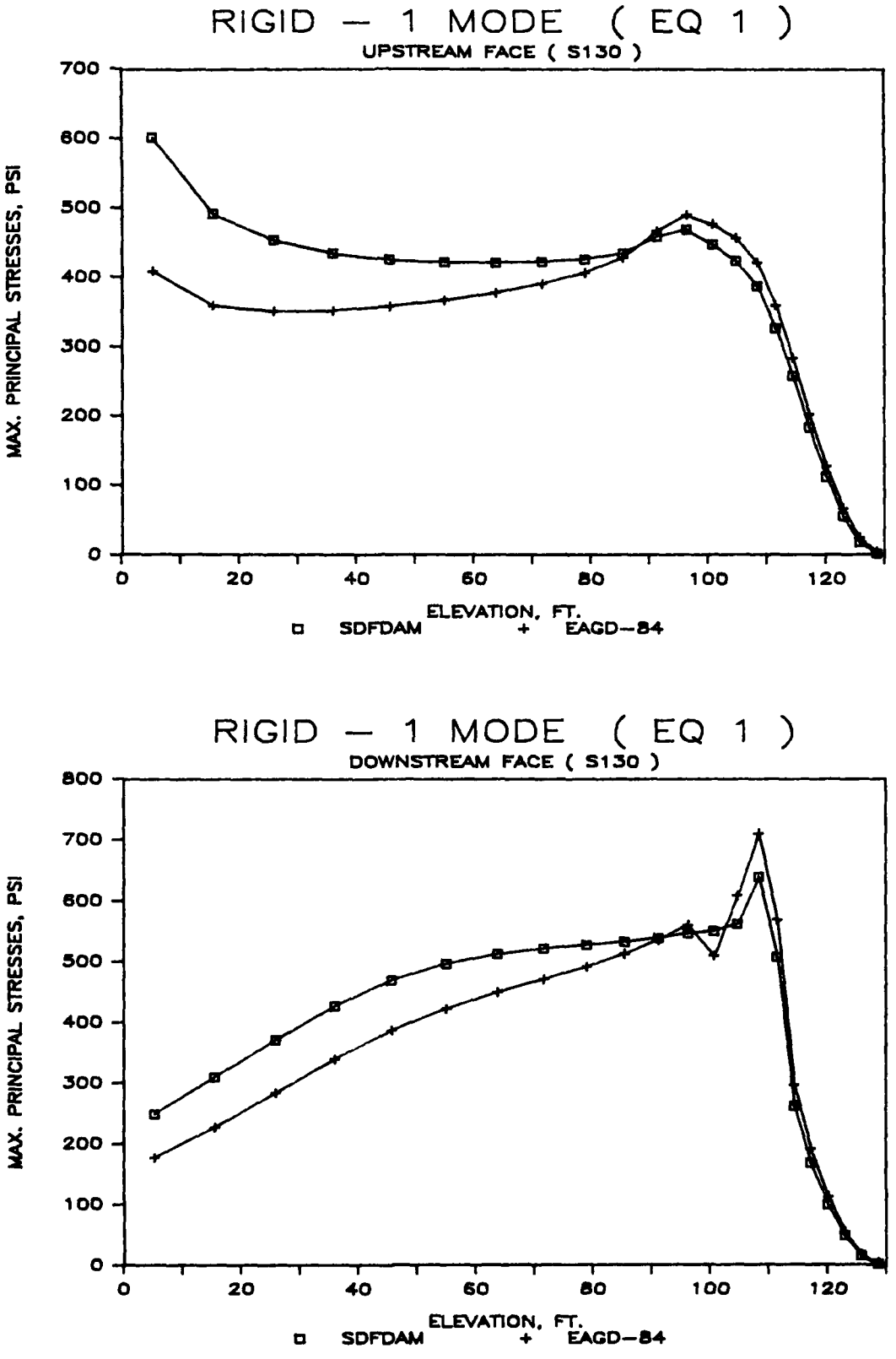

Figure 29. Comparison of Fundamental Mode Response of SDFDAM and EAGD-84 (Case 4)

7. APPENDIX

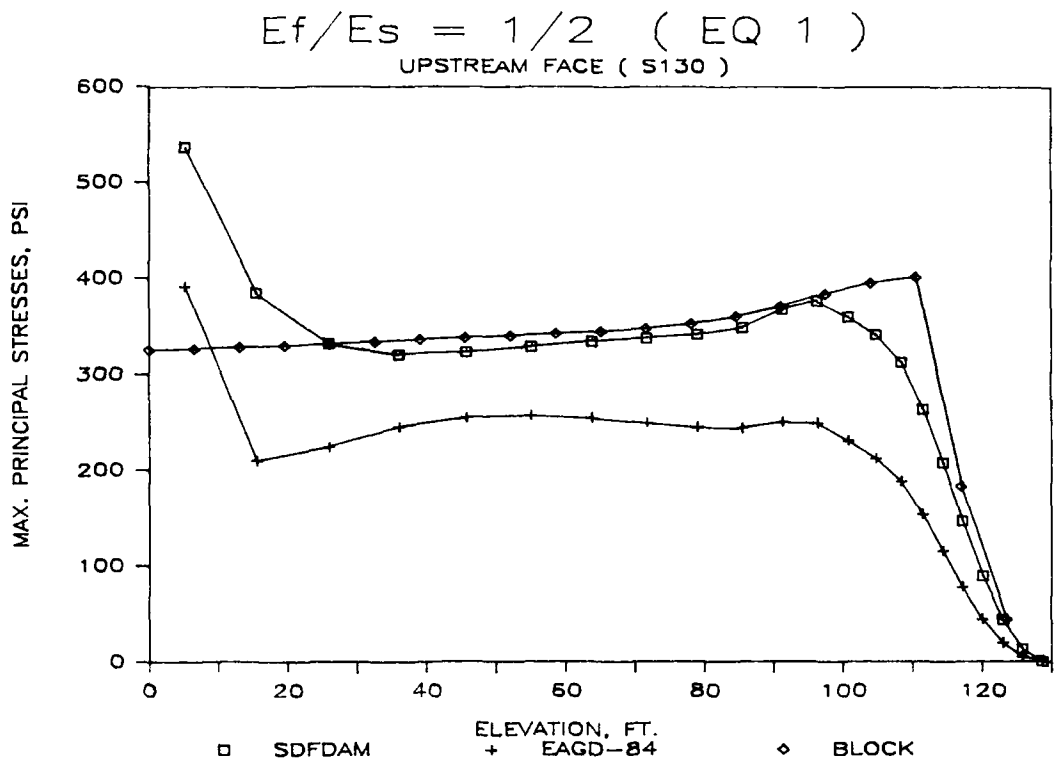
Ef/Es = 1/2 (EQ 1)
UPSTREAM FACE (S130)
MAX. PRINCIPAL STRESSES, PSI
600
500
400
300
200
100
0
0
20
40
60
80
100
120
ELEVATION, FT.
SDFDAM
EAGD-84
BLOCK

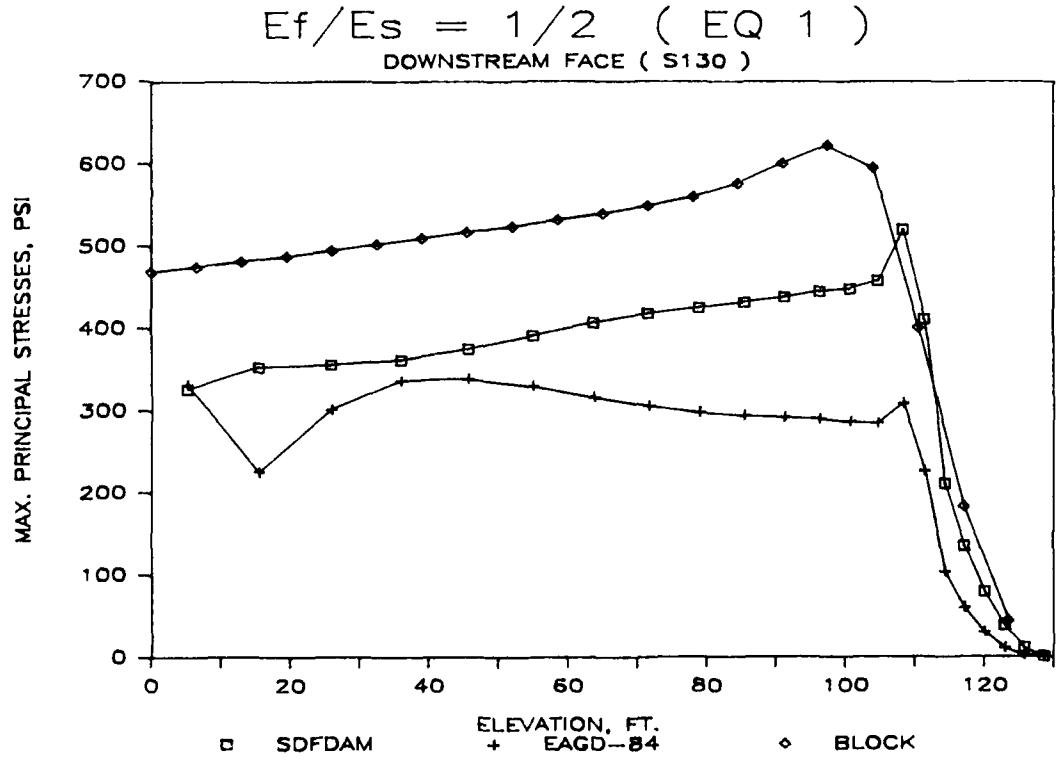
Ef/Es = 1/2 (EQ 1)
DOWNSTREAM FACE (S130)
MAX. PRINCIPAL STRESSES, PSI
700
600
500
400
300
200
100
0
0
20
40
60
80
100
120
ELEVATION, FT.
SDFDAM
EAGD-84
BLOCK

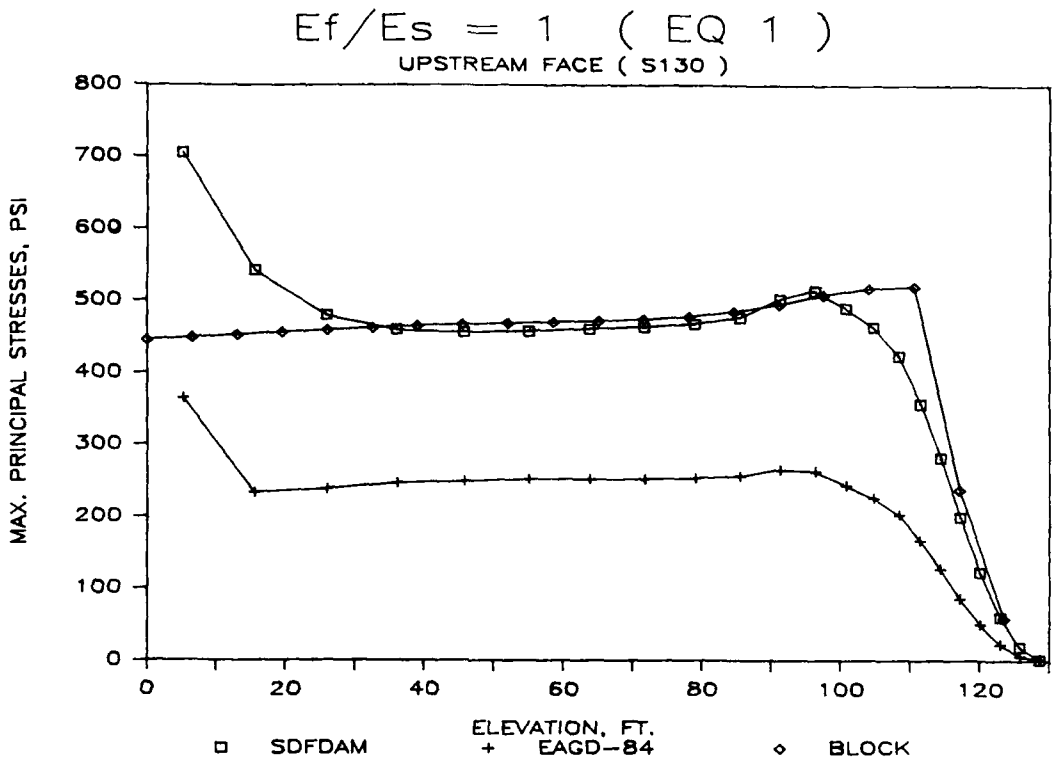
Ef/Es = 1 (EQ 1)
UPSTREAM FACE (S130)
MAX. PRINCIPAL STRESSES, PSI
800
700
600
500
400
300
200
100
0
0
20
40
60
80
100
120
ELEVATION, FT.
SDFDAM
EAGD-84
BLOCK

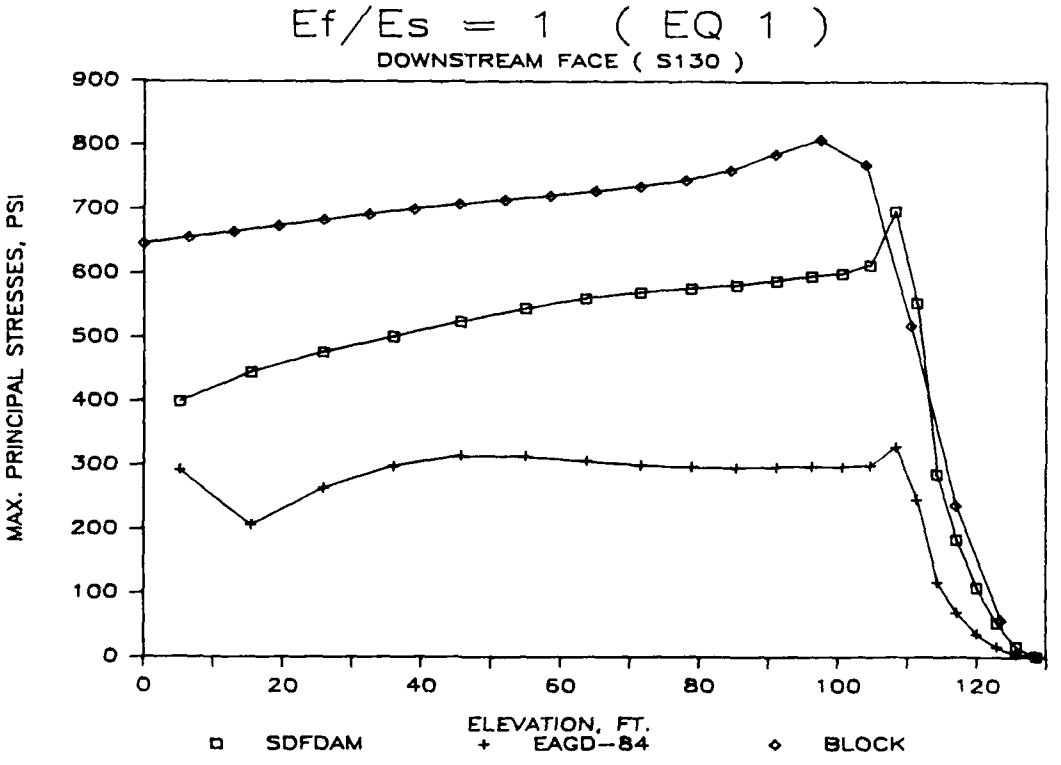
Ef/Es = 1 (EQ 1)
DOWNSTREAM FACE (S130)
MAX. PRINCIPAL STRESSES, PSI
900
800
700
600
500
400
300
200
100
0
0
20
40
60
80
100
120
ELEVATION, FT.
SDFDAM
EAGD-84
BLOCK

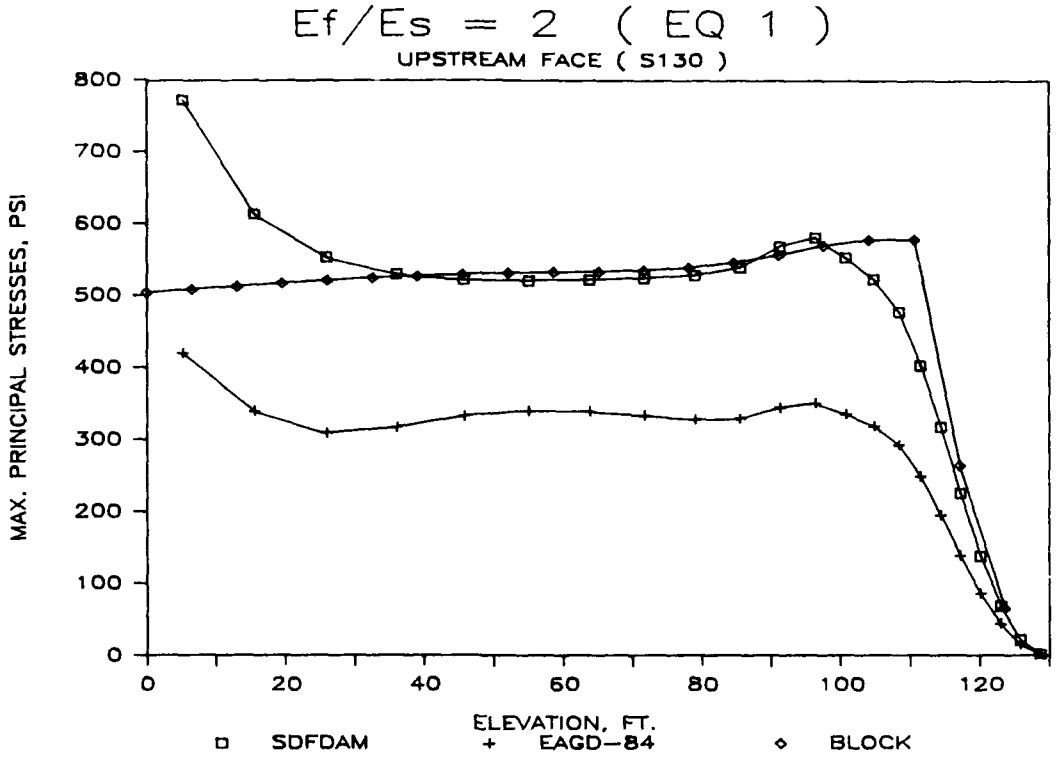
Ef/Es = 2 (EQ 1)
UPSTREAM FACE (S130)
MAX. PRINCIPAL STRESSES, PSI
800
700
600
500
400
300
200
100
0
0
20
40
60
80
100
120
ELEVATION, FT.
SDFDAM
EAGD-84
BLOCK

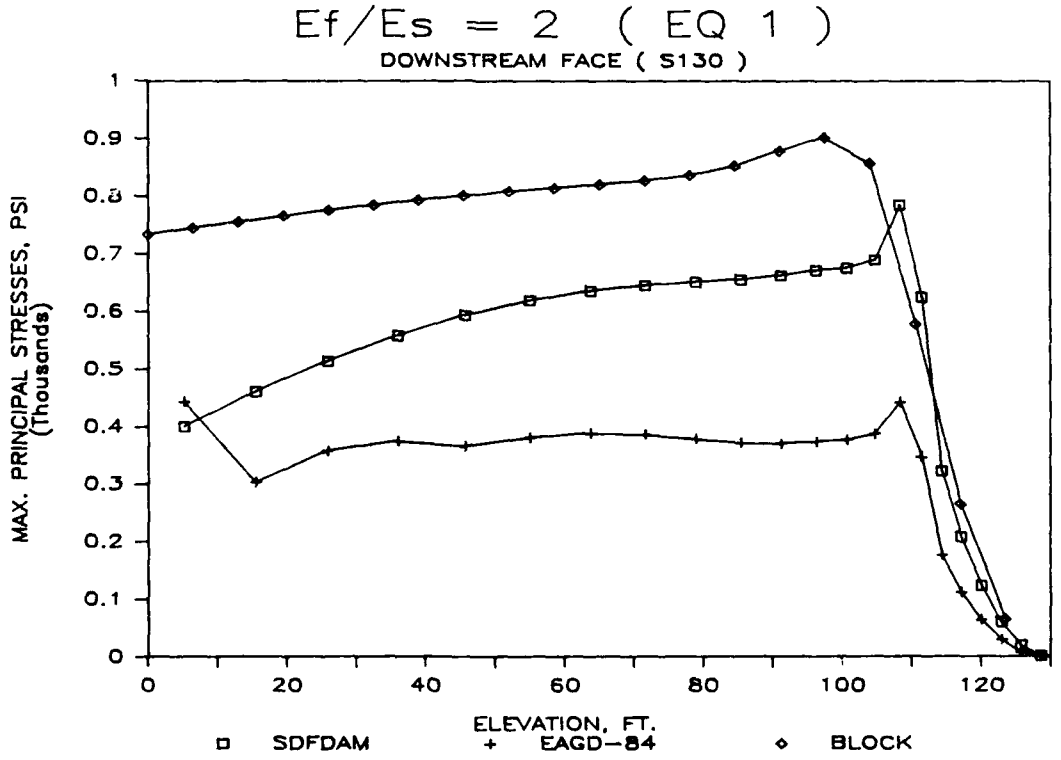
Ef/Es = 2 (EQ 1)
DOWNSTREAM FACE (S130)
MAX. PRINCIPAL STRESSES, PSI
(Thousands)
1
0.9
0.8
0.7
0.6
0.5
0.4
0.3
0.2
0.1
0
0
20
40
60
80
100
120
ELEVATION, FT.
SDFDAM
EAGD-84
BLOCK

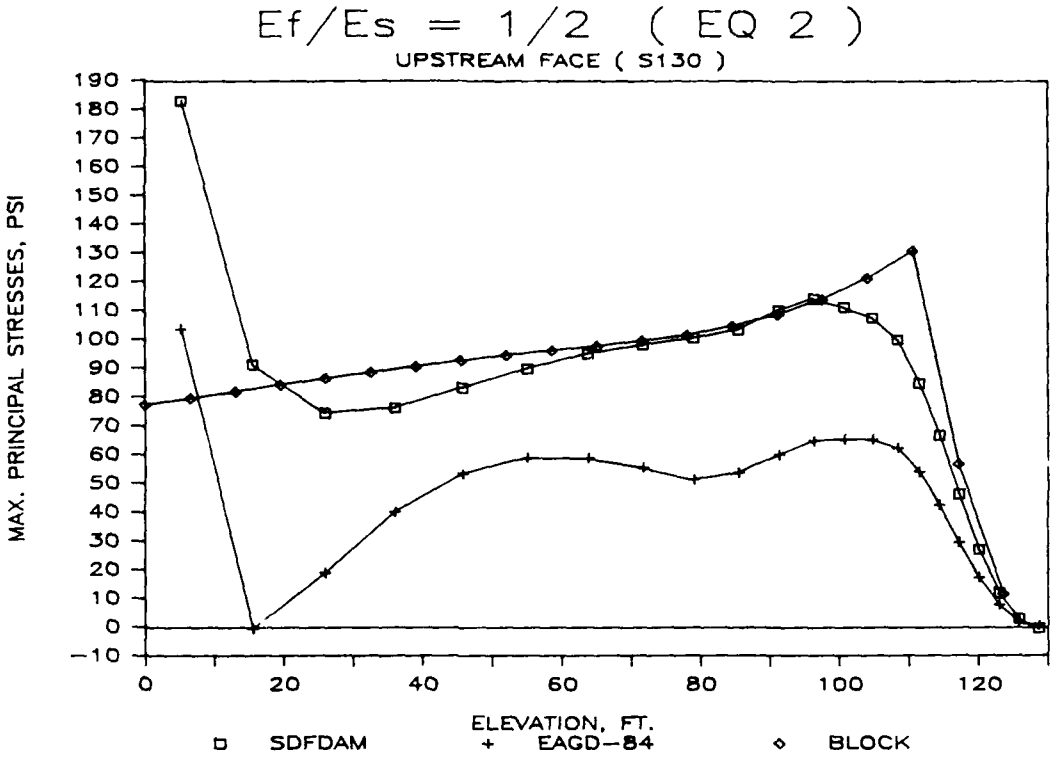
Ef/Es = 1/2 (EQ 2)
UPSTREAM FACE (S130)
MAX. PRINCIPAL STRESSES, PSI
190
180
170
160
150
140
130
120
110
100
90
80
70
60
50
40
30
20
10
0
-10
0
20
40
60
80
100
120
ELEVATION, FT.
SDFDAM
EAGD-84
BLOCK

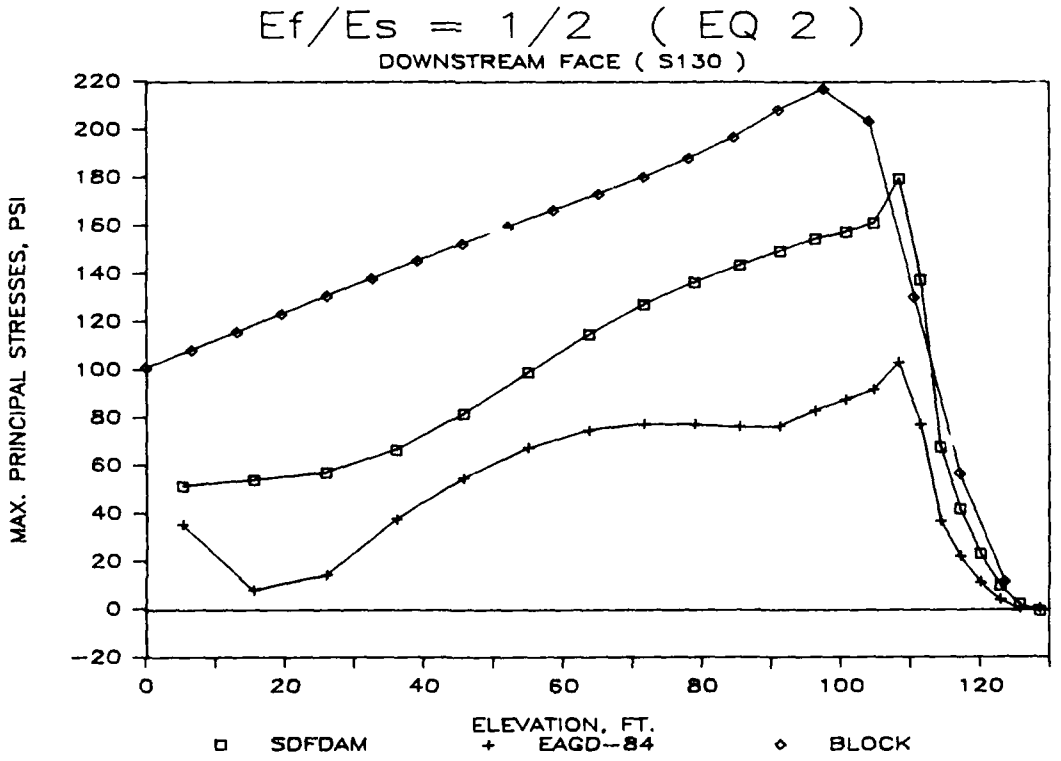
Ef/Es = 1/2 (EQ 2)
DOWNSTREAM FACE (S130)
MAX. PRINCIPAL STRESSES, PSI
220
200
180
160
140
120
100
80
60
40
20
0
-20
0
20
40
60
80
100
120
ELEVATION, FT.
SDFDAM
EAGD-84
BLOCK

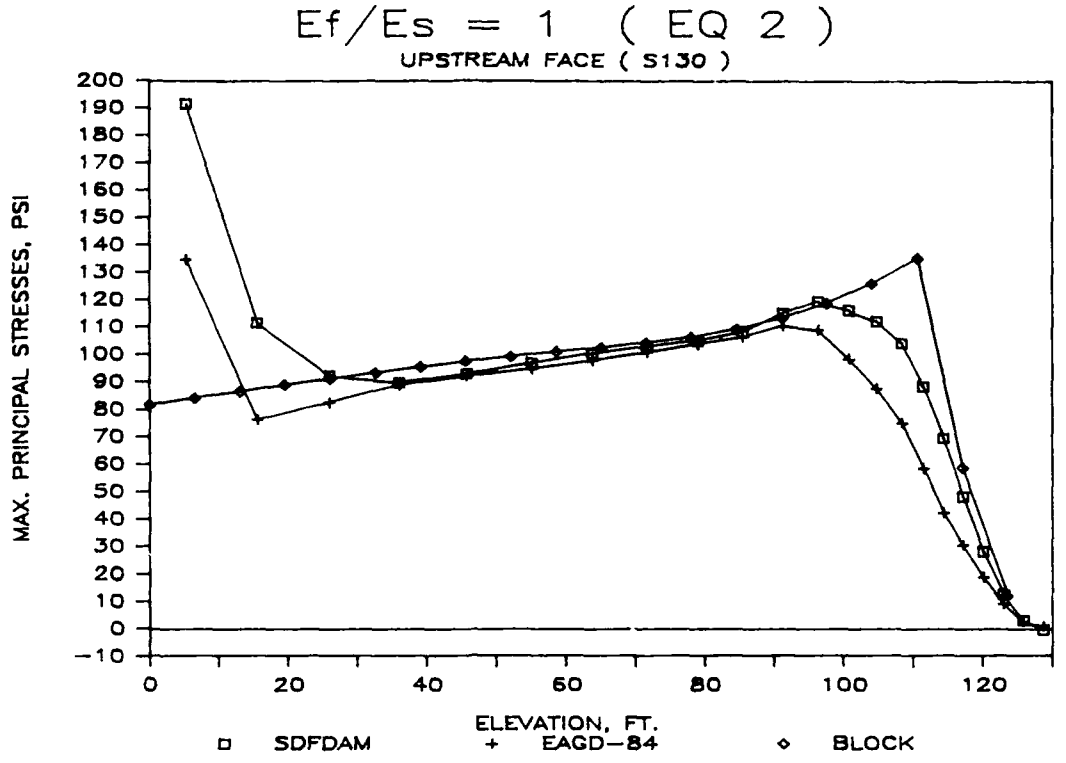
Ef/Es = 1 (EQ 2)
UPSTREAM FACE (S130)
MAX. PRINCIPAL STRESSES, PSI
200
190
180
170
160
150
140
130
120
110
100
90
80
70
60
50
40
30
20
10
0
−10
0
20
40
60
80
100
120
ELEVATION, FT.
SDFDAM
EAGD−84
BLOCK

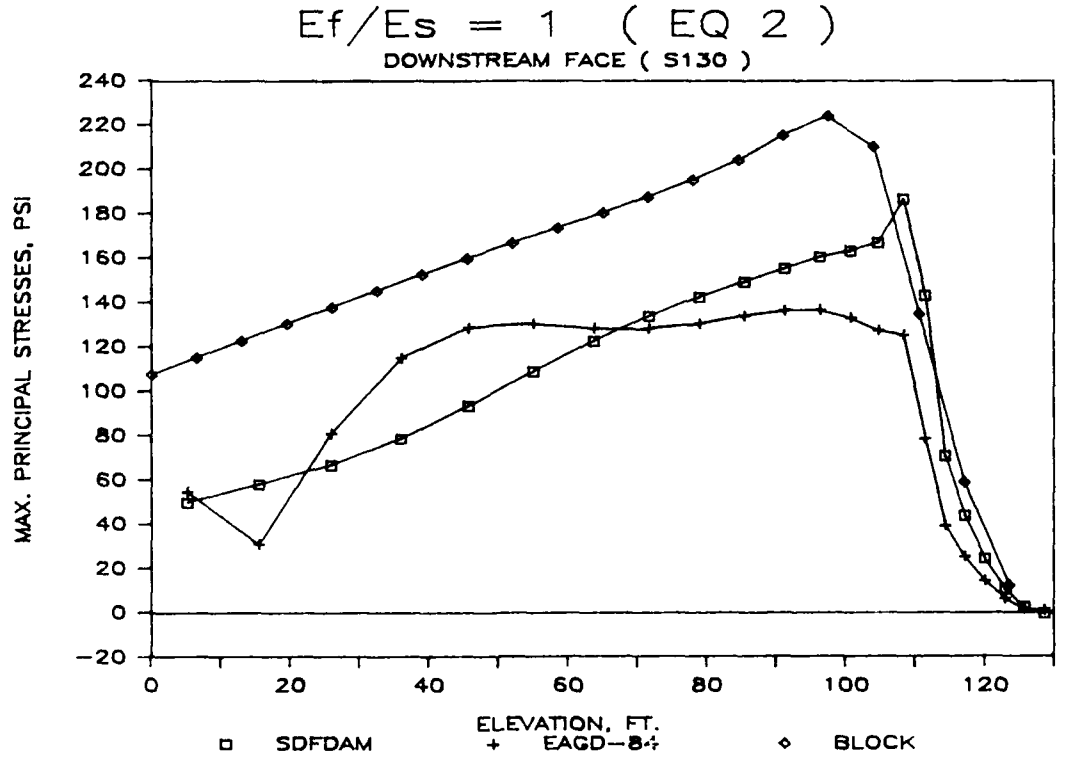
Ef/Es = 1 (EQ 2)
DOWNSTREAM FACE (S130)
MAX. PRINCIPAL STRESSES, PSI
240
220
200
180
160
140
120
100
80
60
40
20
0
−20
0
20
40
60
80
100
120
ELEVATION, FT.
SDFDAM
EAGD−84
BLOCK

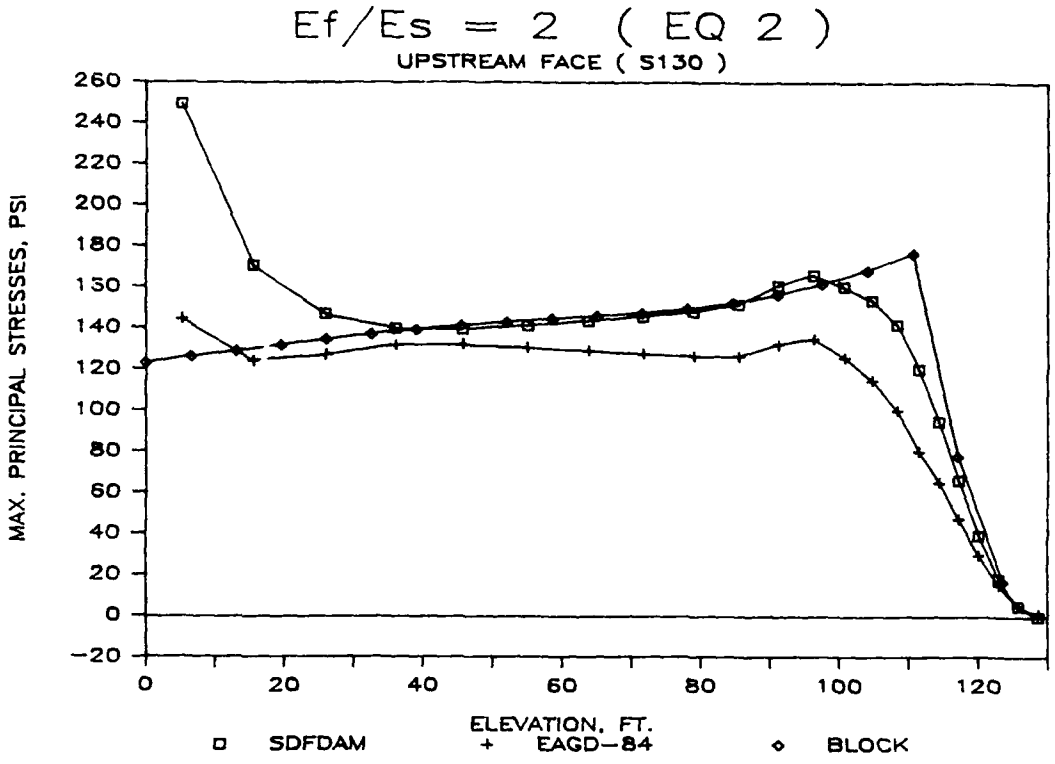
Ef/Es = 2 (EQ 2)
UPSTREAM FACE (S130)
MAX. PRINCIPAL STRESSES, PSI
260
240
220
200
180
130
140
120
100
80
60
40
20
0
-20
0
20
40
60
80
100
120
ELEVATION, FT.
SDFDAM
EAGD-84
BLOCK

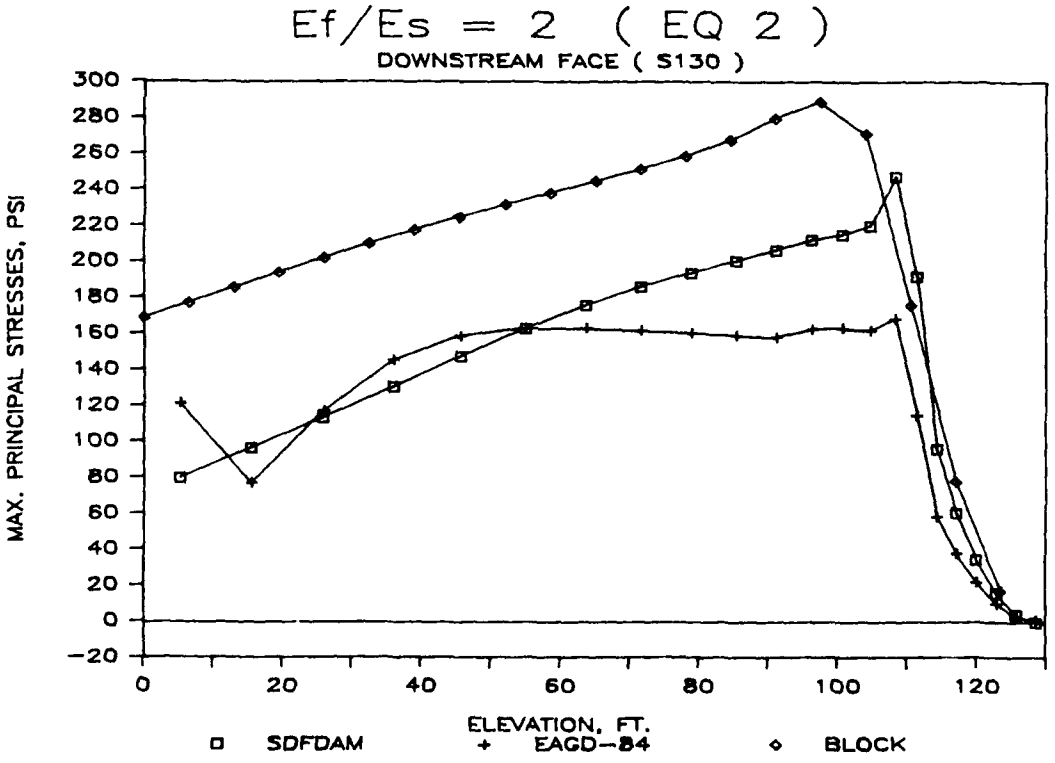
Ef/Es = 2 (EQ 2)
DOWNSTREAM FACE (S130)
MAX. PRINCIPAL STRESSES, PSI
300
280
260
240
220
200
180
160
140
120
100
80
60
40
20
0
-20
0
20
40
60
80
100
120
ELEVATION, FT.
SDFDAM
EAGD-84
BLOCK

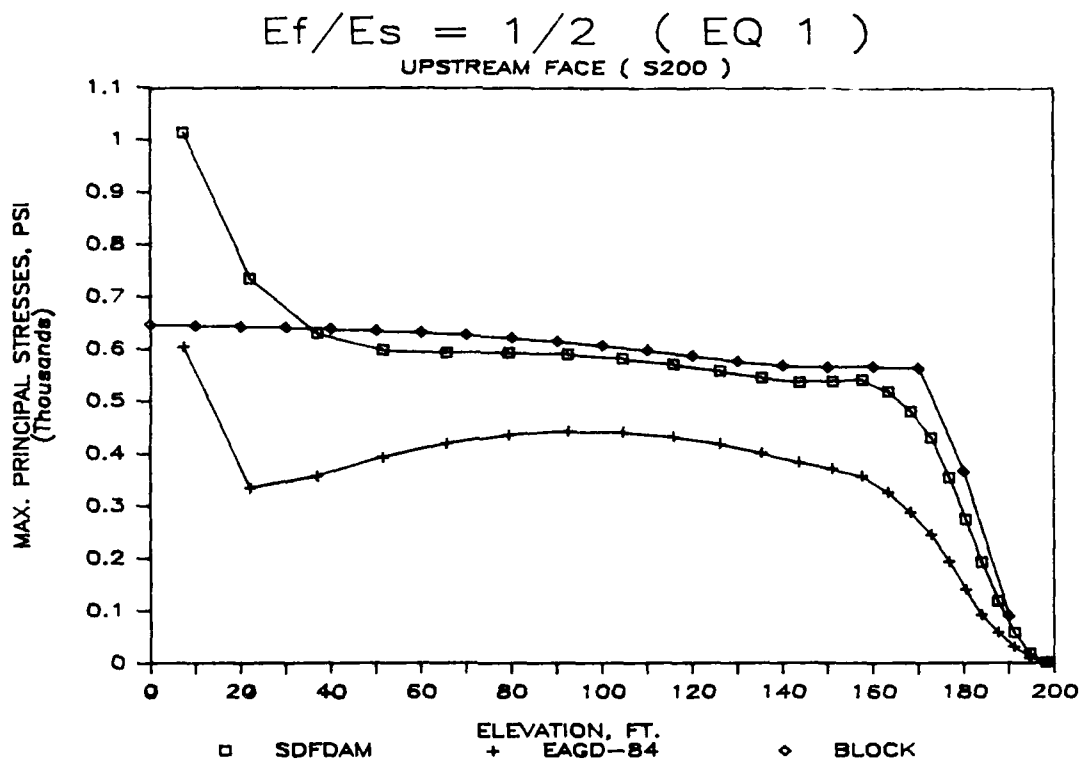
Ef/Es = 1/2 (EQ 1)
UPSTREAM FACE (S200)
MAX. PRINCIPAL STRESSES, PSI
(Thousands)
1.1
1
0.9
0.8
0.7
0.6
0.5
0.4
0.3
0.2
0.1
0
0
20
40
60
80
100
120
140
160
180
200
ELEVATION, FT.
SDFDAM
EAGD-84
BLOCK

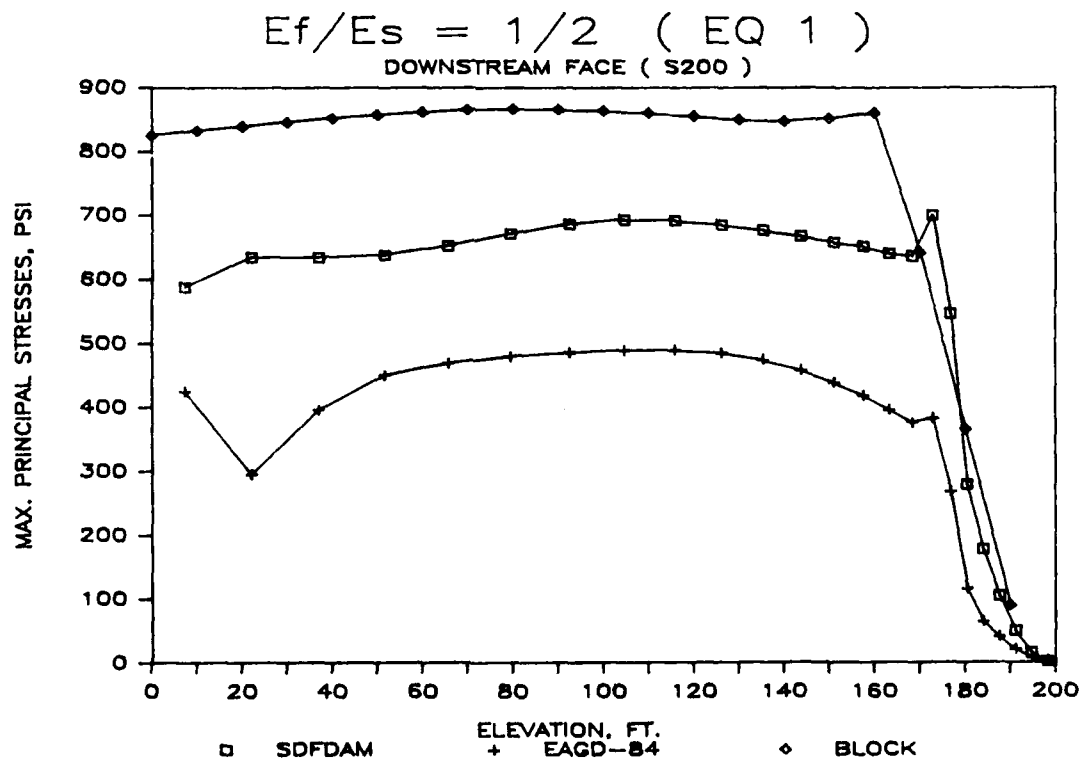
Ef/Es = 1/2 (EQ 1)
DOWNSTREAM FACE (S200)
MAX. PRINCIPAL STRESSES, PSI
900
800
700
600
500
400
300
200
100
0
0
20
40
60
80
100
120
140
160
180
200
ELEVATION, FT.
SDFDAM
EAGD-84
BLOCK

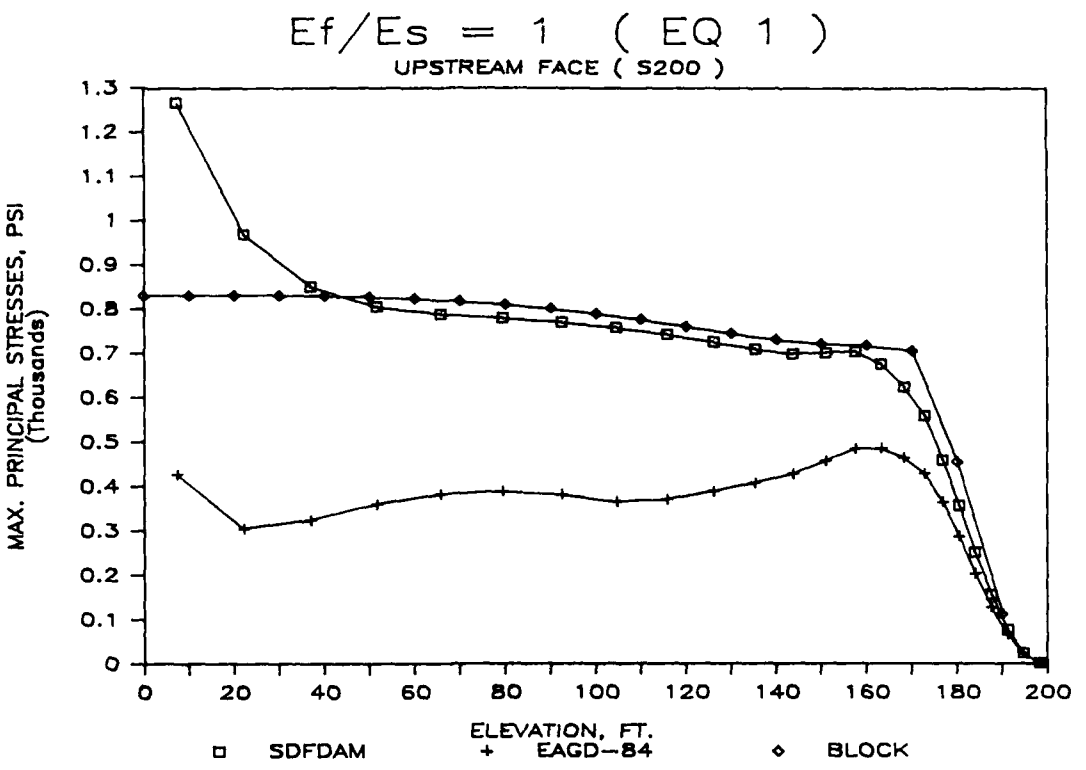
Ef/Es = 1 (EQ 1)
UPSTREAM FACE (S200)
MAX. PRINCIPAL STRESSES, PSI (Thousands)
1.3
1.2
1.1
1
0.9
0.8
0.7
0.6
0.5
0.4
0.3
0.2
0.1
0
0 20 40 60 80 100 120 140 160 180 200
ELEVATION, FT.
SDFDAM
EAGD-84
BLOCK

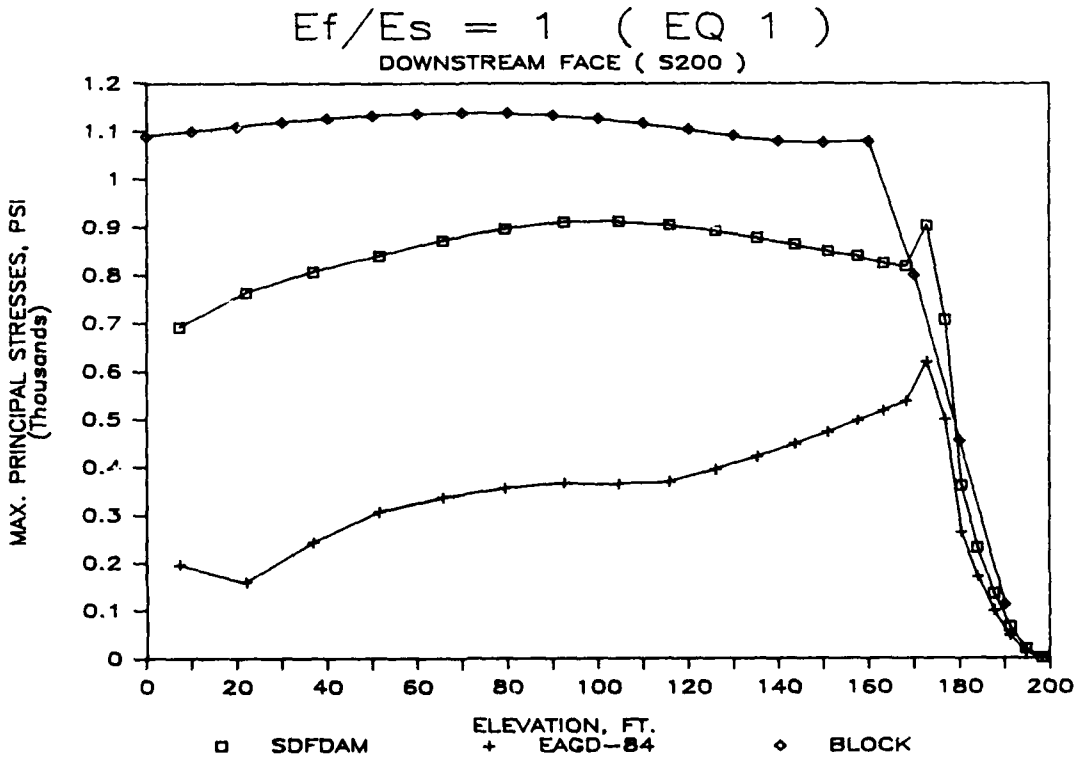
Ef/Es = 1 (EQ 1)
DOWNSTREAM FACE (S200)
MAX. PRINCIPAL STRESSES, PSI (Thousands)
1.2
1.1
1
0.9
0.8
0.7
0.6
0.5
0.4
0.3
0.2
0.1
0
0 20 40 60 80 100 120 140 160 180 200
ELEVATION, FT.
SDFDAM
EAGD-84
BLOCK

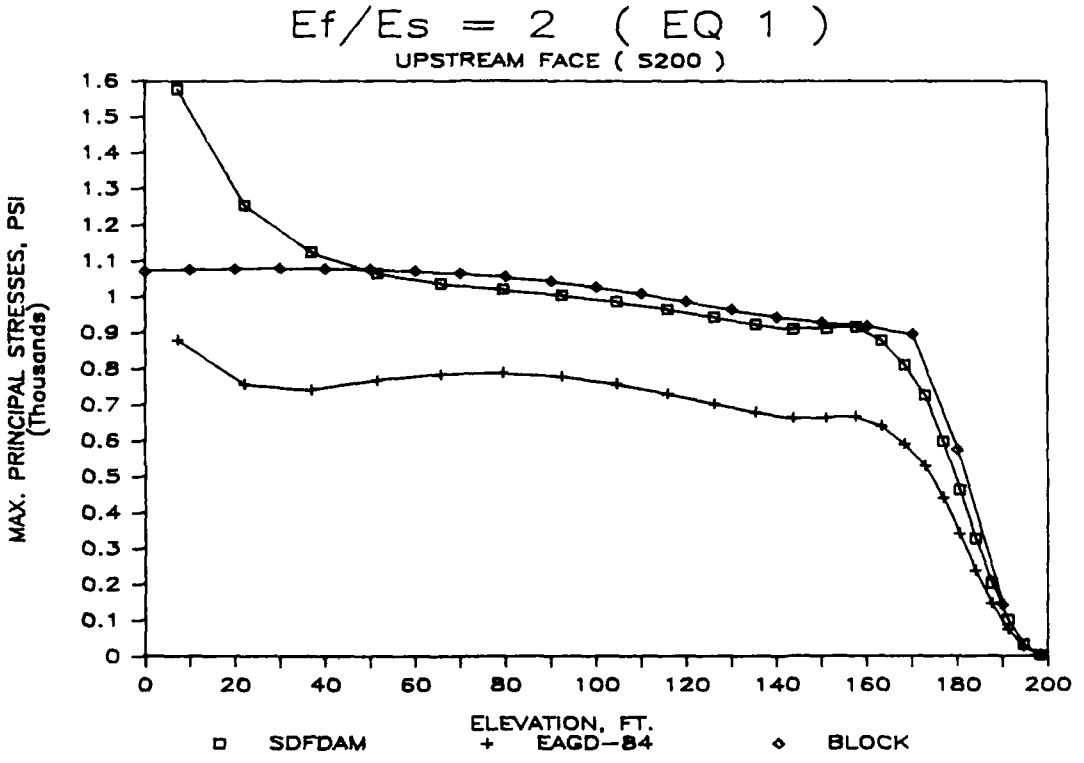
Ef/Es = 2 (EQ 1)
UPSTREAM FACE (S200)
MAX. PRINCIPAL STRESSES, PSI (Thousands)
1.6
1.5
1.4
1.3
1.2
1.1
1
0.9
0.8
0.7
0.6
0.5
0.4
0.3
0.2
0.1
0
0 20 40 60 80 100 120 140 160 180 200
ELEVATION, FT.
SDFDAM
EAGD-84
BLOCK

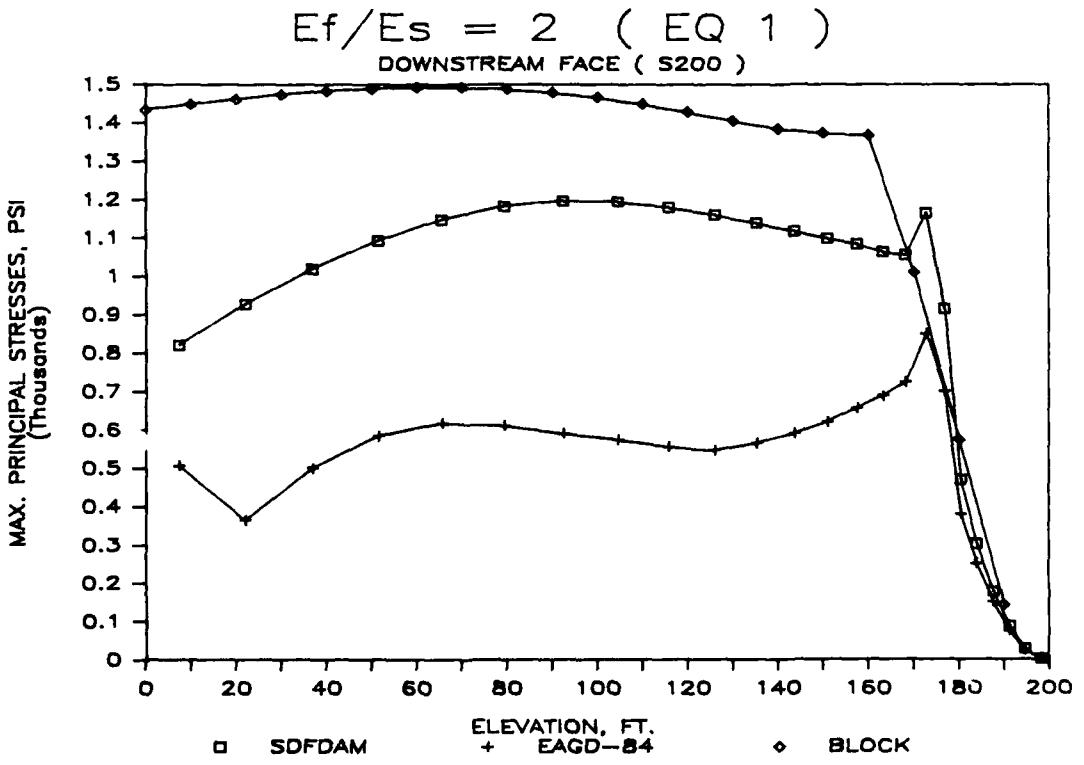
Ef/Es = 2 (EQ 1)
DOWNSTREAM FACE (S200)
MAX. PRINCIPAL STRESSES, PSI (Thousands)
1.5
1.4
1.3
1.2
1.1
1
0.9
0.8
0.7
0.6
0.5
0.4
0.3
0.2
0.1
0
0 20 40 60 80 100 120 140 160 180 200
ELEVATION, FT.
SDFDAM
EAGD-84
BLOCK

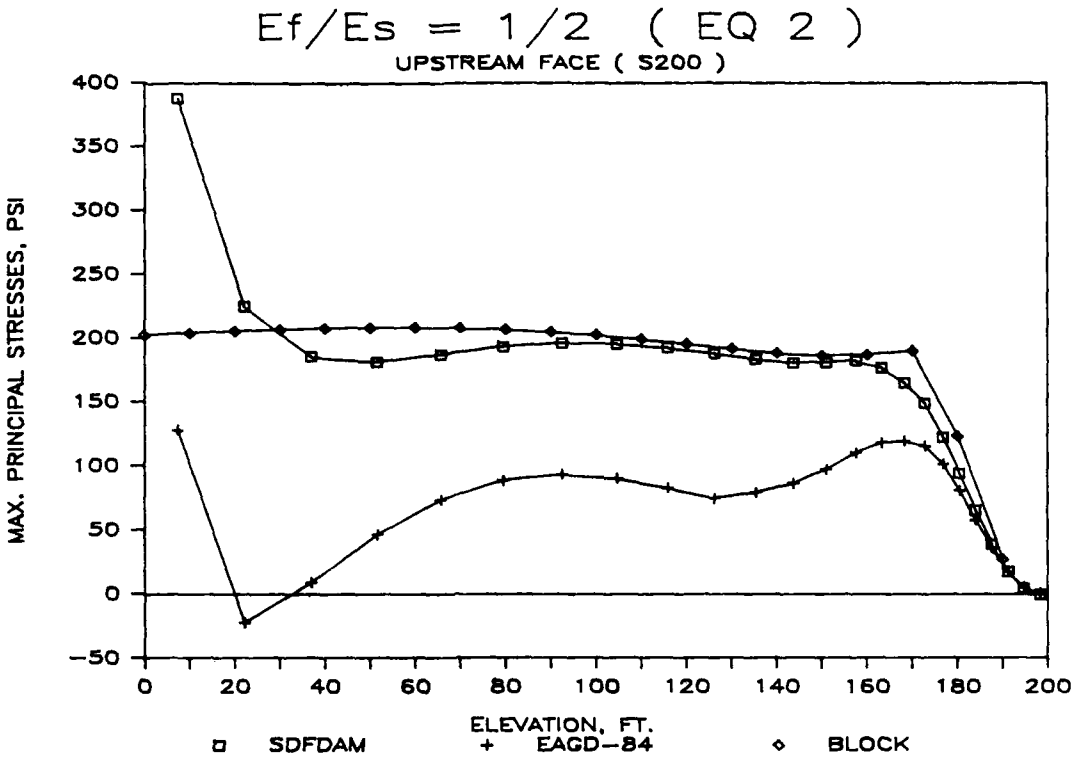
Ef/Es = 1/2 (EQ 2)
UPSTREAM FACE (S200)
MAX. PRINCIPAL STRESSES, PSI
400
350
300
250
200
150
100
50
0
-50
0
20
40
60
80
100
120
140
160
180
200
ELEVATION, FT.
SDFDAM
EAGD-84
BLOCK

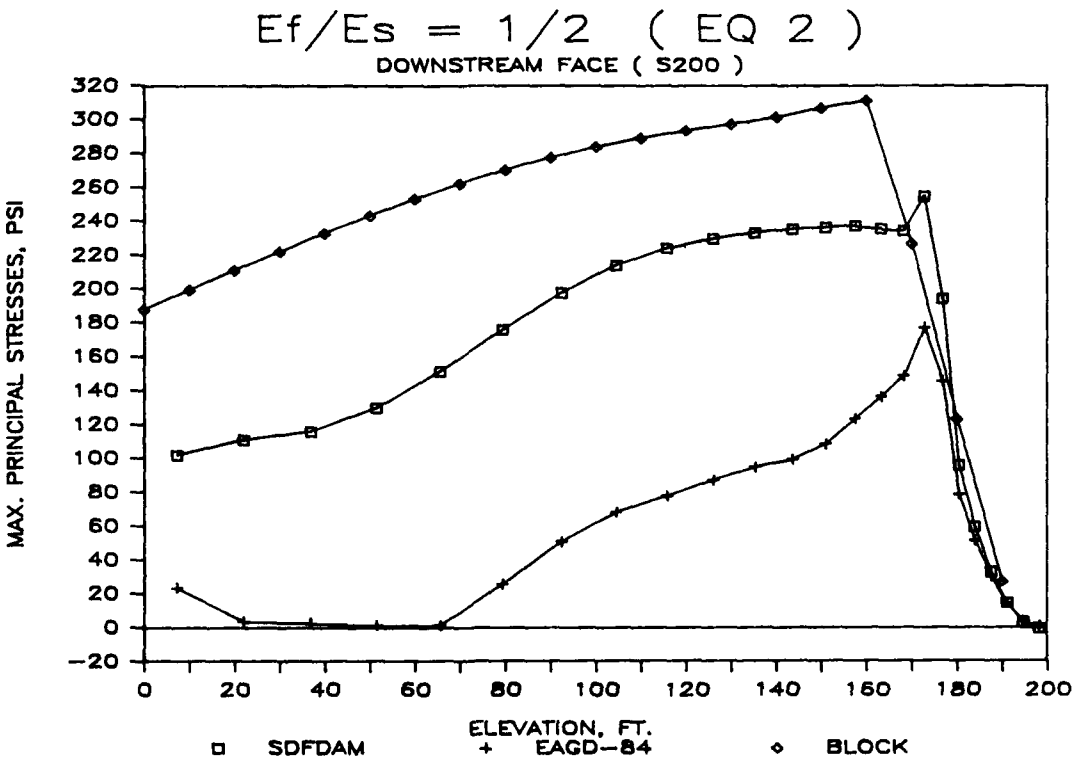
Ef/Es = 1/2 (EQ 2)
DOWNSTREAM FACE (S200)
MAX. PRINCIPAL STRESSES, PSI
320
300
280
260
240
220
200
180
160
140
120
100
80
60
40
20
0
-20
0
20
40
60
80
100
120
140
160
180
200
ELEVATION, FT.
SDFDAM
EAGD-84
BLOCK

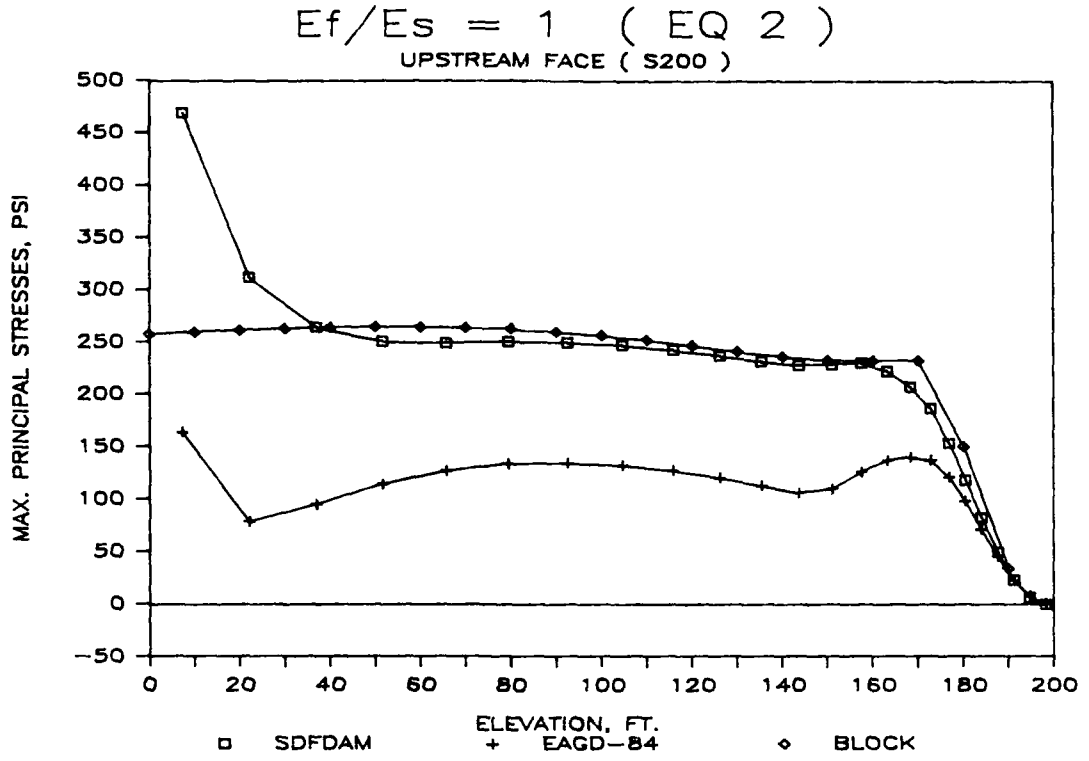
Ef/Es = 1 (EQ 2)
UPSTREAM FACE (S200)
MAX. PRINCIPAL STRESSES, PSI
500
450
400
350
300
250
200
150
100
50
0
-50
0
20
40
60
80
100
120
140
160
180
200
ELEVATION, FT.
SDFDAM
EAGD-84
BLOCK

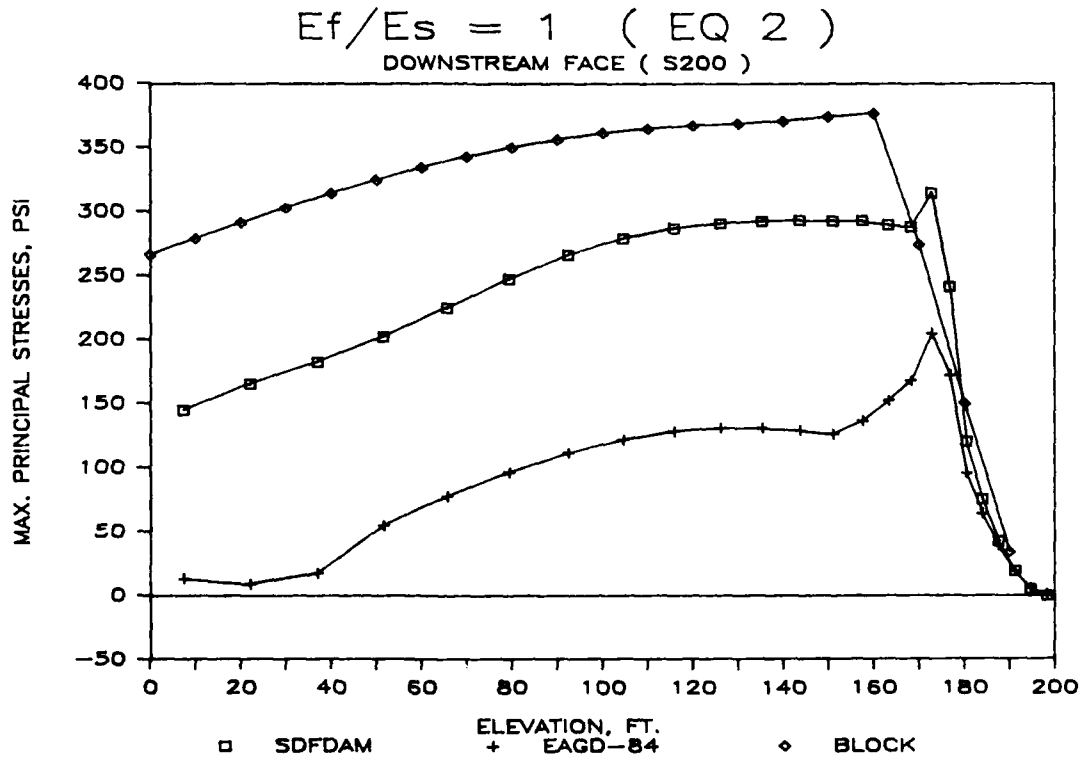
Ef/Es = 1 (EQ 2)
DOWNSTREAM FACE (S200)
MAX. PRINCIPAL STRESSES, PSI
400
350
300
250
200
150
100
50
0
-50
0
20
40
60
80
100
120
140
160
180
200
ELEVATION, FT.
SDFDAM
EAGD-84
BLOCK

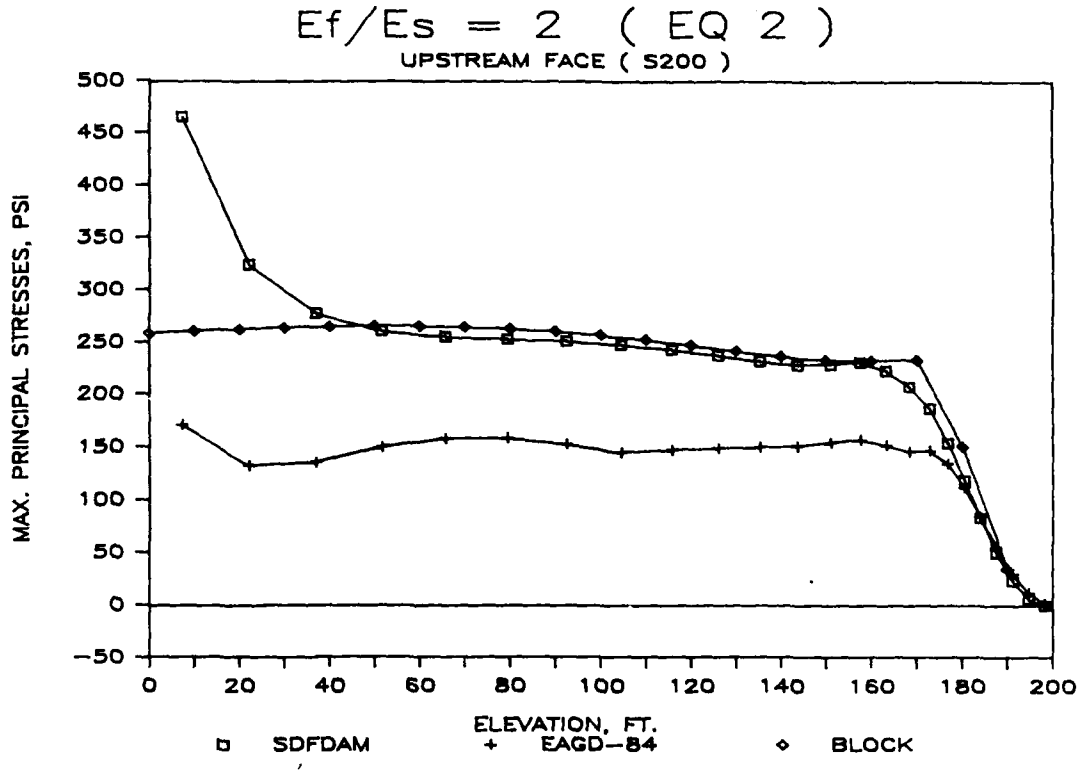
Ef/Es = 2 (EQ 2)
UPSTREAM FACE (S200)
MAX. PRINCIPAL STRESSES, PSI
500
450
400
350
300
250
200
150
100
50
0
-50
0
20
40
60
80
100
120
140
160
180
200
ELEVATION, FT.
SDFDAM
EAGD-84
BLOCK

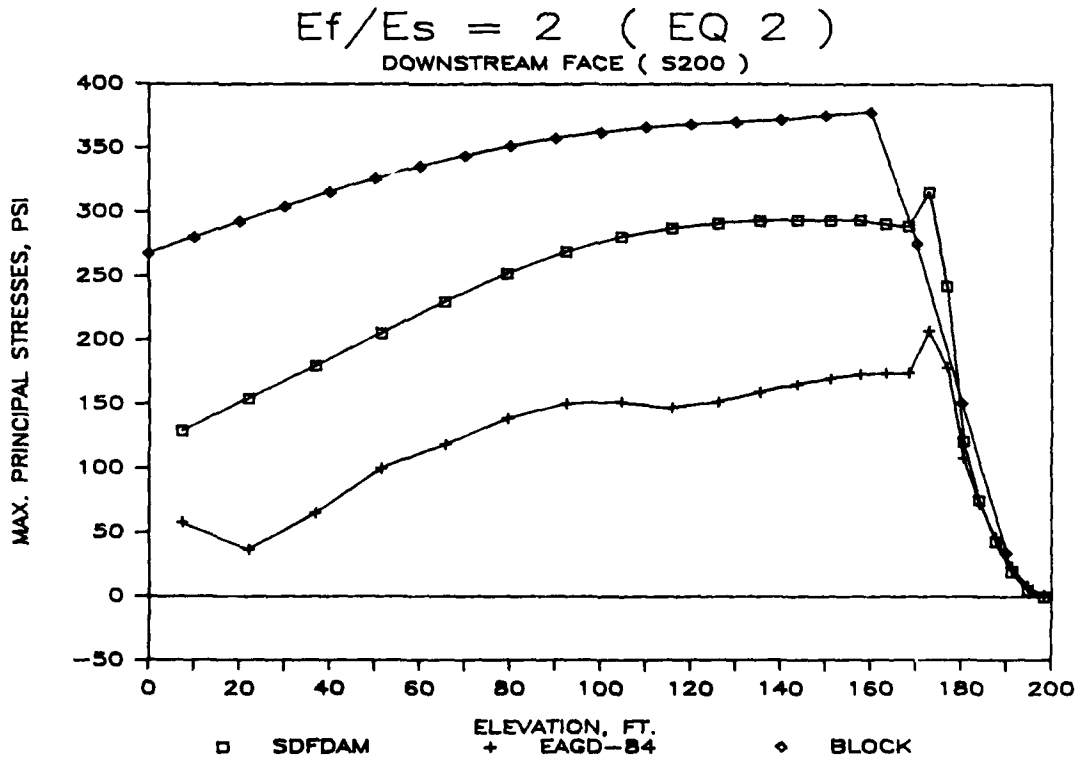
Ef/Es = 2 (EQ 2)
DOWNSTREAM FACE (S200)
MAX. PRINCIPAL STRESSES, PSI
400
350
300
250
200
150
100
50
0
-50
0
20
40
60
80
100
120
140
160
180
200
ELEVATION, FT.
SDFDAM
EAGD-84
BLOCK

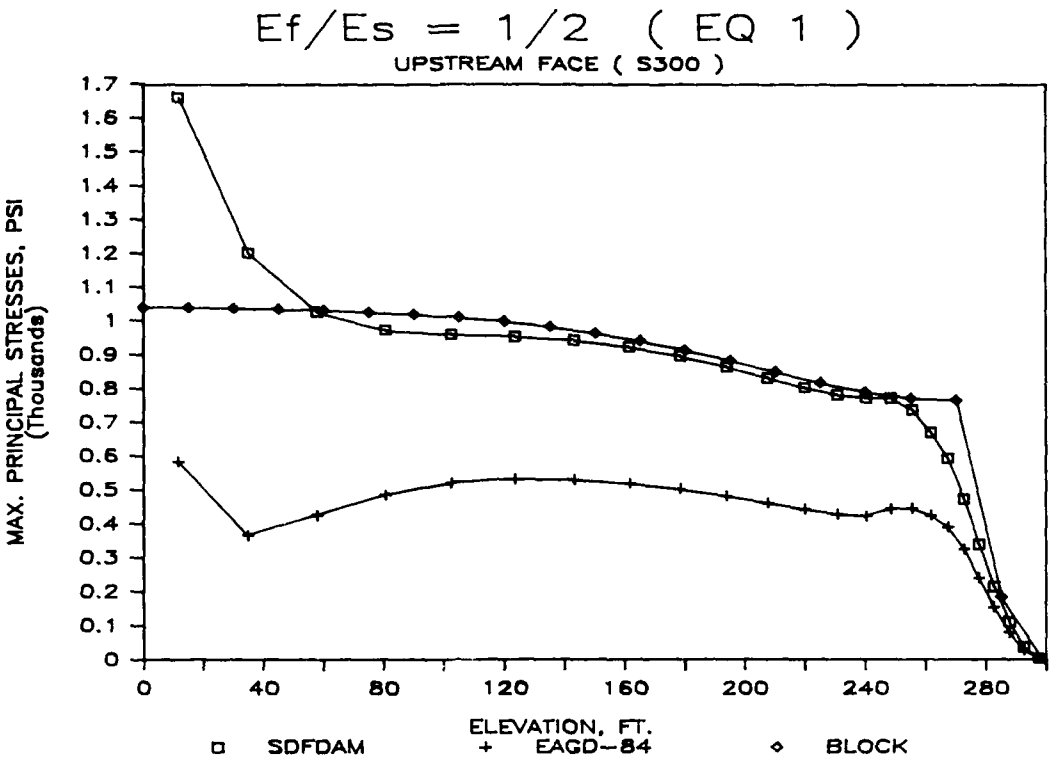
Ef/Es = 1/2 (EQ 1)
UPSTREAM FACE (S300)
MAX. PRINCIPAL STRESSES, PSI (Thousands)
1.7
1.6
1.5
1.4
1.3
1.2
1.1
1
0.9
0.8
0.7
0.6
0.5
0.4
0.3
0.2
0.1
0
0
40
80
120
160
200
240
280
ELEVATION, FT.
SDFDAM
EAGD-84
BLOCK

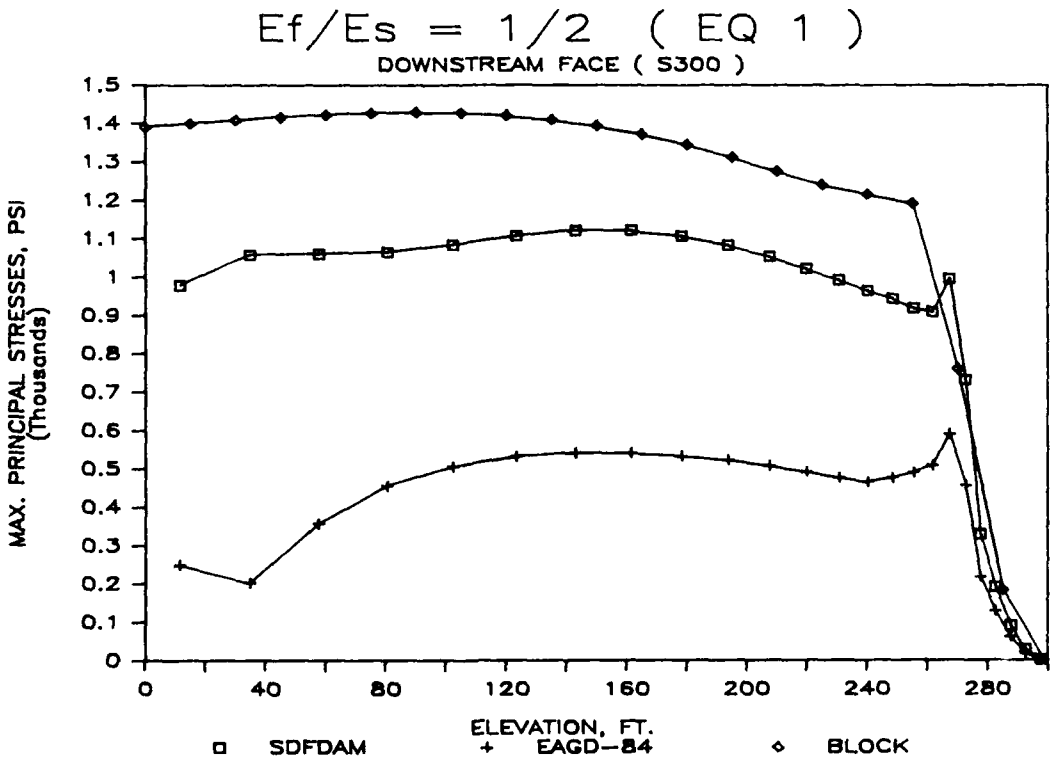
Ef/Es = 1/2 (EQ 1)
DOWNSTREAM FACE (S300)
MAX. PRINCIPAL STRESSES, PSI (Thousands)
1.5
1.4
1.3
1.2
1.1
1
0.9
0.8
0.7
0.6
0.5
0.4
0.3
0.2
0.1
0
0
40
80
120
160
200
240
280
ELEVATION, FT.
SDFDAM
EAGD-84
BLOCK

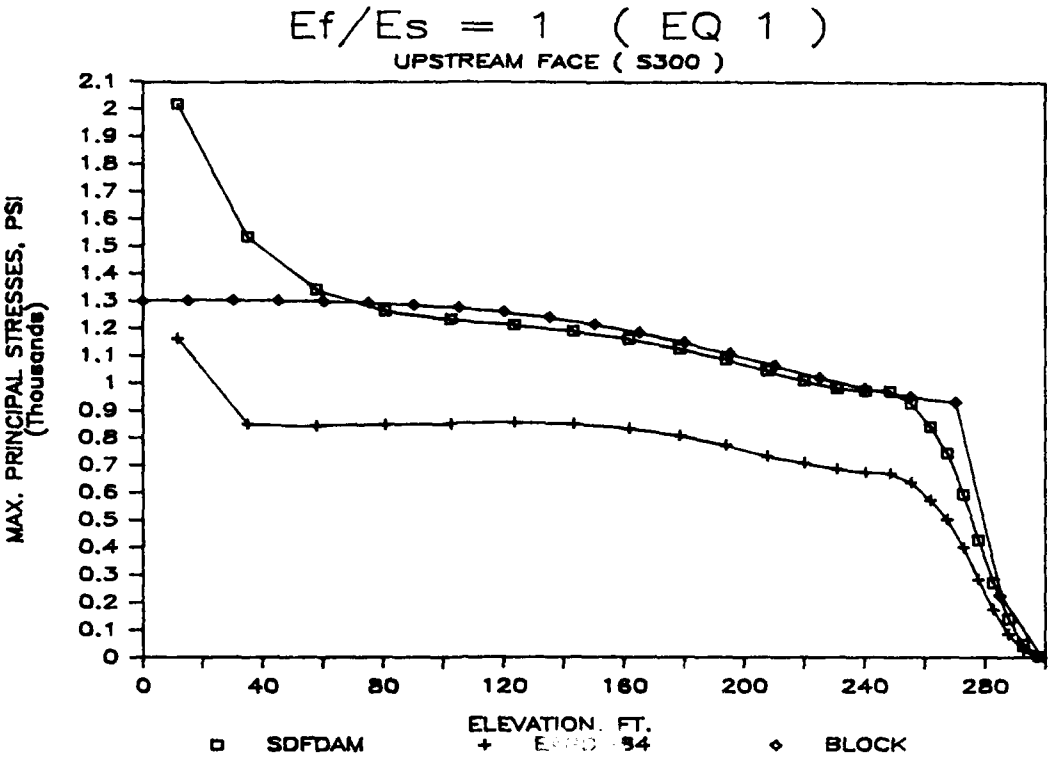
Ef/Es = 1 (EQ 1)
UPSTREAM FACE (S300)
MAX. PRINCIPAL STRESSES, PSI (Thousands)
2.1
2
1.9
1.8
1.7
1.6
1.5
1.4
1.3
1.2
1.1
1
0.9
0.8
0.7
0.6
0.5
0.4
0.3
0.2
0.1
0
0
40
80
120
160
200
240
280
ELEVATION, FT.
SDFDAM
BLOCK

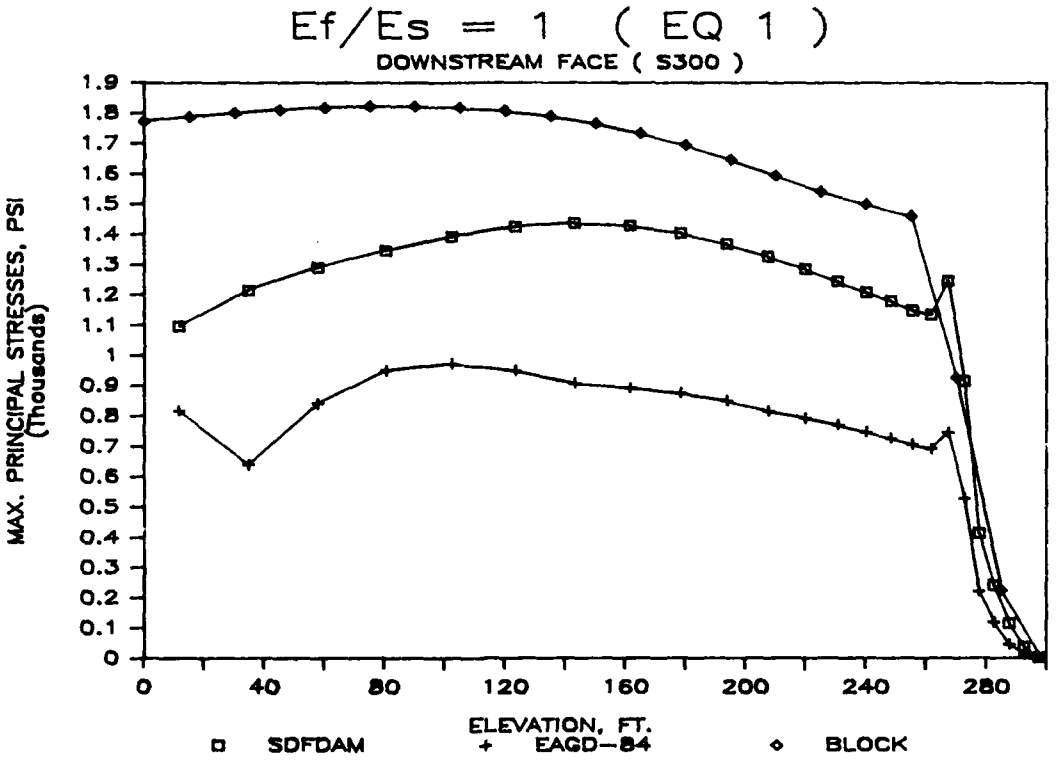
Ef/Es = 1 (EQ 1)
DOWNSTREAM FACE (S300)
MAX. PRINCIPAL STRESSES, PSI (Thousands)
1.9
1.8
1.7
1.6
1.5
1.4
1.3
1.2
1.1
1
0.9
0.8
0.7
0.6
0.5
0.4
0.3
0.2
0.1
0
0
40
80
120
160
200
240
280
ELEVATION, FT.
SDFDAM
EAGD-84
BLOCK

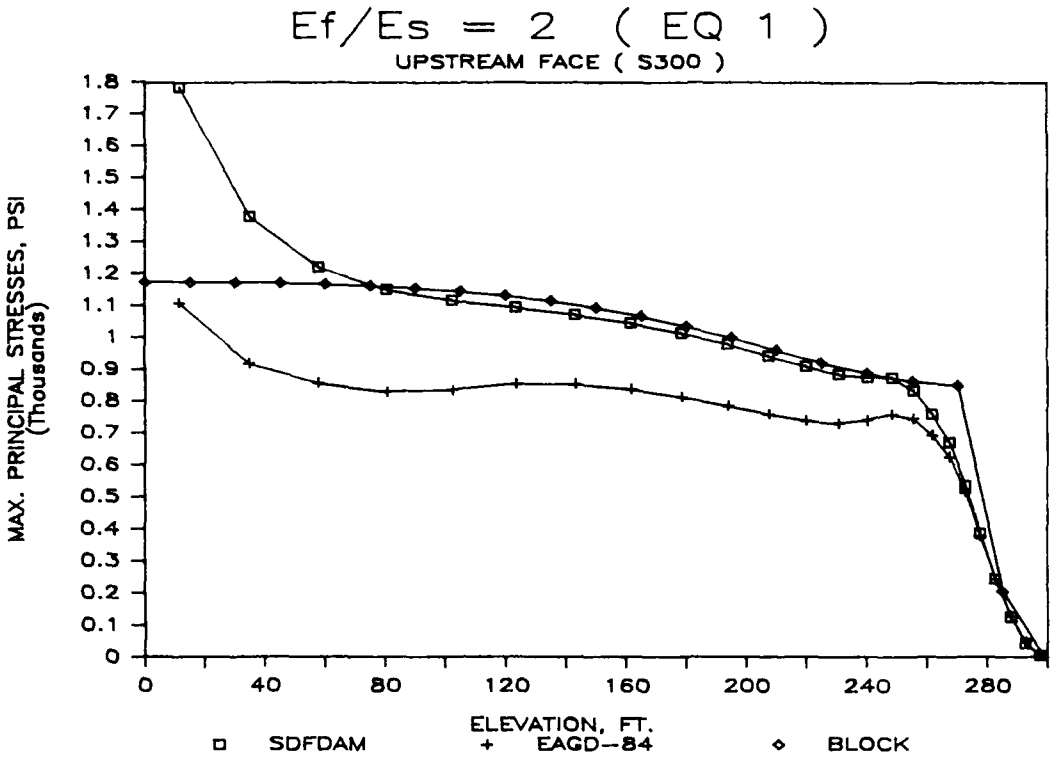
Ef/Es = 2 (EQ 1)
UPSTREAM FACE (S300)
MAX. PRINCIPAL STRESSES, PSI (Thousands)
1.8
1.7
1.6
1.5
1.4
1.3
1.2
1.1
1
0.9
0.8
0.7
0.6
0.5
0.4
0.3
0.2
0.1
0
0
40
80
120
160
200
240
280
ELEVATION, FT.
SDFDAM
EAGD-84
BLOCK

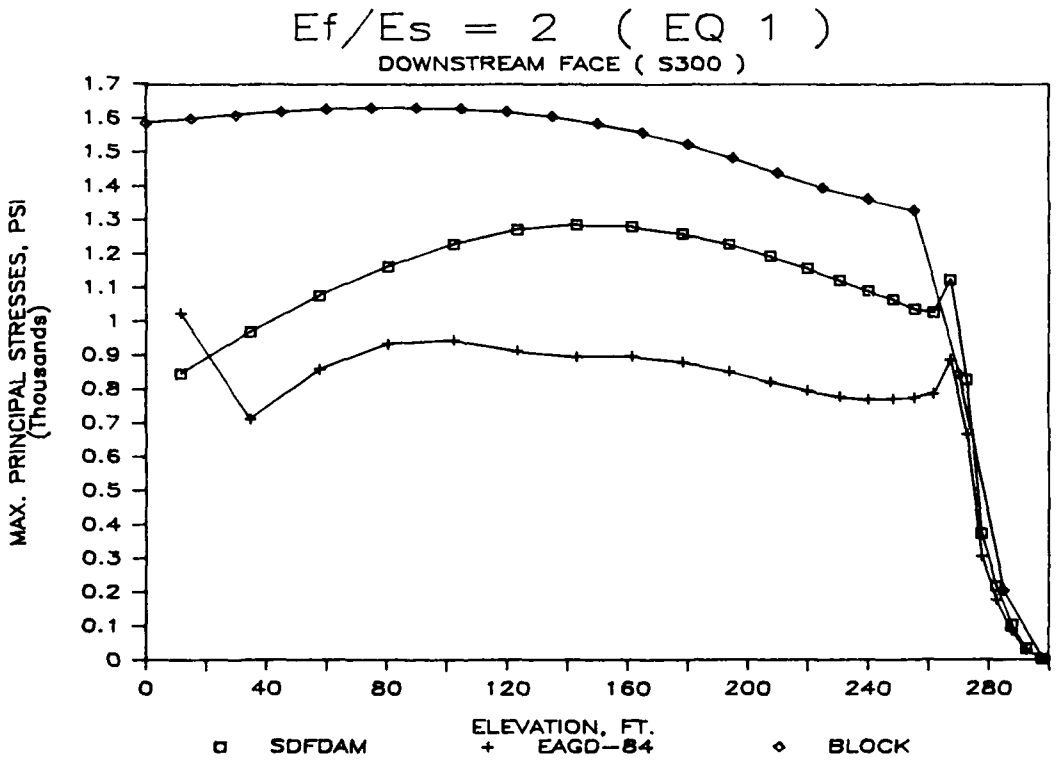
Ef/Es = 2 (EQ 1)
DOWNSTREAM FACE (S300)
MAX. PRINCIPAL STRESSES, PSI (Thousands)
1.7
1.6
1.5
1.4
1.3
1.2
1.1
1
0.9
0.8
0.7
0.6
0.5
0.4
0.3
0.2
0.1
0
0
40
80
120
160
200
240
280
ELEVATION, FT.
SDFDAM
EAGD-84
BLOCK

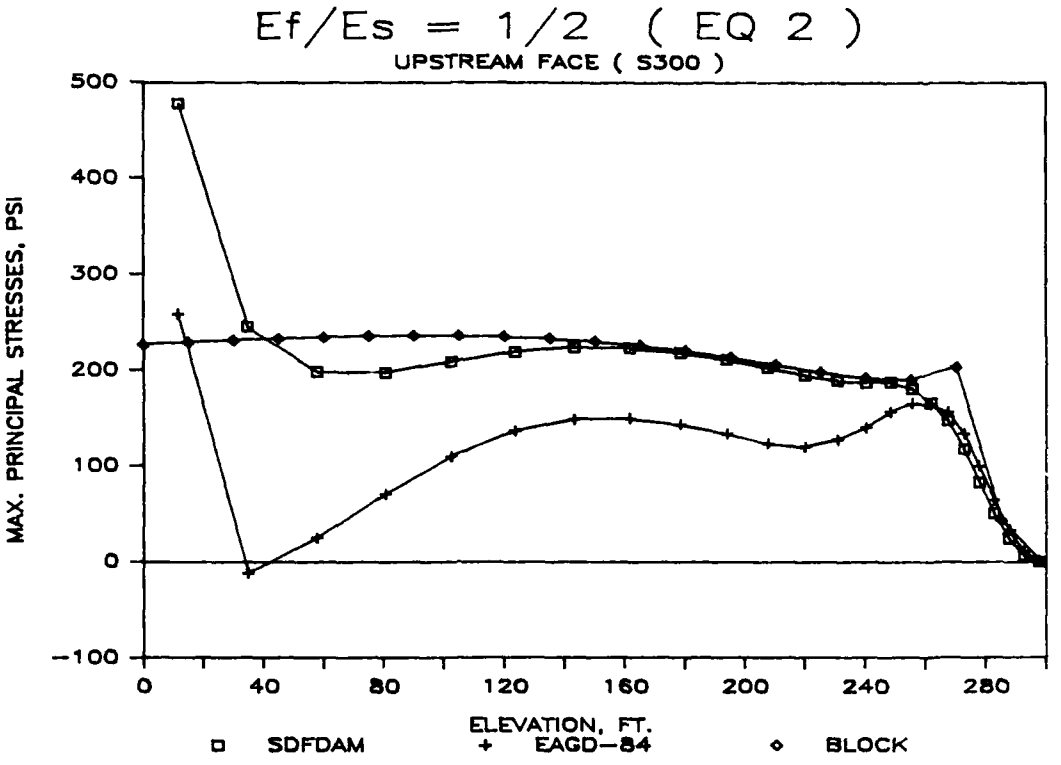
Ef/Es = 1/2 (EQ 2)
UPSTREAM FACE (S300)
MAX. PRINCIPAL STRESSES, PSI
500
400
300
200
100
0
-100
0
40
80
120
160
200
240
280
ELEVATION, FT.
SDFDAM
EAGD-84
BLOCK

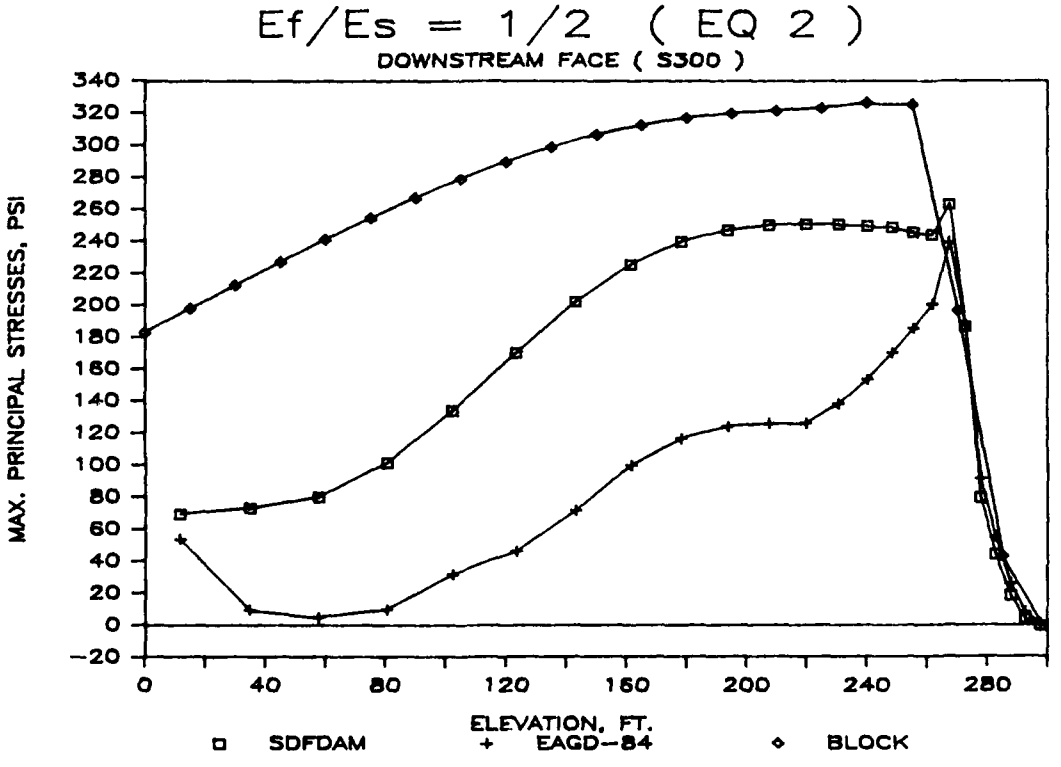
Ef/Es = 1/2 (EQ 2)
DOWNSTREAM FACE (S300)
MAX. PRINCIPAL STRESSES, PSI
340
320
300
280
260
240
220
200
180
160
140
120
100
80
60
40
20
0
-20
0
40
80
120
160
200
240
280
ELEVATION, FT.
SDFDAM
EAGD-84
BLOCK

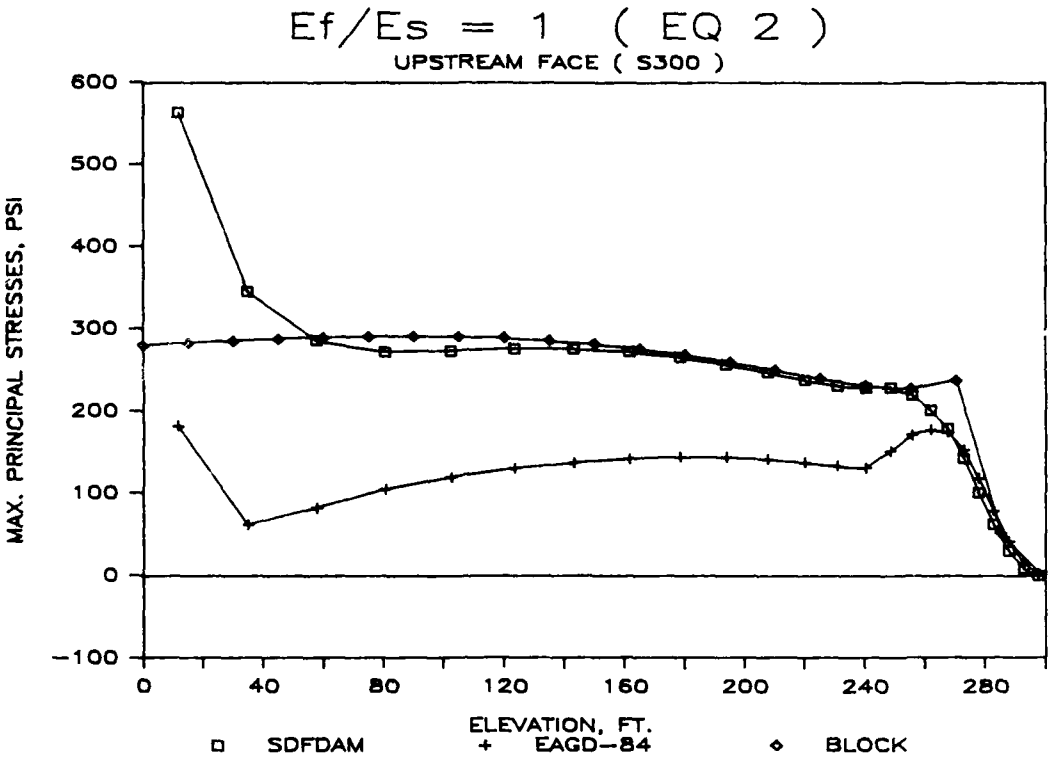
Ef/Es = 1 (EQ 2)
UPSTREAM FACE (S300)
MAX. PRINCIPAL STRESSES, PSI
600
500
400
300
200
100
0
-100
0
40
80
120
160
200
240
280
ELEVATION, FT.
SDFDAM
EAGD-84
BLOCK

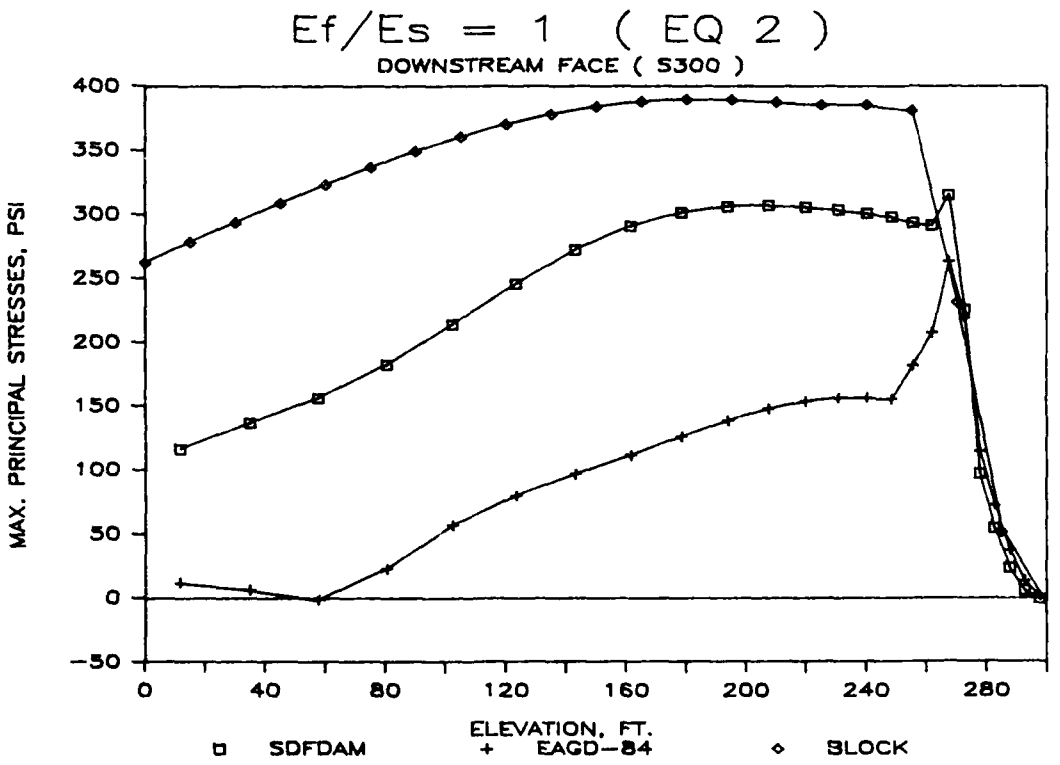
Ef/Es = 1 (EQ 2)
DOWNSTREAM FACE (S300)
MAX. PRINCIPAL STRESSES, PSI
400
350
300
250
200
150
100
50
0
-50
0
40
80
120
160
200
240
280
ELEVATION, FT.
SDFDAM
EAGD-84
BLOCK

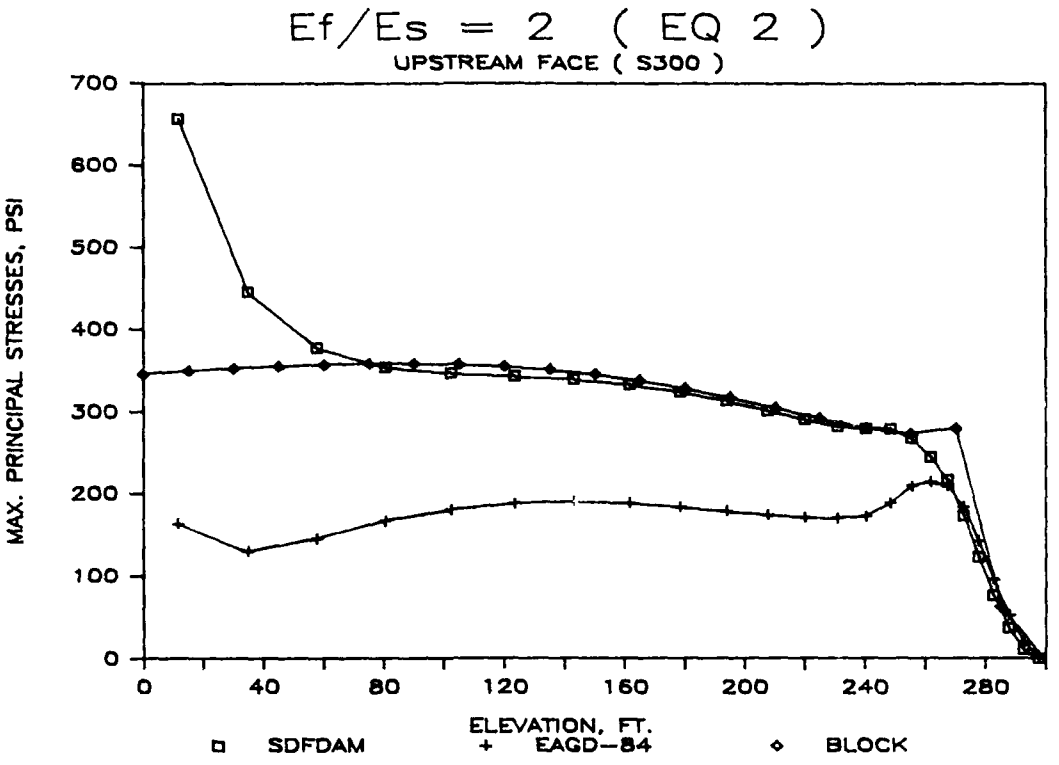
Ef/Es = 2 (EQ 2)
UPSTREAM FACE (S300)
MAX. PRINCIPAL STRESSES, PSI
700
600
500
400
300
200
100
0
0
40
80
120
160
200
240
280
ELEVATION, FT.
SDFDAM
EAGD-84
BLOCK

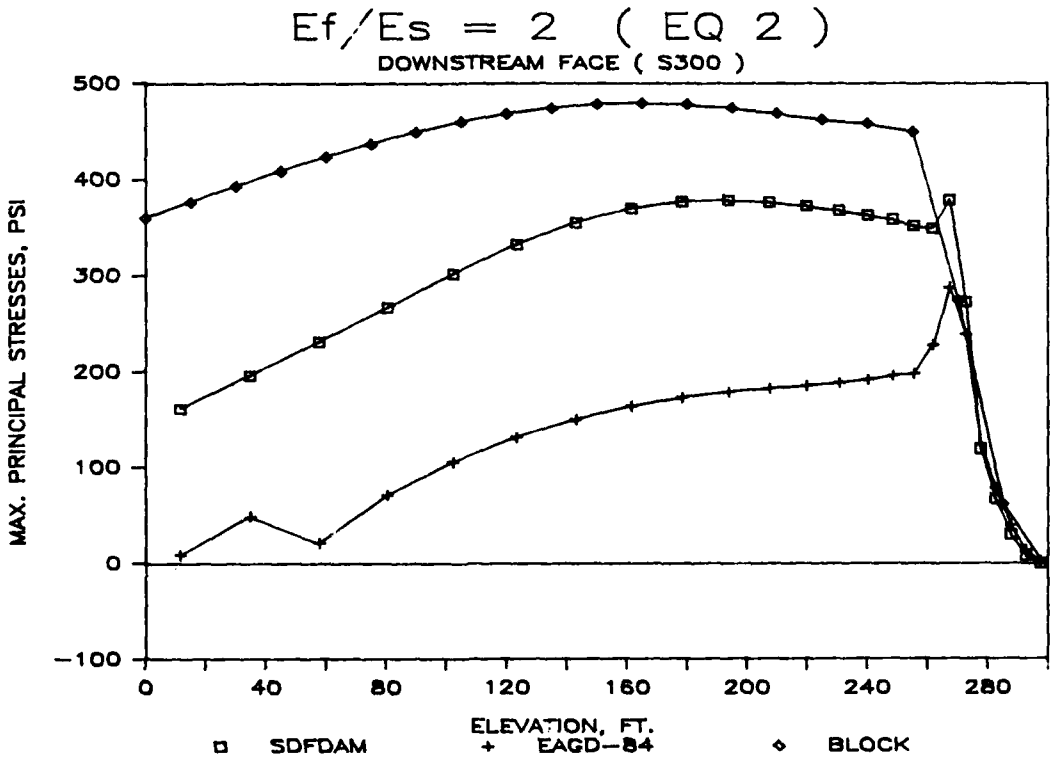
Ef/Es = 2 (EQ 2)
DOWNSTREAM FACE (S300)
MAX. PRINCIPAL STRESSES, PSI
500
400
300
200
100
0
-100
0
40
80
120
160
200
240
280
ELEVATION, FT.
SDFDAM
EAGD-84
BLOCK